Analysis of the molecular interactions of tissue-invasive M1 *Streptococcus pyogenes* with primary human endothelial cells

Von der Fakultät für Lebenswissenschaften

der Technischen Universität Carolo-Wilhelmina

zu Braunschweig

zur Erlangung des Grades einer

Doktorin der Naturwissenschaften

(Dr. rer. nat.)

genehmigte

D i s s e r t a t i o n

von Anja Ochel, geb. Grützner
aus Bottrop

1. Referentin: Privatdozentin Dr. Simone Bergmann
2. Referent: Professor Dr. Michael Steinert
eingereicht am: 23.09.2013
mündliche Prüfung (Disputation) am: 16.01.2014

Druckjahr 2014

Vorveröffentlichungen der Dissertation

Teilergebnisse aus dieser Arbeit wurden mit Genehmigung der Fakultät für Lebenswissenschaften, vertreten durch die Mentorin der Arbeit, in folgenden Beiträgen vorab veröffentlicht:

Publikationen

Ochel, A., Rohde, M., Chhatwal, G. S. & Talay, S. T. The M1 protein of *Streptococcus pyogenes* triggers an innate uptake mechanism into polarized human endothelial cells. Journal of Innate Immunity 2014 (DOI: 10.1159/000358085).

Tagungsbeiträge

Grützner, A., Chhatwal, G. S. & Talay, S. T. Analysis of the interaction of M1 *Streptococcus pyogenes* with human endothelial cells. (Poster) 4th International PhD Symposium, Helmholtz International Graduate School for Infection Research, Braunschweig (2010).

Grützner, A., Chhatwal, G. S. & Talay, S. T. Analysis of the interaction of M1 *Streptococcus pyogenes* with human endothelial cells. (Poster) 2nd Public Retreat, Helmholtz International Graduate School for Infection Research, Hahnenklee (2011).

Grützner, A., Rohde, M., Chhatwal, G. S. & Talay, S. T. Analysis of the interaction of invasive M1 *Streptococcus pyogenes* with human endothelial cells. (Poster) 5th International PhD Symposium, Helmholtz International Graduate School for Infection Research, Braunschweig (2011).

Grützner, A., Rohde, M., Chhatwal, G. S. & Talay, S. T. Analysis of the interaction of invasive M1 *Streptococcus pyogenes* with human endothelial cells. (Talk) Jahrestagung der Vereinigung für Allgemeine und Angewandte Mikrobiologie (VAAM), Tübingen (2012).

Ochel, A., Rohde, M., Chhatwal, G. S. & Talay, S. T. Analysis of the molecular interactions of invasive M1T1 *Streptococcus pyogenes* with primary human endothelial cells. (Talk) 3rd Public Retreat, Helmholtz International Graduate School for Infection Research, Bad Bevensen (2012).

Ochel, A. Analysis of the interaction of M1 *S. pyogenes* with human endothelial cells. (Talk) Progress Seminar, Helmholtz Centre for Infection Research, Braunschweig (2012).

Table of contents

List of figures

List of tables

List of abbreviations

%	percentage
℃	degree Celsius
µF	microfarad
µg	microgram
µl	microlitre
µm	micrometre
µM	micromol
3’	three prime end
5’	five prime end
∞	infinitely
A	adenine
ad	*ad* (Latin ‘up to’)
APS	ammonium persulfate
aq.	aqueous
Arp2/3	actin-related protein 2/3
ATP	adenosine-5’-triphosphate
bp	base pairs
BSA	bovine serum albumin
C	cytosine
Ccl	capacitance
CD	cluster of differentiation
cfu	colony forming units
cm^2	centimetre squared
CO_2	carbon dioxide
compl.	complemented
C-terminus	carboxy-terminus
ctr	control

DAG	diacylglycerol
dH_2O	deionized water
DMSO	dimethyl sulfoxide
DNA	deoxyribonucleic acid
DNase	deoxyribonuclease
dNTP	deoxyribonucleotide triphosphate
DTT	dithiotretol
E. coli	*Escherichia coli*
e.g.	*exempli gratia* (Latin 'for example')
EBM	endothelial basal medium
ec	extracellular
EC	endothelial cell
ECM	extracellular matrix
EDTA	ethylenediaminetetraacetic acid
EEA1	early endosomal antigen 1
EGM	endothelial growth medium
EM	electron microscopy
EsB	energy selective backscattered electron
et al	*et alii* (Latin 'and others')
FACS	fluorescence activated cell sorting
FAK	focal adhesion kinase
FbaB	fibronectin binding protein of group A streptococci type B
FCS	fetal calf serum
FESEM	field emission scanning electron microscopy
FHL-1	factor H-like protein 1
FnBP	fibronectin binding protein
fwd	forward
G	guanine
g	gram

GA	glutaraldehyde
GAS	group A streptococcus
GST	glutathione-S-transferase
GTPase	guanosine triphosphatase
h	hour
HA	hyaluronic acid
HDLEC	human dermal lymphatic endothelial cells
HIS	histidine
HPMEC	human pulmonary microvascular endothelial cells
HUVEC	human umbilical vein endothelial cells
i.e.	*id est* (Latin 'that is')
ic	intracellular
IF	immunofluorescence
IFNγ	interferon gamma
IgG (H+L)	immunoglobulin G (heavy and light chain)
IL	interleukin
ILK	integrin linked kinase
IP_3	inositol-3,4,5-trisphosphate
IPTG	isopropyl-β-D-thiogalactopyranoside
kb	kilobase
kDa	kilodalton
kV	kilovolt
l	litre
L. lactis	*Lactococcus lactis*
Lamp-1	lysosomal associated membrane protein 1
LB	Luria Bertani
LTA	lipoteichoic acid
M	molarity
mAB	monoclonal antibody

MCS	multiple cloning site
mg	milligram
MHC	major histocompatibility complex
min	minute(s)
ml	millilitre
mm	millimetre
mM	millimol
MOPS	3-(N-morpholino)propanesulfonic acid
MQ H_2O	milli-Q water
MW	molecular weight
MWCO	molecular weight cut off
N	nucleus
n.s.	non-significant
NETs	neutrophil extracellular traps
ng	nanogram
nm	nanometre
N-terminus	amino-terminus
ø	diameter
O_2	oxygen
OD_{600}	optical density at 600 nm
p value	probability value
PBS	phosphate buffered saline
PBST	phosphate buffered saline with Tween-20
PCR	polymerase chain reaction
Pen	penicillin
PET	polyethylene terephthalate
PFA	paraformaldehyde
pH	*potentia Hydrogenii*
$PI(4,5)P_2$	phosphatidylinositol-4,5-bisphosphate

PI3K	phosphatidylinositol-3-kinase
PKC	protein kinase C
PLC	phospholipase C
PMNs	polymorphonuclear neutrophils
pmol	picomol
PrtF1	protein F1
rev	reverse
RGD	arginine-glycine-aspartic acid
RNase	ribonuclease
rpm	rotations per minute
S. pyogenes	*Streptococcus pyogenes*
SD	standard deviation
SDS	sodium dodecyl sulphate
SDS-PAGE	SDS-polyacrylamide gel electrophoresis
sec	second(s)
SfbI	streptococcal fibronectin binding protein I
sic	streptococcal inhibitor of complement-mediated lysis
SLO	streptolysin O
SLS	streptolysin S
Spe	streptococcal pyrogenic exotoxin
Strep	streptomycin
STSS	streptococcal toxic shock syndrome
T	thymine
T_A	annealing temperature
TAE	Tris-acetate-EDTA
TCH	thiocarbocyanide
TCR	T cell receptor
TE	Tris/EDTA
T_E	elongation time

TEM	transmission electron microscopy
TEMED	N,N,N,N-tetramethylethylenediamine
TER	transendothelial electric resistance
TES	Tris/EDTA/saline
THB	Todd Hewitt broth
THY	Todd Hewitt broth with yeast extract
TNFα	tumor necrosis factor alpha
TSB	tryptic soy broth
TSBY	tryptic soy broth with yeast
™	trademark
U	units
Uac	uranyl acetate
UV	ultraviolet
V	volt
v/v	volume/volume
w/v	weight/volume
WASP	Wiskott-Aldrich Syndrome proteins
WAVE	WASP family verprolin-homologous proteins
wt	wild type
α	alpha
β	beta
γ	gamma
Δ	delta
Ω	ohm

1. Abstract

Streptococcus pyogenes (*S. pyogenes*, GAS) is a major human pathogen that causes severe invasive diseases associated with high morbidity and mortality. Although various serotypes of *S. pyogenes* are associated with invasive tissue infections, serotype M1 *S. pyogenes* is frequently isolated from patients with necrotizing fasciitis. The development of an invasive disease implies that the pathogen has to be able to overcome tissue barriers, one of which is the endothelial cell (EC) lining separating the blood stream from the underlying soft tissue.

This study demonstrates for the first time a direct interaction of serotype M1 GAS with human EC. Infection assays using a complex *in vitro* EC barrier model highlight that M1 GAS efficiently invades into human umbilical cord, dermal and lung endothelial cells. A tight confluent polarized EC layer proofed to be essential for efficient invasion. The M1 protein expressed by serotype M1 *S. pyogenes* is identified as a strong invasin which mediates internalization into EC. Heterologous expression of M1 as well as the use of a M1 knock out mutant clearly demonstrates that the M1 protein is sufficient to mediate uptake into EC via a phagocytosis-like mechanism. Activation of phospholipase C, protein kinase C and the release of intracellular calcium are crucial for efficient invasion of M1 GAS, as inhibition of either of those significantly reduces streptococcal uptake. On a cellular level the activation of these signalling molecules leads to the formation of membrane protrusions which tightly engulf the streptococcal chain resulting in zipper-like uptake of M1 GAS into EC. This process comprises a reorganization of the actin cytoskeleton, activation of the Arp2/3 actin nucleation complex and accumulation of F-actin at the entry port. Internalized streptococci are incorporated into phagosomes which traffic along the classical endocytic pathway, accumulate late endosomal/lysosomal markers and finally fuse with lysosomes. However, M1 GAS evades the phagolysosome to reside and persist within the cytoplasm of the host cell and subsequently crosses the EC lining and is released at the basolateral side of the EC layer, facing the underlying soft tissue.

In conclusion, this study provides new major insights in the invasion of serotype M1 GAS into EC and strongly indicates that EC represent target cells for M1 GAS invasion. Invasion into EC represents one potential general mechanism of M1 GAS to efficiently evade innate host immune responses and to persist intracellular. Subsequent transmigration into underlying soft tissue might represent a crucial step in the dissemination into deep tissue and thus, would explain why M1 GAS is frequently associated with invasive diseases such as necrotizing fasciitis.

2. Introduction

2.1 The genus Streptococcus

The genus *Streptococcus* encompasses non-motile, gram-positive, non-spore-forming cocci 0.6-1 µm in diameter which grow in pairs or chains. As facultative anaerobes with a fermentative metabolism, streptococci obtain energy from homolactic fermentation of sugars (e.g. glucose) to lactic acid rather than by electron transport and oxidative phosphorylation (Olsen *et al.*, 2010).

The genus *Streptococcus* comprises various human pathogenic strains including *Streptococcus pyogenes*, *Streptococcus dysagalactiae* subsp. *equisimilis*, *Streptococcus agalactiae* and *Streptococcus pneumoniae*. One major characteristic, which is wildly used for taxonomic classification, is the ability of streptococci to lyse red blood cells (Schottmüller, 1903). According to the lysis capabilities streptococci are divided into α-, β- and γ-haemolytic species. The group of β-haemolytic streptococci creates a zone of complete clearing when grown on blood agar plates which is characterized by complete lysis of nearby erythrocytes. α-haemolysis, on the other hand, is characterized by an incomplete lysis of erythrocytes causing a greenish zone surrounding the streptococcal colonies. γ-haemolytic streptococci show no haemolysis pattern (Prescott *et al.*, 2005, Salyers *et al.*, 2002).

2.2 Streptococcus pyogenes

Streptococcus pyogenes (*S. pyogenes*), the β-haemolytic group A streptococcus (GAS), is an important human pathogen which is considered as the most pathogenic species of the genus streptococcus (Facklam, 2002). It is an exclusively human pathogen causing a large variety of diseases ranging from mild superficial infections to severe invasive diseases (Cunningham, 2000, Carapetis *et al.*, 2005). When grown on blood agar plates it shows the typical zone of β-haemolysis around the colonies. This feature allows the clear discrimination of *S. pyogenes* from members of the α- and γ-haemolytic streptococci. Within the group of β-haemolytic streptococci *S. pyogenes* is further distinguished from other members of this group e.g. *Streptococcus agalactiae* on the basis of serological typing of the group A specific surface carbohydrate antigen within the bacterial cell wall. This so called Lancefield grouping schema was developed by Rebecca Lancefield in 1933 and divides β-haemolytic streptococci into 20 serogroups designated A-H and K-V (Lancefield, 1933). In addition, the streptococcal M protein on the cell surface of *S. pyogenes* has been used for further differentiation of *S. pyogenes* strains. Serological typing of the M protein antigen, firstly introduced by Rebecca Lancefield, allows further differentiation of group A streptococci into

serotypes (Lancefield, 1928, Lancefield, 1962, Facklam, 2002). This technique is still used today and more than 100 different serotypes have been identified so far. Nowadays, sequence analysis of the hypervariable region of the *emm* gene (*emm* typing) is conducted alternatively to serological typing and allows additional classification of GAS into *emm* types. Over 120 *emm* types have been identified which correlate in most cases with serogroups obtained by serological analysis (Beall *et al.*, 1996, Facklam, 2002).

S. pyogenes is an extremely versatile organism and a major cause for morbidity and mortality worldwide (Carapetis *et al.*, 2005). Since *S. pyogenes* colonizes the throat and the skin, superficial infections of the mucous and epithelial membranes such as pharyngitis, tonsillitis, impetigo and pyoderma are the most common diseases caused by GAS (Tart *et al.*, 2007). The prevalence of GAS pharyngitis is estimated with 616 million cases per year. In addition, 111 million incidents of GAS pyoderma, an infection of the epidermis of the face or the extremities, have been reported each year (Carapetis *et al.*, 2005). Although these are usually mild and uncomplicated infections, they provide a constant reservoir and represent a major burden on healthcare (Bisno, 2001, Carapetis *et al.*, 2005, Tart *et al.*, 2007). Post infection immune sequelae like rheumatic fever and post-streptococcal glomerulonephritis can develop as a complication of untreated upper respiratory tract or skin infections. Rheumatic fever mostly affects children with untreated pharyngitis and is the major cause for acquired cardiovascular conditions (Guilherme *et al.*, 2000, Olivier, 2000). Although rheumatic fever today is relatively uncommon in the industrialized world, high frequencies are found in underdeveloped countries and populations with low access to medical health care institutions for example the native population in Northern Australia. In these populations among 100-200 children out of 100.000 children are affected by rheumatic fever each year (Olivier, 2000). Although the exact mechanism of the development of post streptococcal conditions remains unclear, there is evidence that molecular mimicry between streptococcal components (e.g. the M protein) and components of human tissue (e.g. heart) account for the development of these auto-immune conditions (Dale *et al.*, 1985, Kaplan *et al.*, 1964, Cunningham, 2000, Guilherme *et al.*, 2000). In addition to superficial infections, GAS is able to cause severe invasive and life threatening diseases like sepsis, necrotizing fasciitis and streptococcal toxic shock syndrome (STSS). With over 500.000 deaths per year due to severe diseases, *S. pyogenes* is placed among the top ten global killers. It is estimated that the prevalence of invasive diseases is 663.000 new cases and 163.000 deaths annually (Carapetis *et al.*, 2005). The pathogenesis of invasive streptococcal diseases is covered in further detail in chapters 2.3 and 2.4.

For treatment of GAS infections Penicillin is still the antibiotic of choice. To date, GAS remains exquisitely sensitive to Penicillin and no resistances have been reported (Kaplan,

1997, Horn *et al.*, 1998, Macris *et al.*, 1998). However, in around 35% of the pharyngitis patients treated with Penicillin a failure in complete eradication of GAS is observed (Sela *et al.*, 1999) suggesting that *S. pyogenes* has evolved mechanisms to evade the antimicrobial effect of Penicillin. An intracellular niche within tonsillar epithelial cells and the poor cell penetration of Penicillin as well as the presence of β-lactamase producing commensal bacteria (e.g. *Bacillus fragilis*) might account for protection and survival of *S. pyogenes* despite antibiotic treatment (Sela *et al.*, 1999, Brook, 2010, Brook, 2013, Kaplan *et al.*, 2006).

Considering the significant global burden of GAS diseases, research has focused on the development of an efficient and safe vaccine which would ideally prevent both pharyngeal and skin colonization, invasive diseases as well as rheumatic fever and rheumatic heart disease (Dale *et al.*, 2013). However, vaccine development is hindered by the diversity of conserved surface antigens, the varying geographic distribution of GAS diseases among industrialized and developing countries and the diverging global prevalence of *emm* types. Furthermore, the problem of vaccine safety and the issue of auto-immunity due to cross-reactivity with human tissue are still major factors contributing to the problems impeding vaccine development (Cunningham, 2000, Dale *et al.*, 2013). The streptococcal M protein has been the major target for vaccine development and several strategies have focused on the type-specific N-terminal region of the M protein which is known to induce type specific antibodies (Cunningham, 2000, Dale *et al.*, 2013). A 26- and a 30-valent vaccine candidate containing peptides from multiple N-terminal regions of the M protein have turned out as promising candidates and are in various stages of clinical and pre-clinical trials (McNeil *et al.*, 2005, Dale *et al.*, 2011, Dale *et al.*, 2013). In addition, various conserved GAS antigens, including the C-terminal region of the M protein, known to be protective against multiple serotypes, as well as non-M protein based vaccine candidates (e.g. C5a peptidase, fibronectin-binding proteins, pili) and anchorless surface antigens have been considered as target antigens and are currently under investigation (Batzloff *et al.*, 2003, Batzloff *et al.*, 2004, Bauer *et al.*, 2012, Shet *et al.*, 2003, Kawabata *et al.*, 2001, Koller *et al.*, 2010, Henningham *et al.*, 2012, Cunningham, 2000, Dale *et al.*, 2013).

2.3 Epidemiology of GAS invasive diseases

In addition to superficial diseases, *S. pyogenes* infection may lead to severe invasive diseases like necrotizing fasciitis and streptococcal toxic shock syndrome, conditions causing substantial morbidity and mortality worldwide (Cunningham, 2000, Carapetis *et al.*, 2005). The global burden of severe invasive diseases is estimated with 663.000 new cases and 163.000 deaths per year and places *S. pyogenes* among the top ten pathogens responsible for global mortality (Carapetis *et al.*, 2005). Necrotizing fasciitis is an infection of the subcutaneous tissue that is characterized by rapid destruction of the skin, subcutaneous and deep soft tissue and muscle. The disease progresses within hours from a seemingly harmless skin lesion to rapid tissue destruction and necrosis (Stevens, 2001, Olsen *et al.*, 2010). Invasive diseases may also be accompanied by streptococcal toxic shock syndrome, a disease characterized by massive release of pro-inflammatory cytokines in response to streptococcal superantigens resulting in hypotension, toxic shock and multi organ failure (Cunningham, 2000, Long *et al.*, 2012).

Since the late 1980s a resurgence of severe invasive streptococcal diseases has been observed worldwide. Various serotypes of *S. pyogenes* have been associated with invasive diseases, however serotype M1 and M3 GAS are most prevalent and together account for more than 50% of the severe invasive diseases (Stevens, 2001, Tart *et al.*, 2007, Aziz *et al.*, 2008). For the development of an invasive disease, the pathogen has to gain access to naturally sterile tissue. *S. pyogenes* may gain access to deeper tissue through a break in the epithelial cell layer as a consequence of an injury (Olsen *et al.*, 2009). In addition, risk factors include burns, insect bites, varicella, diabetes and intravenous drug abuse (Stevens, 2001). However, in a substantial number of cases invasive conditions develop in previously healthy individuals with no obvious port of entry (Johansson *et al.*, 2010).

2.4 Pathogen-host interactions underlying invasive GAS diseases

The major characteristics of severe invasive GAS diseases are substantial tissue destruction, bacterial dissemination and systemic disease manifestations (Olsen *et al.*, 2009). The key steps in the pathogenesis involve successful colonization of the host, adaptation to the host environment and expression of factors that allow subversion of host immune defences and vascular dissemination (Olsen *et al.*, 2009). To ensure its survival within the host, *S. pyogenes* expresses an array of surface bound and secreted virulence factors which will be discussed in the following chapters (Figure 1, (Nizet, 2007)).

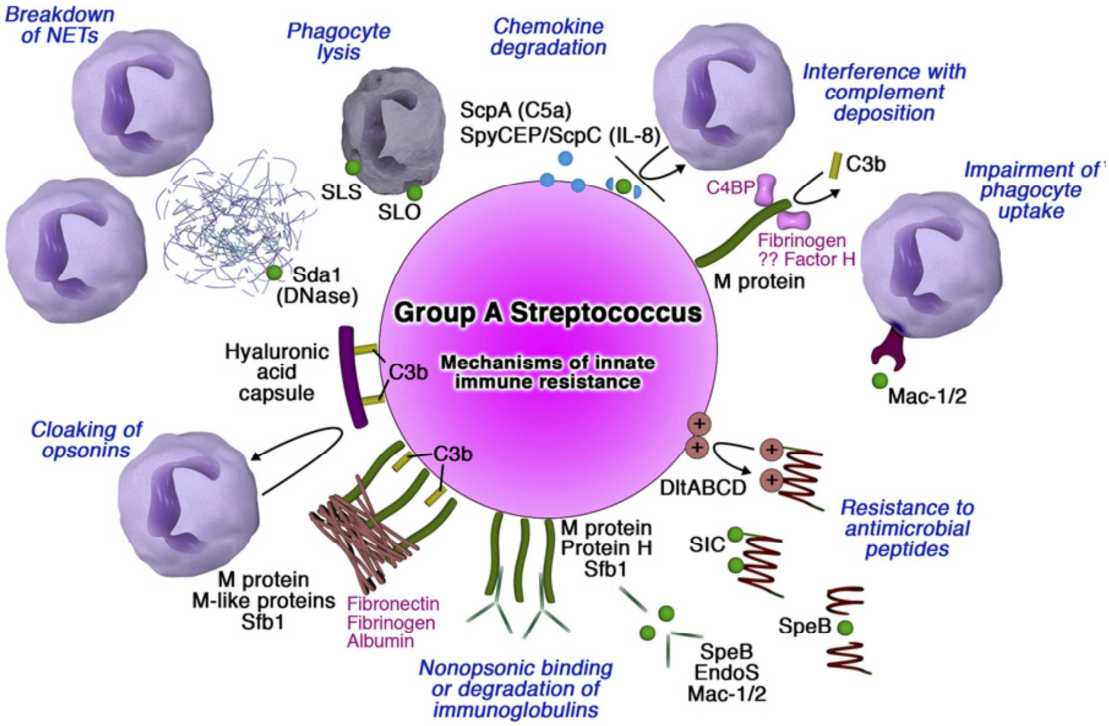

Figure 1: Schematic representation of the variety of virulence factors expressed by *S. pyogenes* to circumvent host cell immune defences

Taken from (Nizet, 2007)

2.4.1 Attachment to the host cell surface

Adhesion to host cells represents the initial step in establishing a disease and allows the pathogen to attach to and subsequently colonize the host (Cunningham, 2000, Yamaguchi *et al.*, 2012). To ensure colonization *S. pyogenes* expresses a large variety of adhesins that mediate initial attachment to the mucosal surfaces of the upper respiratory tract and the dermal epithelial cells of the skin. The expression of multiple adhesins might favour colonization of different tissue sites under varying host environmental conditions and at different stages of infection ensuring successful establishment of an infection (Cunningham, 2000, Bisno *et al.*, 2003, Schwarz-Linek *et al.*, 2006). Binding of bacterial adhesins to cell surface receptors frequently involves engagement of extracellular host cell molecules in particular components of the extracellular matrix e.g. fibronectin, collagen, vitronectin, and laminin which are ubiquitously expressed within the host (Cunningham, 2000). Binding to fibronectin has been shown to play a major role for attachment of streptococci to epithelial and endothelial cells by acting as a molecular bridge between the bacterial and the host cell surface (Yamaguchi *et al.*, 2012, Schwarz-Linek *et al.*, 2006).

S. pyogenes expresses multiple adhesins that mediate attachment to various host cells. The streptococcal cell wall contains glycolipids such as lipoteichoic acid (LTA) which was identified as a streptococcal adhesin for buccal epithelial cells. LTA binds to fibronectin and thereby mediates attachment to epithelial cells. The use of anti-LTA antibodies inhibits adhesion of streptococci to epithelial cells (Beachey *et al.*, 1976, Simpson *et al.*, 1983, Courtney *et al.*, 1983, Courtney *et al.*, 1992, Cunningham, 2000). It has been proposed that LTA mediates the first contact of the bacterium to the host cell and that other adhesins are required to establish high affinity binding (Hasty *et al.*, 1992, Bisno *et al.*, 2003).

A large group of GAS adhesins represents the family of fibronectin binding proteins (FnBPs) which mediate host pathogen interactions by recognition and binding of extracellular fibronectin (Schwarz-Linek *et al.*, 2006, Yamaguchi *et al.*, 2012). Binding of fibronectin to the bacterial surface triggers engagement of $\alpha_5\beta_1$-integrins on the host cell surface and subsequently successful attachment to the target cell. To date, at least 11 fibronectin binding proteins have been described (Yamaguchi *et al.*, 2012). These include SfbI/PrtF1, and related proteins SfbII, FBP54, protein 2 and PFBP (Bisno *et al.*, 2003, Talay, 2005). SfbI and its allelic variant PrtF1 are the best characterised fibronectin binding proteins of GAS and have been shown to mediate adhesion to respiratory epithelial cells (Talay *et al.*, 1992, Hanski *et al.*, 1992, Schwarz-Linek *et al.*, 2006). The *sfbI* (or *prtF*) gene can be found in more than 70% of clinical GAS isolates (Valentin-Weigand *et al.*, 1994).

In addition, the streptococcal M protein, pili and the hyaluronic acid capsule (HA) act as potent adhesins for various cell types. The M1 protein was identified as a potent adhesin on human lung epithelial cells. Several studies have shown that serotype M1 GAS mediates attachment and subsequent uptake into epithelial cells by binding of the M1 protein to fibronectin and subsequent engagement of $\alpha_5\beta_1$-integrins on the host cell surface. Blocking of either the M1 protein on the bacterial surface or the host cell fibronectin binding receptor significantly decreased adherence and invasion of serotype M1 GAS into epithelial cells. (Cue *et al.*, 1998, Dombek *et al.*, 1999, Cue *et al.*, 2000). Furthermore, the M protein of GAS has been demonstrated to recognize membrane cofactor protein CD46 thereby mediating attachment to keratinocytes in skin infections (Okada *et al.*, 1995, Cunningham, 2000). The M3 protein of GAS was shown to target type I and type IV collagen fibres, a process which favours colonization (Dinkla *et al.*, 2003). The hyaluronic acid capsule also acts as a potent adhesin either by binding of cell surface receptors via collagen or by directly binding to human CD44 the cell surface receptor of keratinocytes on epithelial cells (Schrager *et al.*, 1998, Dinkla *et al.*, 2003).

2.4.2 Resistance to host immune defence mechanisms

Professional phagocytic cells e.g. macrophages and polymorphonuclear neutrophils (PMNs) represent major cell types of the innate immune system which represent an important line of defence against invading pathogens. Professional phagocytes efficiently internalize and eliminate bacterial pathogens (Sarantis *et al.*, 2012). However, *S. pyogenes* has evolved multiple mechanisms to circumvent phagocytosis which is important to ensure successful survival within the human host.

Both, the M protein and the hyaluronic acid capsule of GAS, have been described to confer antiphagocytic properties (Moses *et al.*, 1997, Wessels *et al.*, 1991). The streptococcal M protein is composed of two polypeptide chains which form an alpha-helical dimer which protrudes from the streptococcal cell surface. The C-terminal region of the M protein is highly conserved among GAS strains and is anchored to the cell membrane via a LPXTG motif. The hypervariable N-terminal region extends from the cell surface and constitutes for the production of type specific antibodies (Phillips *et al.*, 1981, Cunningham, 2000, Bisno *et al.*, 2003). The M protein of GAS is known to exert its antiphagocytic properties in non-immune individuals by interfering with the activation of the alternative complement pathway (Bisno, 1979). Several mechanisms have been described so far. On the one hand the M protein binds to regulatory components of the complement pathway like factor H or factor H-like protein (FHL-1) (Horstmann *et al.*, 1988, Bisno *et al.*, 2003, Nizet, 2007). Binding of factor H to the C-terminal region of the M protein impedes the deposition of soluble complement factor C3b resulting in inhibition of the activation of the alternative complement pathway and in turn inhibition of phagocytosis (Cunningham, 2000, Bisno *et al.*, 2003). On the other hand the M protein binds human fibrinogen to its surface. Binding of fibrinogen blocks the activation of the alternative complement pathway, again by diminishing the amount of C3b deposited on the bacterial cell surface and thereby inhibiting phagocytosis by polymorphonuclear leukocytes (Cunningham, 2000, Bisno *et al.*, 2003). In addition, several other M related surface proteins (e.g. M49, Mrp, Enn-49, FcrA) of GAS have been identified and have been shown to contribute to the antiphagocytic properties of GAS (Podbielski *et al.*, 1996, Ji *et al.*, 1998, Bisno *et al.*, 2003).

Another major streptococcal factor which promotes resistance to phagocytosis is the capsule (Nizet, 2007). It is composed of a polymer of hyaluronic acid similar to hyaluronate present in human connective tissue. Due to these similarities the hyaluronic acid capsule of GAS is a poor immunogen. Studies have shown that non-encapsulated strains are more susceptible to phagocytosis and are less virulent in mice than encapsulated strains. In addition, GAS strains which are highly encapsulated and produce high amounts of M protein are found to

be extremely virulent for humans and the cause of severe invasive diseases (Cunningham, 2000, Bisno *et al.*, 2003, Nizet, 2007).

The recruitment of professional phagocytic cells from the vasculature to the site of infection is mediated by the release of chemoattractants for example the chemokine interleukin-8 (IL-8) and the complement factor C5a. *S. pyogenes* interferes with host cell chemotactic components by the production of factors with enzymatic activities e.g. SpyCEP and C5a peptidase. The streptococcal protease SpyCEP inactivates IL-8 by specific cleavage of the C-terminus, thereby impairing leucocyte recruitment (Nizet, 2007, Tart *et al.*, 2007). Furthermore, the C5a peptidase of GAS which is anchored to the streptococcal cell wall cleaves complement factor C5a. By inactivating C5a streptococci inhibit the recruitment of polymorphonuclear neutrophils to the site of infection, hence promoting resistance to phagocytosis and aiding dissemination within the host (Wexler *et al.*, 1985, Ji *et al.*, 1996, Cunningham, 2000, Nizet, 2007).

An additional streptococcal factor possibly contributing to GAS virulence is the streptococcal inhibitor of complement-mediated lysis (SIC) which blocks the assembly of the complement membrane attack complex thereby preventing lysis of the bacterium (Cunningham, 2000, Bisno *et al.*, 2003).

2.4.3 Extracellular virulence factors

In addition to surface bound virulence factors, *S. pyogenes* produces several extracellular proteins which contribute to virulence favouring rapid tissue destruction, streptococcal spread and inducing the clinical manifestations observed in severe invasive diseases e.g. necrotizing fasciitis and STSS (Bisno *et al.*, 2003).

S. pyogenes produces two exotoxins streptolysin O (SLO) and streptolysin S (SLS) which are major virulence factors that contribute to the pathogenesis of invasive diseases (Nizet, 2007, Tart *et al.*, 2007). Both belong to the family of pore-forming cytolysins and have been shown to be toxic for a variety of cell types including erythrocytes, polymorphonuclear neutrophils, platelets and subcellular organelles such as lysosomes and mitochondria. SLO is an oxygen labile haemolysin produced by almost all GAS strains and which is, therefore, inhibited in an oxygen rich environment (Bisno *et al.*, 2003, Nizet, 2002).

In addition to their function as professional phagocytes, neutrophils are also able to capture and subsequently kill pathogens by their entrapment in a mesh of DNA and histone molecules so called neutrophil extracellular traps (NETs). The production of DNases (e.g. SdaI) which degrade DNA enables *S. pyogenes* to successfully escape from NETs (Nizet,

2007, Tart *et al.*, 2007). Streptococcal tissue spread is further facilitated by degradation of hyaluronic acid components of human connective tissue by the streptococcal enzyme hyaluronidase (Bisno *et al.*, 2003). Streptokinase, a plasminogen binding protein found in almost all GAS isolates, also plays an important role in GAS virulence. Streptokinase binds plasminogen and converts it to plasmin which in turn dissolves fibrin clots, a process favouring tissue spread (Cunningham, 2000, Bisno *et al.*, 2003). Furthermore, *S. pyogenes* produces streptococcal pyrogenic exotoxin B (SpeB), a cysteine protease, which exerts multiple functions contributing to the tissue damage observed in invasive diseases (Cunningham, 2000, Bisno *et al.*, 2003). Beside its role in the activation of human matrix metalloproteinases it is able to degrade several components of the extracellular matrix e.g. vitronectin and fibronectin (Kapur *et al.*, 1993, Burns *et al.*, 1996). On the other hand SpeB activates the pro-inflammatory cytokine interleukin 1 beta (IL-1β) by conversion of the precursor into its active form (Kapur *et al.*, 1993) which suggests a role of SpeB in the pathogenesis of STSS (Bisno *et al.*, 2003).

In addition to SpeB, a large variety of streptococcal pyrogenic exotoxins (Spe's) has been identified including SpeA, SpeC, SpeD, SpeF, SpeG, SpeH, SpeJ, SpeK, SpeL, SMEZ, SMEZ-2 and SSA. The family of Spe's acts as bacterial superantigens which unspecifically bind to the T-cell receptor (TCR) and MHC class II molecules without prior processing by antigen-presenting cells. Binding results in activation and proliferation of large numbers of T-cells which in turn release massive amounts of pro-inflammatory cytokines such as tumor necrosis factor alpha (TNFα), IL-1β, IL-2 and interferon gamma (IFNγ). This overshooting inflammatory response may lead to endocytic shock, fever, hypotension and multi organ failure representing the clinical characteristics of STSS (Cunningham, 2000, Bisno *et al.*, 2003).

2.4.4 Invasion into eukaryotic cells

Internalization into host cells represents another successful mechanism of *S. pyogenes* that might contribute to the pathogenesis of invasive diseases. Although traditionally viewed as an extracellular pathogen, various studies have shown that *S. pyogenes* is able to induce invasion into non-phagocytic cells with internalization rates comparable to those of classical intracellular pathogens (LaPenta *et al.*, 1994, Greco *et al.*, 1995, Molinari *et al.*, 1997, Jadoun *et al.*, 1998, Rohde *et al.*, 2003, Nerlich *et al.*, 2009, Amelung *et al.*, 2011). The biological relevance of an intracellular state has been controversial but might represent several biological advantages. On the one hand an intracellular 'lifestyle' might provide a niche which allows streptococci to be protected from phagocytes, humoral antibodies and antibiotic treatment. This might promote carriage and streptococcal persistence within the

human host. On the other hand invasion into host cells might represent the first step in the dissemination from the primary site of infection into deep tissue (Cunningham, 2000, Bisno *et al.*, 2003, Schwarz-Linek *et al.*, 2006). A study of Osterlund and colleagues gave first evidence that an intracellular habitat of GAS might constitute a relevant mechanism for *in vivo* persistence. This study showed that viable GAS could be recovered from biopsies of infected tonsils from patients with recurrent pharyngotonsillits. This suggests that an intracellular niche constitutes an essential step for streptococcal persistence within the host and hence contributes to the pathogenesis of GAS infections (Osterlund *et al.*, 1997).

2.5 Invasion mechanisms of S. pyogenes

Since various reports have shown that *S. pyogenes* is able to trigger its own uptake into host cells, research has focused on the identification of bacterial and host cell factors as well as the molecular mechanisms that contribute to the internalization process.

The streptococcal surface proteins M1 and the major fibronectin-binding protein SfbI (and its allelic variant protein F1) not only mediate adhesion to host cells, as previously described, but also represent potent invasins mediating efficient internalization into epithelial cells (Molinari *et al.*, 1997, Talay *et al.*, 2000, Jadoun *et al.*, 1998, Ozeri *et al.*, 1998, Rohde *et al.*, 2003, Cue *et al.*, 1998, Dombek *et al.*, 1999). Studies of the invasion mechanism using different GAS strains have identified distinct invasion patterns dependent on the invasin expressed on the streptococcal surface (Molinari *et al.*, 2000). M1-expressing and SfbI-negative strains invade host cells by cytoskeletal rearrangements characterized by the formation of membrane protrusion that tightly engulf the streptococcal chain and subsequent zipper-like uptake of streptococci into epithelial cells (Dombek *et al.*, 1999, Molinari *et al.*, 2000). On the other hand SfbI-expressing strains use the formation of large membrane invaginations for internalization into host cells (Molinari *et al.*, 2000, Rohde *et al.*, 2003).

Studies on the cellular processes triggered by M1 or SfbI revealed common pathways as well as characteristic features initiated by each invasin. Figure 2 shows a schematic representation of the signalling pathways initiated by M1- and SfbI/F1 protein leading to *S. pyogenes* uptake into epithelial cells. A pre-requisite for both, M1- and SfbI-mediated invasion processes, is binding of the extracellular matrix protein fibronectin. Fibronectin acts as a bridging molecule by binding to $\alpha_5\beta_1$-integrins on the host cell surface via its RGD (arginine, glycine, aspartic acid) motive (Cue *et al.*, 1998, Molinari *et al.*, 1997, Molinari *et al.*, 2000, Talay *et al.*, 2000, Jadoun *et al.*, 1998, Ozeri *et al.*, 1998). Integrin engagement on the host cell surface leads to the formation of focal adhesions which function as signalling and docking sites for a variety of cytoskeletal proteins, thereby linking the extracellular matrix

(ECM) to the actin cytoskeleton (Brakebusch *et al.*, 2003, Wang *et al.*, 2007). Upon association with integrins both, M1 and SfbI, initiate the recruitment and phosphinositide 3-kinase (PI3K) dependent activation of the integrin linked kinase (ILK) and subsequent phosphorylation and assembly of paxillin and the focal adhesion kinase (FAK) at the port of entry (Purushothaman *et al.*, 2003, Wang *et al.*, 2006, Wang *et al.*, 2007, Ozeri *et al.*, 2001). In the case of M1-expressing strains, phosphorylation of paxillin is absolutely essential for efficient uptake processes. It provides additional docking sites for cytoskeletal proteins promoting cytoskeletal rearrangements (Wang *et al.*, 2007). In contrast to this, in SfbI/F1-mediated entry processes paxillin phosphorylation is also induced but does not seem to be necessarily required for SfbI/F1-mediated entry processes. Instead, Wang *et al* speculated that in SfbI-mediated uptake paxillin acts as a scaffold for additional signalling molecules such as the src family kinases (Wang *et al.*, 2007). Recruitment of src kinases causes the phosphorylation of caveolin-1 and the formation of membrane invaginations (Wang *et al.*, 2007). In addition, Ozeri and colleagues have observed involvement of the small GTPase Rac and Cd42 in internalization of SfbI/F1 expressing streptococci (Ozeri *et al.*, 2001).

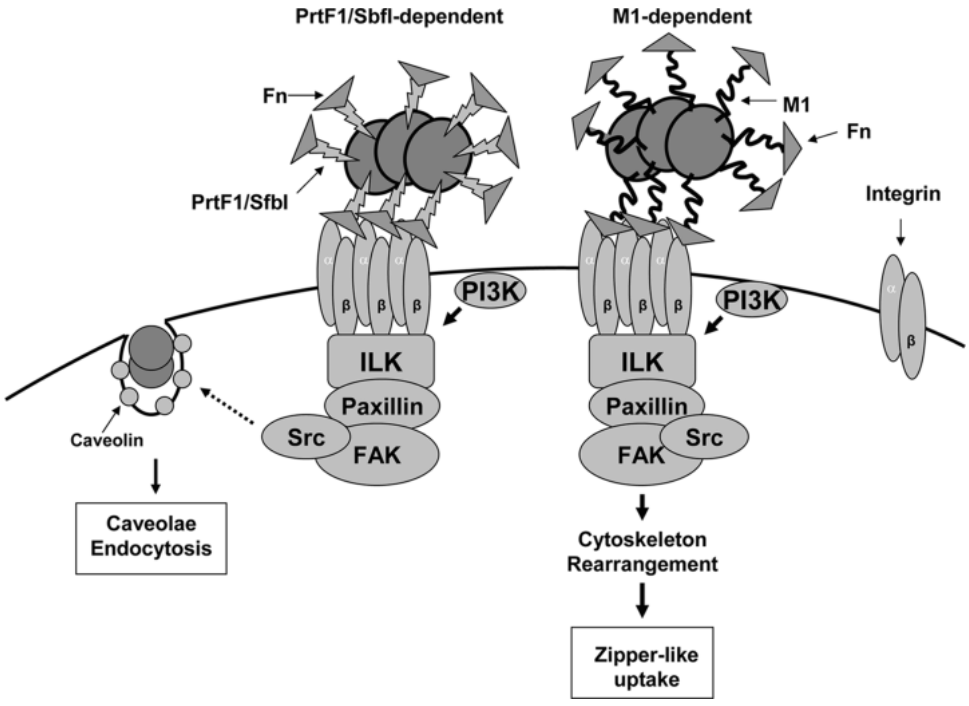

Figure 2: Schematic representation of signalling pathways and corresponding uptake processes initiated by M1- and SfbI/F1- expressing *S. pyogenes*

Both M1 and SfbI/F1 protein bind to soluble fibronectin and subsequently bind to $\alpha_5\beta_1$-integrins on the host cell surface. Integrin engagement triggers an intracellular signalling cascade including assembly and activation of PI3K, ILK, paxillin and FAK. In the case of M1-mediated entry signalling cascades lead to actin cytoskeletal rearrangements and zipper-like uptake of M1-expressing strains. SfbI/F1-mediated signalling pathways trigger caveolae formation via the phosphorylation of caveolin-1 by src family kinases and subsequent uptake of *S. pyogenes* by caveolae-mediated endocytosis (Taken from (Wang *et al.*, 2007)).

Initiation of different signalling cascades correlates with the observation of distinct uptake and intracellular trafficking processes of M1- and SfbI/F1-expressing streptococci. M1-mediated internalization is characterized by great cytoskeletal rearrangements of the host cell membrane. The re-organization of the cytoskeleton is accompanied with actin polymerization and actin recruitment to the site of streptococcal entry. Membrane microvilli and pseudopod-like structures are formed which tightly engulf invading streptococci resulting in zipper-like uptake of M1-expressing streptococci into epithelial cells. Following uptake, internalized streptococci reside within membrane-bound phagocytic vacuoles which are positive for the late endosomal/lysosomal marker protein 1 (Lamp-1) indicating trafficking along the classical endosomal pathway with subsequent lysosomal fusion (Dombek *et al.*, 1999). The association of streptococci containing vacuoles with Lamp-1 is in line with previous observations of Greco and colleagues who showed fusion of phagocytic compartments with lysosomes (Greco *et al.*, 1995).

In contrast, in SfbI-expressing strains co-operative binding of fibronectin results in the presentation of multiple RGD binding sites in fibronectin, thus, triggering integrin clustering and subsequent accumulation of small omega shaped cavities in the vicinity of attached streptococci (Rohde *et al.*, 2003). These cavities were identified as caveolae which have already been described as entry ports for other bacteria (e.g. FimH expressing *Escherichia coli*, *Chlamydia trachomatis*), viruses (e.g. echovirus, SV40 virus) as well as parasites (Shin *et al.*, 2001c, Shin *et al.*, 2001a, Shin *et al.*, 2001b, Baorto *et al.*, 1997, Norkin *et al.*, 2001, Marjomaki *et al.*, 2002, Pelkmans *et al.*, 2001). At later stages caveolae aggregate and fuse forming large invaginations enabling uptake of SfbI-expressing streptococci. Subsequently streptococci are incorporated into caveosomes which are positive for caveolin-1 but lack markers of the classical endocytic pathway like Lamp-1 and Rab7. In addition, neither acidification of caveosomes nor lysosomal fusion events are detectable. Thus, by co-opting caveloae-mediated endocytosis, SfbI-expressing streptococci bypass the classical endosomal/lysosomal pathway, prevent fusion with lysosome and thereby ensure protection from host cell defence mechanisms (Rohde *et al.*, 2003).

The development of diverse uptake mechanisms, in spite of the initiation of similar signalling pathways triggered by binding of M1/SfbI to fibronectin and subsequent engagement of integrins on the host cells surface, demonstrates the high variability of *S. pyogenes*. Wang *et al* hypothesized that different binding properties and binding affinities of M1 and SfbI to fibronectin might account for the initiation of distinct uptake mechanisms (Wang *et al.*, 2007). Furthermore, the expression of M1 and SfbI is tightly regulated. The M1 protein is expressed under high CO_2 conditions while SfbI is expressed in O_2-rich environments (Caparon *et al.*, 1992, Gibson *et al.*, 1995, Wang *et al.*, 2007). Thus, the initiation of different signalling and

uptake processes might favour streptococcal survival at different tissue sites under various host environmental conditions and at different stages of infection ensuring successful establishment of a disease (Wang *et al.*, 2007).

2.6 Streptococcal dissemination from the primary site of infection into deeper tissue

A pre-requisite for the development of an invasive disease is the ability of the pathogen to overcome tissue barriers. Breaks of the epithelial cell layer, for example as a consequence of physical injury, burns and viral infections, provide entry ports for the transition of *S. pyogenes* into deep tissue and, thus, constitute risk factors for the development of invasive diseases (Olsen *et al.*, 2009, Stevens, 2001). However, in a substantial number of cases invasive diseases develop in previously healthy individuals with no obvious port of entry. It has been suggested that the source of bacteria in these cases is a transient bacteremia originating from the oropharynx (Johansson *et al.*, 2010). The transition of *S. pyogenes* from the blood stream into deeper tissue requires its ability to overcome the endothelium of the blood vessel which is one of the strongest cellular barriers in the human body. Thus, the endothelial cell lining of the vascular system might possibly represent target cells for *S. pyogenes* invasion.

The endothelium constitutes the inner layer of the blood vessels of the entire vascular system within the human body (Figure 3). Endothelial cells form a continuous single layer lining the interior of the blood vessel wall thereby forming an active barrier between the blood and the underlying tissue, allowing selective transport of metabolites and nutrients (Sumpio *et al.*, 2002). In addition to its barrier function, it also plays a major role in the regulation of homeostasis, the modulation of blood flow and vessel tone, coagulation, fibrinolysis as well as angiogenesis and vasculogenesis (Sumpio *et al.*, 2002, Pries *et al.*, 2006). In immune reactions and inflammatory responses the endothelium regulates the extravasation of leukocytes from the blood stream into the tissue to the site of infection (Sumpio *et al.*, 2002).

Staali and colleagues have demonstrated that serotype M1 GAS ensures its survival within human PMNs by impairing fusion of azurophilic granules with phagosomes containing intracellular streptococci thereby avoiding intracellular killing (Staali *et al.*, 2003, Staali *et al.*, 2006). In addition, Medina and colleagues could re-isolate viable *S. pyogenes* from neutrophils after *in vivo* infection of mice (Medina *et al.*, 2003). The ability of neutrophils to move from the blood stream into tissue together with the observation of intracellular survival of *S. pyogenes* within neutrophils led the authors to hypothesise that *S. pyogenes* might exploit neutrophils as vehicles for the transport across the endothelium (Trojan horse theory), a process which facilitates dissemination into deeper tissue (Medina *et al.*, 2003). Recent studies have further highlighted the import role of the endothelium during the pathogenesis of

S. pyogenes deep tissue infections. Serotype M3 GAS has been shown to directly interact with and invade endothelial cells (Nerlich *et al.*, 2009). The fibronectin-binding protein FbaB has been identified as the endothelial cell invasin which mediates phagocytosis-like uptake of *S. pyogenes* into endothelial cells of the umbilical cord (Amelung *et al.*, 2011). It has been shown that after transcytosis viable serotype M3 GAS are released at the basement membrane via lysosomal exocytosis (Talay, unpublished data).

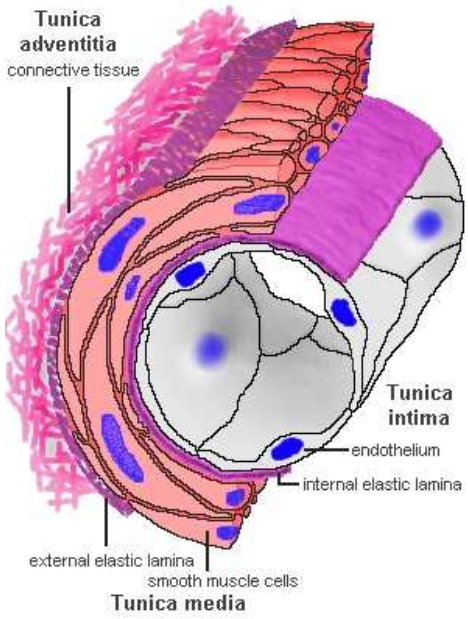

Figure 3: Schematic representation of the composition of a blood vessel

(http://www.siumed.edu/~dking2/crr/cvguide.htm)

2.7 Aim of the study

S. pyogenes has been the cause for severe life-threatening invasive infections including sepsis, necrotizing fasciitis and streptococcal toxic shock syndrome (Cunningham, 2000). Although various serotypes have been associated with these severe invasive infections, serotype M1 is frequently isolated from patients with necrotizing fasciitis (Stevens, 2001, Tart *et al.*, 2007). A pre-requisite for the development of invasive infections is the ability of the pathogen to disseminate from the primary site of infection, a process which requires crossing of cellular and tissue barriers, one of which is the endothelial cell lining of the blood vessels. Studies have already identified a role of invasion of endothelial cells in the pathogenesis of serotype M3 *S. pyogenes*. However, despite the well characterized interaction of the most invasive serotype M1 *S. pyogenes* with epithelial cells, nothing is known about its interaction with endothelial cells. Thus, the focus of this study is the characterization of the molecular interactions of tissue-invasive serotype M1 *S. pyogenes* with human endothelial cells of the umbilical cord. By using a complex *in vitro* infection model, i.e. the establishment of an artificial EC barrier model, the invasion potential, in particular the mode of internalization, intracellular trafficking as well as the mechanism of survival of serotype M1 GAS within endothelial cells was to be elucidated. The use of defined M1 GAS knock out mutants, heterologous expression of M1 GAS factors and blocking experiments aimed to identify relevant bacterial and host cell factors that determine endothelial cell interaction as well as underlying signalling cascades in endothelial cells.

3. Materials and Methods

3.1 Materials

3.1.1 Chemicals/solutions

Table 1: Chemicals and solutions used in this study

Chemical/solution	Company
10x coral load PCR buffer	Qiagen
5x phusion high fidelity PCR buffer	Thermo Scientific
6x loading dye (agarose gel electrophoresis)	Fermentas
Acetic acid	Merck
Acrylamide 30% (Rotiphorese Gel 30)	Roth
Agar-Agar, Kobe I	Roth
Agarose Broad range (NEEO Ultra quality)	Roth
Ammoniumpersulfate (APS)	Serva
Ampicillin	Applichem
Bacto™ Tryptic Soy Broth (TSB)	Becton Dickinson
Bacto™ Tryptone	Becton Dickinson
Bacto™ Yeast Extract	Becton Dickinson
BAPTA-AM	Calbiochem
Bovine serum albumin (BSA)	Sigma Aldrich
Bromophenol blue	Sigma Aldrich
Calcium chloride ($CaCl_2$)	Merck
Calphostin C	Enzo
Chloroform	Sigma Aldrich

Colloidal gold nanoparticles	BBInternational
Columbia blood agar plates	Becton Dickinson
Coomassie Brilliant Blue R-250	Sigma Aldrich
Cu grids	Plano
Difco™ M17 broth	Becton Dickinson
Dimethylsulfoxid (DMSO)	Sigma Aldrich
Di-sodiumhydrogenphosphat (Na_2HPO_4)	Merck
dNTPs	Fermentas
Edelfosine (ET-18-OCH3)	Calbiochem
Erythromycin	Sigma Aldrich
Ethanol	J. T. Baker
Ethidium bromide	Applichem
Ethylenediaminetetraacetic acid (EDTA)	Gibco
Fetal calf serum (FCS)	PAA
Gelatine	Sigma Aldrich
Gene ruler™ DNA ladder mix, 100-1000 bp	Fermentas
Gentamycin	Sigma Aldrich
Glucose	Roth
Glutaraldehyde 25%	Merck
Glutathion S-Transferase (GST) protein	Abcam
Glycerol	Roth
Glycine	Roth
HEPES-BSS	Promocell
Immersol 518N	Zeiss

Isopropyl alcohol	Merck
Isopropyl β-D-1-thiogalactopyranoside (IPTG)	Applichem
Kanamycin	Roth
Lactose	Roth
LysoTracker® Red DND-99	Invitrogen
Lysozyme	Sigma
Magnesium chloride ($MgCl_2$)	Qiagen
Manganese chloride	Riedel-de Haën
Methanol	J. T. Baker
MOPS (3-(N-morpholino)propanesulfonic acid)	Roth
Mutanolysine	Sigma
Osmium tetroxide 1%, aqueous	Roth
Page Ruler™ Plus Pre-stained Protein Ladder	Fermentas
Paraformaldehyde (PFA) solution, 4% in PBS	USB Corporation
Pb citrate (ultrastain 2)	Leica
Penicillin G	Sigma Aldrich
Penicillin/Streptomycin	Pan Biotech GmbH
Paraformaldehyde, 25% in H_2O	Sigma Aldrich
Phusion® Hot Start II High fidelity DNA Polymerase	Thermo Scientific
Potassium acetate (KAc)	Sigma
Potassium carbonate (K_2CO_3)	Merck
Potassium chloride (KCl)	Riedel- de Haën
Potassium dihydrogenphosphate (KH_2PO_4)	Roth
ProLong® Gold antifade reagent	Invitrogen

ProLong® Gold antifade reagent with DAPI	Molecular probes
Proteinase K	Fluka
RNase (DNase-free)	Applichem
Roti®-Phenol	Roth
Rubidium chloride	Applichem
Saponin	Fluka
Sodium acetate	Fluka
Sodium chloride (NaCl)	Roth
Sodium dodecyl sulphate (SDS)	Sigma Aldrich
Sodium hydroxide (NaOH)	Merck
Spectinomycin	Sigma Aldrich
Spurr resin	Sigma/Fluka
Sucrose	Fluka
T4 DNA ligase	New England Biolabs
Taq DNA polymerase	Qiagen
TEMED	Biorad
Todd Hewitt Broth (THB)	Roth
Tris	Sigma Aldrich
Triton-X-100	Sigma Aldrich
Trizma Base	Sigma Aldrich
Trypsin/EDTA	Promocell
Tween 20	Applichem
Uranyl acetate (Uac) 4%, (w/v)	Serva
β-mercaptoethanol	Serva

3.1.2 Expendable material

Table 2: Expendable material used in this study

Material	Company
Cell culture insert, transparent PET membrane, 24 well (0.4 µm and 3.0 µm pore size)	Becton Dickinson
Cell Star® 15 ml tubes	Greiner bio-one
Cell Star® 50 ml tubes	Greiner bio-one
Coverslips (ø 12 mm)	Thermo Scientific
Cryo tube™ vial	Nunc™
Cuvettes polystyrene 10x 4x 45 mm	Sarstedt
Electroporation cuvettes, 2 mm electrode gap	Peqlab Biotechnologie GmbH
Gelatine capsules, operculatae No.2	Pharmapol
Latex beads (ø 3 µm)	Sigma Aldrich
Micro tube 1.5 ml	Sarstedt
Microscope slides 76x 26 mm	Thermo Scientific
PCR tubes 0.2 ml	Starlab
Petri dish	Greiner bio-one
Safe seal micro tube 2 ml	Sarstedt
Servpor® dialysis tubing (MWCO 12-14000)	Serva
TPP Tissue culture dish 100, growth area 60.1 cm^2	Sigma Aldrich
TPP Tissue culture test plate 24 well	Sigma Aldrich
TPP Tissue culture test plate 96 well	Sigma Aldrich

3.1.3 Instruments

Table 3: Instruments and equipment used in this study

Instrument	Company
Agarose gel chambers	Horizon™ 58
Autoclave-steam sterilizer	Biomedis
Biofuge primo	Heraeus
CellZscope®	Nano Analytics
Centrifuge 5417R	Eppendorf
Centrifuge 5804R	Eppendorf
CO_2 water jacketed incubator	Forma Scientific
Critical point dryer (CPD030, CPD300)	BalTec, Leica
Cryo 1℃ freezing container	Nalgene™
FACS Calibur BD	Becton Dickinson
FESEM DSM 982 Gemini	Zeiss
FESEM Merlin	Zeiss
French® pressure cell press (SLM Aminco, 40.000 PSI)	Thermo Fisher
Gene Pulser™ and pulse controller	BioRad
HERA Cell 150i CO_2 Incubator	Thermo Scientific
Incubator Kelvitron®	Heraeus Instruments
Infors HT multitron shaking incubator	Tuttnauer
Kodak IS2000R gel documentation unit	Intas
Megafuge 1.0	Heraeus
Microwave Pro 825	Whirlpool

Mini Protean II™ system	BioRad
Nano Drop®	Thermo Scientific
Novaspec II spectophotometer	Amersham Pharmacia Biotech
pH-meter 766	Calimatic Knick
Power pack 200	BioRad
Power pack 300	BioRad
Roller mixer SRT6	Stuart
Rotor TLA 100.2	Beckmann
Shaking device Unimax 2010	Heidolph Instruments
Sorvall® RC 6 Plus, rotor SLA-3000	Thermo Electron Corporation
Sorvall® RC 6 Plus, rotor SS-34	Thermo Electron Corporation
Special accuracy weighing machine AE 260 Delta Range®	Mettler
Sputter coater SCD 500	BalTec
TEM EM 910	Zeiss
Thermocycler	Biometra
Thermomixer Comfort	Eppendorf
Transferpette® S-8 (multichannel pipet)	Brand
Ultra centrifuge TL-100	Beckmann
Ultramicrotome, Reichert ultracut	Leica
Ultratrimm, Reichert	Leica
UV-transilluminator	Herolab UVT 2020
Vortex Genie 2™	Bender + Hobein AG
Wallac 1470 Wizard gamma counter	Perkin Elmer
Waterbath	GFL

Weighing machine PC 2000	Mettler
Zeiss Axio Cam MRm camera	Zeiss
Zeiss Axio Imager A2	Zeiss
Zeiss AxioCam HRc digital camera	Zeiss
Zeiss Axiophot	Zeiss
Zeiss Microscope ID03	Zeiss

3.1.4 Oligonucleotides

Table 4: Oligonucleotides used in this study

Name	Sequence 5'-3'	Annotation/ reference
	Primer for amplification of *emm1* (complementation of M1 knock out mutant)	
M1_fwd_*KpnI*	GCGGTACCCCTGAAAATGAGGGTTTCTTC	*KpnI* restriction site
M1_rev_*XbaI*	GCGTCTAGAACTCCTTAACCTCATTCTTCTATAC	*XbaI* restriction site
	Primer for amplification of *emm1* (expression of recombinant M1-HIS fusion protein)	
His_M1_fwd	GCCGCCATGGGATTAAAAACAGGAACGGCTTC AGTAGCG	*NcoI* restriction site
His_M1_rev	GCCGGGATCCCTGTCTCTTAGTTTCCTTCATTG GTGC	*BamHI* restriction site

Name	Sequence 5'-3'	Annotation/ reference
	Primer for colony PCR and sequencing of pDC_{erm}	
pDC_MCS_fw	GCCATACCACAGATGTTCCA	provided by S. Amelung (HZI, Braunschweig)
pDC_MCS_rev	GCTTTTTCAGATTCAGTTGCCTTC	provided by S. Amelung (HZI, Braunschweig
	Primer for colony PCR and sequencing of pQE60	
pQE60_5'	CCGTGAGCGGATAACAATTTCACACAGGG	provided by K. Branitzki-Heinemann (HZI, Braunschweig)
pQE60_3'	CCGATGGAGTTCTGAGGTCATTACTGGGG	provided by K. Branitzki-Heinemann (HZI, Braunschweig)
	Primer for 16s RNA sequencing	
16s_fwd	AGAGTTTGATCCTGGCTC	provided by A. Babbar (HZI, Braunschweig)
16s_rev	GGTTACTTGTTACGACTT	provided by A. Babbar (HZI, Braunschweig)

3.1.5 Antibodies

Table 5: Primary antibodies used in this study

Antibody/serum	Dilution immunofluorescence	Source/company
Rabbit anti-*S. pyogenes* serum, polyclonal (anti-GAS)	1:100	(Molinari *et al.*, 1997)
Rabbit anti-*Lactococcus lactis* serum	1:100	Kindly provided by Dr. S. Talay (HZI, Braunschweig)
Mouse anti-human beta 1 integrin labelling antibody (MAB 2079Z)	5 µg/well	Chemicon International
Mouse anti-human beta 1 integrin blocking antibody (MAB 1987Z)	1:100	Millipore
Mouse anti-human alpha 1 integrin blocking antibody (MAB 1973Z)	1:100	Chemicon International
Mouse anti-human alpha 2 integrin blocking antibody (MAB 1950Z)	1:100	Chemicon International
Mouse anti-Arp2/3 (p16 #323H3)	1:50	Kindly provided by Dr. C. Erck (Research Group Cellular Proteome Research, HZI, Braunschweig)
Mouse anti-human CD107a (Lamp-1)	1:50	BD Pharmingen™
Rabbit anti-GST (ab 9085)	1:100	Abcam
Rabbit anti-M1	1:100	Kindly provided by Dr. S. Talay (HZI, Braunschweig)
ALEXA Fluor® 488 phalloidin	1:100	Invitrogen
ALEXA Fluor® 568 phalloidin	1:100	Invitrogen

Table 6: Secondary antibodies used in this study

Antibody	Dilution	Source/company
ALEXA Fluor® 488 goat-anti-rabbit IgG (H+L)	1:200	Invitrogen
ALEXA Fluor® 568 goat-anti-rabbit IgG (H+L)	1:300	Invitrogen
ALEXA Fluor® 488 goat-anti-mouse IgG (H+L)	1:200	Invitrogen

3.1.6 Vectors

Table 7: Vectors used in this study

Vector	Vector size	Selection conditions	Reference/source
pDC_{erm}	4690 bp	500 µg ml^{-1} erythromycin	Kindly provided by Prof. V. Nizet, UCSD, San Diego
pQE60	3431 bp	100 µg ml^{-1} ampicillin	Qiagen

3.1.7 Restriction endonucleases

All enzymes and corresponding enzyme buffers were purchased from New England Biolabs.

3.1.8 Antibiotics

Table 8: Antibiotics used in this study

Name	Application	Final concentration	Source/company
Ampicillin	Culturing of *Escherichia coli* (*E. coli*) carrying pQE60 and its derivatives	100 µg ml^{-1}	Applichem
Erythromycin	*E. coli* carrying pDC_{erm} and its derivatives	500 µg ml^{-1}	Sigma Aldrich
	S. pyogenes carrying pDC*erm* derivatives	2 µg ml^{-1}	
	Lactococcus lactis (*L. lactis*) carrying pLM1 or pP59	5 µg ml^{-1}	
Gentamycin	Killing of extracellular bacteria during survival assays	100 µg ml^{-1}	Sigma Aldrich
Kanamycin	Culturing of *E. coli* M15	25 µg ml^{-1}	Roth
	Culturing of *S. pyogenes* mutant strain A528	150 µg ml^{-1}	
Penicillin G	Killing of extracellular bacteria during survival assays	5 µg ml^{-1}	Sigma Aldrich
Penicillin/Streptomycin	Cell culture	100 U Penicillin/ml 0.1 mg Streptomycin/ml	PAN™ Biotech GmbH
Spectinomycin	Culturing of *S. pyogenes* mutant strains A585 and A591	80 µg ml^{-1}	Sigma Aldrich

3.1.9 Kits

Table 9: Kits used in this study

Kit	Company
QIAprep® Spin Miniprep Kit	Qiagen
PCR Extract & Gel Extract Mini Kit	5Prime
QIAquick PCR Purification Kit	Qiagen
Protino® Ni-TED 150 Purification of polyhistidine-tagged proteins Kit	Macherey-Nagel
Live/Dead® Baclight™ Bacterial Viability Kit	Invitrogen

3.1.10 Buffers

Table 10: Buffers used in this study

10x PBS	
NaCl	80 g
KCl	2 g
$Na_2HPO_4 \cdot 2H_2O$	7.6 g
KH_2PO_4	2 g
Adjust pH 7.4 with NaOH	
dH_2O	*ad* 1 l

Autoclave 15 min at 121℃.

1x PBS	
10x PBS (pH 7.4)	100 ml
dH_2O	*ad* 1 l

PBST	
PBS	
Tween 20	0.05% (v/v)

Tris/EDTA buffer (TE), **10 mM Tris/0,1 mM EDTA**	
1M Tris pH 7.5	2.5 ml
0.5 M EDTA pH 8.0	50 µl
MQ H_2O	*ad* 250 ml

3.2 Bacterial strains, media and culture conditions

3.2.1 Bacterial strains

Table 11: *S. pyogenes* strains used for infection studies, survival assays and cloning

Strain	Serotype	Phenotype	Origin/condition	Reference/source
S. pyogenes A527 (KTL3)	M1	wild type	Blood isolate	Strain collection Department of Medical Microbiology, HZI, Braunschweig
S. pyogenes A302 (SF370)	M1	wild type	Genome sequenced M1 *S. pyogenes* strain; wound isolate	Strain collection Department of Medical Microbiology, HZI, Braunschweig; (Ferretti *et al.*, 2001)
S. pyogenes A270 (CanA)	M1T1	wild type	Blood isolate	Strain collection Department of Medical Microbiology, HZI, Braunschweig
S. pyogenes A271 (CanB)	M1T1	wild type	Blood isolate	Strain collection Department of Medical Microbiology, HZI, Braunschweig
S. pyogenes A766 (90-226)	M1	wild type	Blood isolate	(Cue *et al.*, 1997)
S. pyogenes A767 (90-226 Δ*emm1*)	M1	ΔM1	Blood isolate	(Zimmerlein *et al.*, 2005)
S. pyogenes complemented ΔM1 A767 M1pDC$_{erm}$ (clone 2-4)	M1	ΔM1/M1 complemented	2 µg ml^{-1} erythromycin	This study

Strain	Serotype	Phenotype	Origin/condition	Reference/source
S. pyogenes A528 (KTL3 *grab* ko)	M1	ΔGRAB	150 µg ml^{-1} kanamycin	Strain collection Department of Medical Microbiology, HZI, Braunschweig
S. pyogenes A585 (KTL3 *prtS*::*spc*)	M1	ΔPrtS	80 µg ml^{-1} spectinomycin	Strain collection Department of Medical Microbiology, HZI, Braunschweig
S. pyogenes A591 (KTL3 *slo*::*spc*)	M1	ΔSLO	80 µg ml^{-1} spectinomycin	Strain collection Department of Medical Microbiology, HZI, Braunschweig
S. pyogenes A592 (KTL3 pJRS 233-Δ*sagA*)	M1	ΔSagA	1 µg ml^{-1} erythromycin	Strain collection Department of Medical Microbiology, HZI, Braunschweig

Table 12: *E. coli* strains used for protein biochemical studies

Strain	Plasmid	Insert	Culture conditions	Reference/source
E. coli DH5α	-	-	-	Strain collection Department of Medical Microbiology, HZI, Braunschweig
E. coli Top 10	pQE60	-	100 µg ml^{-1} ampicillin	Qiagen
E. coli MC1061	pDC_{erm}	-	500 µg ml^{-1} erythromycin	Provided by Prof. V. Nizet, UCSD, San Diego
E. coli DH5α	pDC_{erm}	*emm1*	500 µg ml^{-1} erythromycin	This study

Strain	Plasmid	Insert	Culture conditions	Reference/source
E. coli M15 pRep4	-	-	25 µg ml^{-1} kanamycin	Qiagen
E. coli M15 pRep4	pQE60	*emm1*	100 µg ml^{-1} ampicillin and 25 µg ml^{-1} kanamycin	This study

Table 13: *L. lactis* strains used for infection studies

Strain	Plasmid	Insert/characteristics	Culture conditions	Reference
L. lactis	pLM1	Replacement of *emm6* within pVE5508 with *emm1* (pLM1)	5 µg ml^{-1} erythromycin; 30℃	(Cue *et al.*, 2001)
L. lactis	pP59	Deletion of emm6 from pVE5508	5 µg ml^{-1} erythromycin; 30℃	(Cue *et al.*, 2001)

3.2.2 Bacterial culture media

Prior to usage media were sterilized by autoclaving in a steam sterilizer for 15 min at 121℃ and 1 bar high pressure. For cultivation of bacteria on agar plates 16 g of agar were added per litre of medium prior to autoclaving.

Table 14: Media used for the cultivation of *S. pyogenes* strains

TSB broth	
Tryptic Soy Broth	30 g
dH_2O	*ad* 1 l

THB broth	
Todd Hewitt Broth	30 g
dH_2O	*ad* 1 l

THY broth	
Todd Hewitt Broth	30 g
Bacto™ Yeast Extract	5 g
dH_2O	*ad* 1 l

TSBY broth	
Tryptic Soy Broth	30 g
Bacto™ Yeast Extract	5 g
dH_2O	*ad* 1 l

Table 15: Media used for the cultivation of *E. coli* strains

Luria Bertani medium (LB)	
Bacto™ Tryptone	10 g
NaCl	10 g
Bacto™ Yeast Extract	5 g
dH_2O	*ad* 1 l

Table 16: Media used for the cultivation of *L. lactis* strains

M17 medium	
Difco™ M17 broth powder	37.25 g
dH_2O	950 ml
Heat with frequent agitation	
Boil 1 min to completely dissolve the powder	
Autoclave 15 min at 121℃	
Cool to 50℃	
10% Lactose	50 ml

3.2.3 Cultivation of bacterial strains and culture conditions

S. pyogenes strains were cultured in TSB medium and supplemented with antibiotics if needed (see Table 8). Bacterial were cultured in a Falcon tube with the lid slightly opened. Cultivation was carried out overnight at 37℃, 5% CO_2 without agitation. For isolation of chromosomal DNA from GAS, bacteria were grown in THY medium overnight at 37℃, 5% CO_2 in a Falcon tube with the lid slightly opened. For the preparation of competent GAS as well as transformation, GAS were grown in TSBY medium or were plated on TSBY agar plates. *E. coli* strains were routinely grown in LB medium in the presence of antibiotics where appropriate (see Table 8, Table 12) overnight at 37℃ shaking (120 rpm). To prepare competent *E. coli* cells bacteria were grown in SOB medium at 37℃ with agitation. *L. lactis* strains were cultured in M17 medium supplemented with 0.5% glucose and 5 µg ml^{-1} erythromycin at 30℃ without agitation. For long term storage of bacteria 750 µl overnight cultures of GAS cultured in THY medium, *E. coli* grown in LB medium and *L. lactis* cultivated in M17 + 0.5% glucose were mixed with 250 µl sterile glycerol. Stocks were stored at -80℃.

3.3 Molecular biological techniques

3.3.1 Isolation of chromosomal DNA from *S. pyogenes* and *L. lactis*

For isolation of chromosomal DNA from *S. pyogenes* an overnight culture in 100 ml THY medium was inoculated (37°C, 5% CO_2). *L. lactis* strains were cultured in M17 medium containing 0.5% glucose. On the following day bacterial cultures were centrifuged for 10 min at 10000 rpm and the pellet was resuspended in 3 ml sucrose/TES-buffer. Afterwards 1 ml lysozyme (5 mg/ml) and 100 µl mutanolysine (5000 U/ml) were added and the suspension was incubated for 1 h at 37°C. Following addition of 100 µl RNase (5 mg/ml) and incubation for 15 min at 37°C, 500 µl of proteinase K (5 mg/ml) were added and samples were incubated for 15 min at 37°C. After the addition of 500 µl 10% sarcosyl/250 mM EDTA-buffer, the tubes were inverted gently and incubated for 1 h at 37°C. Subsequently 2 ml of phenol were added, the samples were mixed and centrifuged for 10 min at 4000 rpm. The upper aqueous phase was removed and transferred to a new eppendorf tube. 2 ml of phenol/chloroform (25:24) were added and the sample was centrifuged for 10 min at 12000 rpm. The supernatant, which contains the DNA, was removed carefully and mixed with 1/10 of the volume of 3M NaAc and 1 volume of isopropanol and precipitated 1 h at room temperature or overnight at -20°C. Following precipitation, the sample was centrifuged for 10 min at 12000 rpm. The supernatant was removed and the pellet was washed with 70% ice cold ethanol. Following a final centrifugation step (5 min at maximum speed), ethanol was removed and the pellet was air dried at room temperature. The dry pellet was then resuspended in 500 µl TE-buffer and analysed by agarose gel electrophoresis (see section 3.3.3).

Table 17: Buffers and solutions used for isolation of chromosomal DNA

TES-buffer (Tris/EDTA/saline-buffer), pH 8.0
50 mM Tris-HCl
5 mM EDTA
10 mM NaCl

TE-buffer (Tris/EDTA buffer), pH 8.0 **10 mM Tris/0,1 mM EDTA**	
1M Tris pH 7.5	2.5 ml
0.5 M EDTA pH 8.0	50 µl
MQ H_2O	*ad* 250 ml

Sucrose-TES
20% sucrose in TES-buffer, pH 8.0

RNase
5 mg/ml in TES-buffer (boil for 15 min to inactivate residual DNase)

Sarcosyl solution
10% sarcosyl in 250 mM EDTA

3.3.2 Isolation of plasmid DNA

Plasmid DNA from *E. coli* was isolated with the QIAprep® Spin Miniprep kit according to the manufacturer's protocol. DNA was eluted in MQ H_2O and stored at -20℃ until used. Isolated plasmid DNA was analysed by agarose gel electrophoresis (see section 3.3.3).

3.3.3 Agarose gel electrophoresis

Agarose gel electrophoresis is used for qualitative and quantitative analysis of DNA molecules, for example after plasmid DNA isolation or to analyse fragment sizes after restriction digest or polymerase chain reaction. It is based on the migration of different sized DNA fragments in an electric field. Small DNA molecules run faster through a mesh of 1% agarose than larger molecules and this allows the separation of DNA fragments according to their sizes. Samples were mixed with 6x loading dye and separated in a 1% (w/v) agarose gel (in 1x TAE buffer) for 30 min at 120 V. 1x TAE buffer was used as running buffer. Gene

Ruler™ DNA ladder mix served as a molecular weight standard. Following gel electrophoresis, gels were incubated in an ethidium bromide solution (1 µg/ml in H_2O) for 10 min. DNA bands were then visualised with an UV-transilluminator and a Kodak IS2000R gel documentation unit (Intas).

Table 18: Buffers and solutions used for gel electrophoresis

50x TAE	
Trizma base	242 g
Acetic acid	51.12 ml
EDTA (0.5 M, pH 8)	100 ml
dH_2O	*ad* 1 l

1x TAE	
50x TAE	20 ml
dH_2O	*ad* 1 l

1% (w/v) agarose	
Agarose	1 g
1x TAE	100 ml
Boil until agarose is completely melted	

3.3.4 Polymerase chain reaction (PCR)

Polymerase chain reaction is used for *in vitro* amplification of defined DNA fragments and was described by Mullis and Faloona 1987 (Mullis *et al.*, 1987). PCR is a cyclic reaction in which the DNA template is amplified exponentially. It encompasses the steps denaturation, annealing of short oligonucleotides (primers) and the synthesis of new DNA fragments by a polymerase (elongation).

3.3.4.1 Standard PCR

The amplification of the *emm1* gene of *S. pyogenes* was performed in a Thermocycler according to the standard PCR protocol described below (see Table 19, Table 20). For standard PCR the Phusion high fidelity polymerase was used.

Table 19: Standard PCR protocol

10-100 ng	Template DNA
10 µl	5x Phusion PCR buffer
5 µl	dNTPs [2 mM]
1 µl	forward primer [10 pmol/µl]
1 µl	reverse primer [10 pmol/µl]
0.5 µl	Phusion high fidelity DNA polymerase [2 U/µl]
ad 50 µl	MQ H_2O

Table 20: Standard PCR program

95℃	2:00 min	Denaturation	
95℃	0:30 min	Denaturation	⎫
T_A℃	0:30 min	Annealing	⎬ 25x
72℃	T_E min	Elongation	⎭
72℃	5:00 min	Final polymerisation	
4℃	∞		

T_A: Annealing temperature, primer specific

T_E: Elongation time, dependent on the processivity of the polymerase used (Phusion polymerase ~1 kb/30 sec, Taq polymerase ~1 kb/1 min)

3.3.4.2 16s RNA sequencing

To verify the provided *L. lactis* strains, 16s RNA was sequenced using a PCR based method. Chromosomal DNA from *L. lactis* was isolated as described above (see 3.3.1) and served as a template for PCR.

Table 21: 16s RNA PCR protocol

10-100 ng	Template DNA
2 µl	10x PCR buffer
0.5 µl	dNTPs [2 mM]
0.5 µl	forward primer [10 pmol/µl]
0.5 µl	reverse primer [10 pmol/µl]
0.2 µl	Taq DNA polymerase [3 U/µl]
ad 20 µl	MQ H_2O

Table 22: 16s RNA PCR program

94℃	5:00 min	Denaturation	
94℃	0:30 min	Denaturation	⎫
54℃	0:45 min	Annealing	⎬ 27x
72℃	0:45 min	Elongation	⎭
72℃	10:00 min	Final polymerisation	
4℃	∞		

3.3.4.3 Colony PCR

Using the colony PCR method positive bacterial clones, carrying the desired insert after transformation, were identified. A single bacterial colony was resuspended in 15 µl MQ H_2O. Subsequently samples were boiled for 10 min at 95℃ to lyse bacteria and to release the DNA. 5 µl of this bacterial suspension was then used as template for PCR. PCR was performed according to the protocol described below (Table 23) using the standard PCR program (Table 20).

Table 23: Colony PCR protocol

5 µl	Template DNA
5 µl	10x CL PCR buffer
5 µl	$MgCl_2$
5 µl	dNTPs [2 mM]
1 µl	forward primer [10 pmol/µl]
1 µl	reverse primer [10 pmol/µl]
0.5 µl	Taq DNA polymerase [5 U/µl]
ad 50 µl	MQ H_2O

Following PCR, 5 µl of the samples were mixed with 1 µl of 6x loading dye and analysed by agarose gel electrophoresis (see 3.3.3).

3.3.5 Purification of PCR products and restriction digests

PCR products and restriction digests were purified using the PCR Extract Mini Kit or the QIAquick PCR Purification Kit according to the manufacturer's protocol. Samples were eluted in 30 µl of MQ H_2O.

3.3.6 Digestion of DNA with restriction endonucleases

PCR amplification products and plasmid DNA vectors were digested with specific restriction endonucleases. Restriction digests were performed using the protocol stated below (Table 24) for 3 h, or alternatively overnight, at 37℃. Afterwards samples were purified with the QIAquick PCR Purification Kit and either directly used for ligation or stored at -20℃.

Table 24: Standard restriction digest protocol

20 µl	DNA (purified PCR product or plasmid DNA)
5 µl	10x NEB buffer
5 µl	10x BSA
1 µl	Restriction endonuclease I [20 U/µl]
1 µl	Restriction endonuclease II [20 U/µl]
ad 50 µl	MQ H_2O

3.3.7 Ligation of DNA fragments

Ligation is a method in which a free 3'-hydroxygroup of one DNA strand is covalently linked to a free 5'-phosphate group of a second DNA strand resulting in a continuous DNA double strand. This reaction is catalysed by T4 ligase and is dependent on ATP. Ligation of digested PCR amplification products and vectors was performed overnight at 16℃ according to the protocol described below (Table 25). Following ligation, samples were either directly used for transformation of competent bacteria or stored at -20℃.

Table 25: Ligation protocol

1 µl	Vector
6 µl	Insert
2 µl	10x T4-Ligase buffer
1 µl	T4 DNA Ligase [400 U/µl]
ad 20 µl	MQ H_2O

3.3.8 Transformation of bacteria

3.3.8.1 Preparation of competent E. coli

E. coli DH5α and *E. coli* M15 pRep4 were grown in SOB medium overnight at 37℃ and 120 rpm agitation. On the following day bacterial cultures were diluted 1:100 in fresh SOB medium and incubated at 37℃ with agitation until exponential growth phase (OD_{578nm} 0.4-0.6). Bacterial cultures were collected and cooled on ice for 15 min followed by centrifugation for 10 min at 5000 rpm (4℃). The bacterial pellet was resuspended in 15 ml Tfb1 and again centrifuged for 10 min (as above). After removal of the supernatant, the bacterial pellet was resuspended in 4 ml Tfb2 und cooled for 15 min on ice. Competent bacteria were distributed in pre-cooled eppendorf tubes, immediately shock-frozen in liquid nitrogen and stored at -80℃.

Table 26: Buffers and media used for preparation of competent *E. coli*

SOB medium	
20 g	Bacto™ Tryptone (= 2%)
5 g	Bacto™ Yeast Extract (= 0.5%)
0.6 g	NaCl (= 10 mM)
2.5 ml	1M KCl (= 2.5 mM)
ad 1 l dH_2O	

TfbI	
588.84 mg	Potassium acetate (= 30 mM)
2.4 g	Rubidium chloride (= 100 mM)
294 mg	Calcium chloride (= 10 mM)
1.62 g	Manganese chloride (= 50 mM)
30 ml	Glycerol
ad 200 ml dH_2O	
Adjusted to pH 5.8, sterile filtered and stored at 4℃	

TfbII	
46.24 mg	MOPS (= 10 mM)
220.53 mg	Calcium chloride (= 74 mM)
24.184 mg	Rubidium chloride (= 10 mM)
3 ml	Glycerol
ad 20 ml dH_2O	
Adjusted to pH 6.5,	
sterile filtered and stored at 4℃	

3.3.8.2 Transformation of competent E. coli

10 µl ligation reaction were carefully mixed with 50 µl competent *E. coli* and incubated for 30 min on ice which allows adsorption of DNA to the bacterial cell surface. Afterwards samples were subjected to a heat shock (90 sec at 42℃). Following heat shock, samples were incubated with 250 µl LB medium for at least 1 h at 37℃ shacking (120 rpm). Bacterial cultures were then selected on LB agar containing antibiotics. Bacterial colonies carrying the desired insert were analysed by colony PCR (see 3.3.4.3). To verify the right DNA sequence of the insert, plasmid DNA was isolated (see 3.3.2) and send for DNA sequencing (Department of Genome Analytics, HZI, Braunschweig).

3.3.8.3 Preparation of competent S. pyogenes

In order to prepare competent *S. pyogenes*, strain ΔM1 GAS (A767) was grown in TSBY medium overnight at 37℃ and 5% CO_2. On the following day the overnight culture was diluted 1:10 in fresh TSBY medium containing 1% glycine and further incubated at 37℃ until OD_{600nm} 0.1-0.2 was reached. Following centrifugation (10 min at 5000 rmp, 6℃), the bacterial pellet was washed twice with 25 ml ice-cold MQ H_2O and resuspended in 2 ml ice-cold MQ H_2O. After a final centrifugation step (2 min, 13.000 rpm) the bacterial pellet was resuspended in 1 ml ice-cold MQ H_2O. Competent *S. pyogenes* were then directly used for transformation.

3.3.8.4 Transformation of competent S. pyogenes

For transformation of competent *S. pyogenes*, 200 µl competent cells were carefully mixed with 5 µl plasmid DNA and incubated on ice for 30 min. After electroporation at 1.6 kV, 200 Ω using the Gene Pulser™ system, 10 ml pre-warmed TSBY medium was added and cultures were incubated for at least 4 h at 37°C and 5% CO_2. Following incubation, cultures were filled up to 50 ml with TSBY medium and incubated in the presence of 1 µg ml^{-1} erythromycin overnight at 37°C and 5% CO_2. On the following day cultures were collected by centrifugation (10 min at 5000 rmp). The bacterial pellet was resuspended in 1 ml TSBY and plated on TSBY agar containing 2 µg ml^{-1} erythromycin. Plates were incubated for 24-48 h at 37°C and 5% CO_2. Bacterial colonies carrying the desired insert were analysed by colony PCR (see 3.3.4.3).

3.4 Cloning techniques

3.4.1 Complementation of the *S. pyogenes* M1 knock out mutant

The full length *emm1* gene (including 51 nucleotides upstream of the start codon and 84 nucleotides downstream from the stop codon) was amplified according to the standard PCR protocol using chromosomal DNA of M1 GAS strain SF370 as template (see 3.3.1 and 3.3.4.1). The primer pair M1_fwd_*KpnI* and M1_rev_*XbaI* was used for amplification (Table 4). The *emm1* gene was then cloned into the *KpnI* and *XbaI* restriction sites of the shuttle vector pDC_{erm} (Jeng *et al.*, 2003) and the resulting plasmid $M1pDC_{erm}$ transformed into *E. coli* DH5α (see 3.3.8.1 and 3.3.8.2). Transformants were selected on LB agar plates containing 500 µg ml^{-1} erythromycin. Positive clones were confirmed by colony PCR (see 3.3.4.3), restriction enzyme analysis and DNA sequencing (Department of Genome Analytics, HZI, Braunschweig). Plasmid DNA was then subcloned into electro-competent *S. pyogenes* ΔM1 90-226 (A767), transformants (complemented ΔM1 GAS A767 $M1pDC_{erm}$ clone 2-4) were selected on TSBY agar plates containing 2 µg ml^{-1} erythromycin (see 3.3.8.3 and 3.3.8.4). The presence of the *emm1* gene was verified by colony PCR (see 3.3.4.3). Surface expression of the M1 protein was assessed by immunofluorescence staining using a M1 specific primary antibody and a fluorescently labelled secondary antibody (see 3.5.8).

3.4.2 Generation of recombinant M1 protein

In order to express C-terminally 6x Histidine tagged recombinant M1 protein in *E. coli*, the *emm1* gene, omitting the sequence of the signal peptide and the membrane anchor, was cloned into the *NcoI* and *BamHI* restriction sites of the plasmid pQE60. Chromosomal DNA from GAS strain SF370 and the primer pair His_M1_fwd and His_M1_rev were used for amplification (see 3.3.1, 3.3.4.1 and Table 4). The resulting plasmid M1pQE60 was transformed into *E. coli* M15pRep4 and transformants were selected on LB plates containing 100 µg ml^{-1} ampicillin and 25 µg ml^{-1} kanamycin (see 3.3.8.1 and 3.3.8.2). Positive clones carrying the *emm1* gene were verified by colony PCR (see 3.3.4.3), restriction enzyme analysis and DNA sequencing (Department of Genome Analytics, HZI, Braunschweig).

3.5 Biochemical techniques

3.5.1 Overexpression of recombinant M1-HIS-fusion protein

E. coli transformants carrying the *emm1* gene were incubated in LB medium containing 100 µg ml^{-1} ampicillin and 25 µg ml^{-1} kanamycin overnight at 37°C with agitation (120 rpm). On the following day overnight cultures were diluted 1:100 in fresh LB medium (500 ml) and were further incubated (37°C, 120 rpm) in the presence of 100 µg ml^{-1} ampicillin and 25 µg ml^{-1} kanamycin until late exponential growth phase (OD_{600nm} 0.8). For SDS-PAGE analysis, 1 ml of the culture was removed, centrifuged (10 min at 5000 rpm) and the bacterial pellet was resuspended in 200 µl of PAGE sample buffer. Samples were boiled for 10 min at 95°C and then stored at -20°C. For the induction of protein expression, 500 ml LB medium containing IPTG (final concentration 1 mM) was added to the remaining *E. coli* culture and samples were further incubated overnight at 37°C and 120 rpm. 1 ml of the induced *E. coli* culture was removed, centrifuged and stored in PAGE sample buffer at -20°C as described above. Cultures were harvested by centrifugation (10 min at 8000 rpm) and the pellet resuspended in 20 ml LEW buffer (Protino® Ni-TED Kit). Following an additional centrifugation step (10 min at 8000 rpm), the bacterial pellet was resuspended in 10 ml LEW buffer und kept on ice. Bacterial lysates were prepared using the French-pressure cell at a pressure of 1000 bar. To remove cell debris bacterial lysates were centrifuged for 15 min at 15.000 rpm. The supernatant was kept in a fresh eppendorf tube and stored at -20°C. 100 µl of the lysate was mixed with PAGE sample buffer, boiled for 10 min at 96°C and also stored at -20°C until SDS-PAGE analysis (see 3.5.4).

3.5.2 Purification of recombinant M1-HIS-fusion protein

Recombinant M1-HIS fusion protein was purified from *E. coli* lysates using the Protino® Ni-TED purification of polyhistidine-tagged proteins kit according to the manufacturer's manual. Samples of the flow through, the wash steps and the eluted proteins were taken, mixed with SDS-PAGE sample buffer, boiled 10 min at 96℃ and stored at -20℃ until SDS-PAGE analysis (see 3.5.4).

3.5.3 Dialysis and quantification of purified proteins

Purified M1-HIS fusion protein was dialyzed against PBS overnight at 4℃ in dialysis tubes with a molecular weight cut off of 12.000-14.000. The protein concentration was measured with the Nano Drop (Thermo Scientific). This technique is based on the measurement of the absorption at a wavelength of 280 nm. According to the Lambert-Beer law the protein concentration of a sample is proportional to the absorbance of light (Hellenthal, 2002). Since the protein was dialyzed against PBS, PBS was used as a blank. Aliquots of the dialyzed protein was stored at -20℃.

3.5.4 SDS polyacrylamide gel electrophoresis (SDS-PAGE)

SDS polyacrylamide gel electrophoresis is a method used to separate proteins in an electric field according to their molecular weight. This method was first described by Laemmli in 1970 (Laemmli, 1970) and is frequently used in protein biochemistry. Samples are mixed with SDS, an anionic detergent, which denatures and dissociates protein structures and also imparts a negative charge to proteins in proportion to their molecular mass. Addition of β-mercaptoethanol or dithiotretol (DTT) further denatures all disulphide bonds present within the molecule. Thus, due to the negative charge of SDS, proteins migrate towards the anode and are separated based on their molecular weight and independent of their charge. Large proteins are retained within the gel matrix and run slower as small molecules. Protein samples were mixed with SDS-PAGE sample buffer, boiled 10 min at 96℃ and are applied to the gel matrix. Proteins are first concentrated in a low percentage stacking gel with a pH of 6.8, then they migrate into a higher percentage resolving gel (10%) with a pH of 8.8 in which they are separated according to size. SDS gel electrophoresis was carried out using the Mini Protean II system with 0.75 mm spacer and 1x SDS running buffer. As a molecular weight standard Page ruler™ plus pre-stained protein ladder was used.

Table 27: Buffers and solutions used for SDS-PAGE

2x SDS-PAGE sample buffer	
Tris-HCl (0.5 M, pH 6.8)	1 ml
Glycerol	0.8 ml
10% SDS	2 ml
H_2O	3.6 ml
0.05% Bromophenol blue	400 µl of a 1% stock solution
β-mercaptoethanol	0.4 ml
Filter sterilize (ø 0.22 µm)	

10x SDS running buffer	
Trizma base	60 g
Glycine	300 g
SDS (ultrapure)	20 g
H_2O	*ad* 2 l

Stacking gel	**Volume for 1 gel**
H_2O	0.68 ml
30% Acrylamide/Bisacrylamide	0.17 ml
1.0 M Tris (pH 6.8)	0.13 ml
10% SDS	0.01 ml
10% APS	0.01 ml
TEMED	0.001 ml

Resolving gel	10% (volume for 1 gel)	12% (volume for 1 gel)
H_2O	1.9 ml	1.6 ml
30% Acrylamide/Bisacrylamide	1.7 ml	2.0 ml
1.5 M Tris (pH 8.8)	1.3 ml	1.3 ml
10% SDS	0.05 ml	0.05 ml
10% APS	0.05 ml	0.05 ml
TEMED	0.002 ml	0.002 ml

3.5.5 Staining of proteins in polyacrylamide gels

After SDS gel electrophoresis, proteins were stained with Coomassie R250 Brilliant Blue (Table 28). Gels were boiled in the staining solution for 30 sec in a microwave and were further incubated in the staining solution for 30 min at room temperature with shaking. Gels were destained by repeated boiling in dH_2O and incubation at room temperature with agitation until protein bands became visible and the gel background was clear.

Table 28: Composition of the Coomassie staining solution

Coomassie staining solution	
Coomassie Brilliant Blue R-250	0.1% (v/v)
Methanol	50% (v/v)
Acetic acid	10% (v/v)
Added to dH_2O	

3.5.6 Coating of latex beads with recombinant proteins

In order to investigate the invasion potential of recombinant proteins, latex beads were coated with purified recombinant M1 protein and GST protein as a negative control. Latex beads ($1x10^8$) with a diameter of 3 µm were used and were washed three times with 500 µl PBS prior to usage. In between the wash steps samples were centrifuged for 10 min at 1500 rpm. Latex beads were then coated with 5 µg of purified M1 or GST protein overnight at 4℃ with rolling. Following two washing steps with PBS (as above), coated beads were blocked with bovine serum albumin [10 mg/ml] in PBS for 1 h at room temperature. After blocking beads were washed once, resuspended in PBS and stored at 4℃ until used.

3.5.7 Analysis of the coating efficiency of M1-coated latex beads by flow cytometry

The coupling efficiency of protein coated latex beads was assessed by flow cytometry. Latex beads were incubated with a polyclonal antibody against M1 or GST for 45 min at room temperature followed by incubation with a goat-anti-rabbit ALEXA Fluor® 488-labelled secondary antibody (30 min at room temperature, Table 5, Table 6). Labelled samples were then measured by flow cytometry using the FACS Calibur BD and cell quest software (BD). FACS measurements of stained samples were kindly performed by Dr. O. Goldmann (Research Group Infection Immunology, HZI Braunschweig).

3.5.8 Analysis of surface localization of M1 on *S. pyogenes* and *L. lactis*

To analyse surface expression of M1 on *S. pyogenes* or *L. lactis*, strains were grown overnight in TSB medium or M17 medium (supplemented with 0.5% glucose) respectively. One drop of the overnight culture was distributed on a glass coverslip, dried and subsequently fixed with 4% paraformaldehyde for at least 30 min at 4℃. The M1 protein on the bacterial surface was labelled with a specific anti-M1 antibody (1:100 in PBS) for 45 min at room temperature. After washing samples were incubated with a species specific ALEXA Fluor® 488 conjugated secondary antibody (goat-anti-rabbit IgG, 1:200 in PBS) for 30 min at room temperature. After another washing step in PBS stained samples were analysed by fluorescence microscopy using a Zeiss Axio Imager A2 microscope. Strains which express the M1 protein showed green fluorescence.

3.5.9 Plasma absorbance assay

Overnight cultures (50 ml in THY medium) of *S. pyogenes* were collected by centrifugation (10 min at 5000 rpm), washed once with PBS and the pellet was resuspended in 500 µl PBST (PBS + 0.05% Tween). 50 µl of this suspension was added to 350 µl PBST and incubated with 100 µl of human plasma (kindly provided by Dr. H. Garritsen, Institute for Transfusion Medicine, Hospital Celler Strasse, Braunschweig) for 1 h at 37℃. During the incubation period samples were inverted occasionally. Following incubation, bacterial pellets were washed twice with 1 ml PBST. In order to elute bound plasma protein from the bacteria cell surface, samples were incubated with 100 µl glycine/HCl (100 mM, pH 2) for 15 min at room temperature. Following a final centrifugation step the supernatant, containing eluted plasma proteins, was collected and mixed with SDS-sample buffer. To neutralize samples 10% 1.5 M Tris buffer (pH 8.8) was added. Samples were then denatured at 95℃ for 5 min and analysed by SDS-PAGE gel electrophoresis on a 12% gel (refer to 3.5.4 and 3.5.5).

3.5.10 Binding assay with radioactively labelled IgG

Overnight cultures of *S. pyogenes* (50 ml in TSB medium) were collected by centrifugation for 10 min at 5000 rpm and washed once with 20 ml PBST (PBS + 0.05% Tween). Afterwards bacterial pellets were resuspended in 500 µl PBST and suspensions were adjusted in PBST to 10% transmission. 250 µl of this bacterial suspension was then mixed with radioactive IgG (100.000 units per sample) and incubated for 1 h at room temperature. Following incubation, unbound radioactive IgG was removed by washing with 1 ml PBST followed by centrifugation. Finally, the radioactive radiation emitted from the bacterial pellets was measured with a Wallac 1470 Wizard gamma counter (Perkin Elmer). The experiment was performed in triplicates. As a positive control with 100% binding FCS (20 µl) was used. FCS was mixed with the same amount of radioactively labelled IgG as used for the samples and precipitated with 1 ml trichloroacetic acid. The percental binding activity of the streptococcal strains was assessed in comparison to the total amount of radioactive protein used in the experiment (100% binding). The radioactive binding assays were performed in collaboration with Dr. M. Fulde (Department of Medical Microbiology, HZI, Braunschweig).

3.6 Cell culture techniques

3.6.1 Primary endothelial cells

Table 29: Primary endothelial cells used in this study

Cells	Culture medium	Culture conditions	Company/source
Human umbilical vein endothelial cells (HUVEC)	EGM-2 + SupplementMix + Pen/Strep [100 U ml^{-1}]/ [0.1 mg ml^{-1}]	37℃, 5% CO_2	Lonza
Human pulmonary microvascular endothelial cells (HPMEC)	EGM MV + SupplementMix + Pen/Strep [100 U ml^{-1}]/ [0.1 mg ml^{-1}]	37℃, 5% CO_2	Promocell
Human dermal lymphatic endothelial cells (HDLEC)	EGM-2 + SupplementMix + 5% FCS + Pen/Strep [100 U ml^{-1}]/[0.1 mg ml^{-1}]	37℃, 5% CO2	Promocell

3.6.2 Cell culture media

Endothelial cell growth medium 2 (EGM-2) used for the cultivation of HUVEC was purchased from Promocell and was supplemented with the SupplementMix provided by the manufacturer. In addition, Penicillin/Streptomycin (100 U ml^{-1} Penicillin; 0.1 mg ml^{-1} Streptomycin) were added. After addition of the supplements the shelf life of the complete endothelial cell growth medium is 6 weeks at 4℃. A liquots of the complete medium were stored at 4℃. Endothelial cell basal medium (EBM-2), which was used during the infection of HUVEC with streptococci, was purchased from Promocell. Aliquots were stored at 4℃.

Endothelial cell growth medium MV (EGM MV) was used for the cultivation of HPMEC and was purchased from Promocell. EGM MV was supplemented with the SupplementMix provided by the manufacturer. Penicillin and Streptomycin was also added and the complete medium was stored as described above for EGM-2 medium. Endothelial cell basal medium MV was also purchased from Promocell.

3.6.3 Cultivation and sub-cultivation of primary endothelial cells

Prior to cultivation all media and solutions were pre-warmed at 37°C. Endothelial cells were cultured in cell specific medium as described in Table 29 at 37°C and 5% CO_2. The medium was replaced every 3 days.

3.6.3.1 Cultivation of HUVEC

HUVEC were sub-cultured when 80% confluence was reached. For sub-cultivation, cells were washed once with 5 ml HEPES-BSS to remove dead cells, cell debris and medium components. Then 3 ml Trypsin/EDTA were added to detach cells from the cell culture dish. Trypsin treatment was stopped by the addition of 7 ml EGM-2. Detached cells were carefully washed from the petri dish, centrifuged 9 min at 900 rpm and resuspended in 4 ml fresh EGM-2. Approximately $4x10^5$ cells were seeded per 10 cm cell culture dish and incubated at 37°C and 5% CO_2. HUVEC were cultured until passage 5.

3.6.3.2 Cultivation of HPMEC and HDLEC

HPMEC and HDLEC were sub-cultured in the appropriate cell culture medium (Table 29) according to the protocol described for HUVEC (see 3.6.3.1). Cells were collected by centrifugation and resuspended in 3 ml EGM-MV. HPMECs were cultured up to passage 5.

3.6.3.3 Freezing and thawing of HUVEC and HPMEC

For long term conservation, endothelial cells were stored in liquid nitrogen. HUVEC and HPMEC were washed and detached from the cell culture dish as described above (see 3.6.3.1 and 3.6.3.2). After centrifugation the pellet of one cell culture dish was resuspended in 1 ml of the corresponding cell culture medium supplemented with 20% FCS and 10% DMSO. 500 µl HUVEC cell suspension and 1 ml HPMEC cell suspension were frozen per cryo vial and stored in an isoproponal filled freezing container for 24 h at -80°C which ensures controlled cooling of 1°C per minute to prevent accumulation of cell damaging ice crystals. After 24 h vials were transferred into liquid nitrogen. For thawing, the cells from one cryo vial were seeded in a 10 cm cell culture dish containing pre-warmed cell culture medium. Cells were incubated at 37°C with 5% CO_2. To diminish the cytotoxic effects of DMSO, the medium was replaced after cells had attached to the cell culture dish (after 4-5 h).

3.7 Infection assays

3.7.1 *In vitro* transwell infection system

For infection assays, an *in vitro* transwell system was used in which endothelial cells were grown on a semi-permeable membrane of cell culture inserts with a pore size of 3.0 or 0.4 µm. This system allows the cultivation of a polarised endothelial cell barrier to study the interaction and transmigration of streptococci. Prior to seeding of endothelial cells, transwell inserts were coated with 1% gelatine for 1 h at 37°C. Gelatine was subsequently cross-linked with 0.5% glutaraldehyde for 25 min at room temperature. Cross-linked gelatine served as a substrate to generate a semi-artificial basement membrane (Smeets *et al.*, 1992). $3x10^4$ endothelial cells were seeded per transwell insert, cultivated at 37°C, 5% CO_2 and grown to confluence. Confluent cell layers were then infected with streptococci or lactococci as described in section 3.7.2.

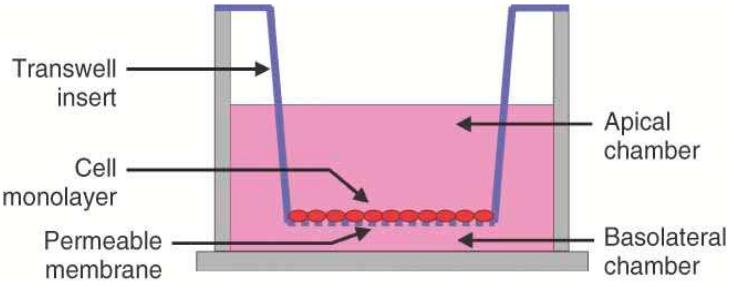

Figure 4: Schematic representation of the transwell system

Taken from (Saunders, 2009)

3.7.2 *In vitro* transwell infection assay of endothelial cells with *S. pyogenes* or *L. lactis*

To study the interaction of *S. pyogenes* with endothelial cells, HUVEC, HPMEC or HDLEC were cultivated on cell culture transwell inserts as described in section 3.7.1. One day prior to infection cell layers were washed three times with endothelial basal medium and were further incubated in antibiotic free endothelial cell growth medium at 37°C and 5% CO_2. For infection assays, streptococcal strains were grown in TSB overnight and on the day of infection sub-cultured in a 1:10 ratio in TSB until exponential growth phase (OD_{600} 0.4). Prior to infection streptococci were harvested by centrifugation at 5000 rpm for 10 min. The pellet of a 50 ml bacterial culture was resuspended in 500 µl PBS and the suspension adjusted to 10% transmission in PBS. The bacterial solution was subsequently diluted 1:8 in basal medium containing 2.5% FCS. To start the infection, 25 µl of the bacterial suspension were added per transwell containing 400 µl medium (final dilution 1:128). Infection was performed

for different time intervals ranging from 1 h till overnight infections. To stop the infection, cell layers were washed three times with endothelial basal medium and fixed with 4% PFA in PBS (immunofluorescence analysis). For electron microscopic analysis samples were fixed with EM-fixans (see Table 31). Invasion rates were determined after immunofluorescence staining of intra- and extracellular bacteria (see 4.8.1) by enumerating intracellular bacteria. Invasion rates are expressed as intracellular bacteria per 10 cells or % invasion.

Infection assays of HUVEC with *L. lactis* strains were performed as described above for *S. pyogenes* except that *L. lactis* strains were cultured in M17 medium supplemented with 5% glucose and 5 µg/ml erythromycin.

3.7.3 Pre-incubation of HUVEC

3.7.3.1 Blocking of integrin subunits on HUVEC

In order to identify the cellular receptor which mediates entry of M1 GAS into HUVEC, blocking experiments of the alpha and beta integrin subunits on HUVEC were performed. HUVEC were pre-incubated with specific monoclonal antibodies against the α_1-, α_2- and β_1-integrin subunit diluted 1:100 in cell culture medium for 75 min. Following blocking, cell layers were washed twice with EBM-2 and infected with M1 GAS A527 for 2 ½ h according to the standard infection protocol described above (see 3.7.2). Invasion rates were determined by enumerating intracellular streptococci. Invasion rates are depicted as % invasion compared to an untreated control with 100% invasion.

3.7.3.2 Pre-incubation of HUVEC with various inhibitors to interfere with host cell signalling pathways

To analyse the involvement of host cell signalling molecules of the phagocytic uptake machinery in M1 GAS invasion into HUVEC, function interfering experiments were performed. A key component of classical phagocytic uptake processes is the protein kinase which was inhibited by calphostin C in the infection experiments. Activation of protein kinase leads to the release of intracellular calcium, which was inhibited by the calcium chelator BAPTA-AM. Treatment with edelfosine inhibits phospholipase C gamma, another essential host cell signalling molecule required for the phagocytic uptake machinery. HUVEC, cultivated in transwell inserts, were pre-treated with the inhibitors specified in Table 30 for 30 min. To exclude toxic effects of the solvent on HUVEC and subsequently on bacterial invasion, cells were also pre-incubated with the corresponding concentration of DMSO alone. All inhibitors were diluted in cell culture medium to the concentration stated in Table 30.

Following pre-incubation, infection of HUVEC cell layers were performed for 3 h according to the standard infection protocol described in section 3.7.2. Inhibitors were present during the whole infection period. Invasion rates were determined by enumerating intracellular streptococci. Invasion rates are depicted as % invasion compared to the DMSO treated control with 100% invasion.

Table 30: Inhibitors used in this study

Inhibitor	Concentration	Solvent
Calphostin C	2 µM	DMSO
Edelfosine	20 µM	DMSO
BAPTA-AM	25 µM	DMSO

3.7.3.3 Pre-incubation of HUVEC with BSA-gold nano particles

Coating of 15 nm gold particles with BSA

10 ml of a colloidal gold solution containing 15 nm nano gold particles were adjusted to pH 6.0-6.5 using 1.1 M K_2CO_3. Subsequently the gold solution was incubated with 100 µl of a BSA stock solution (100 mg/ml) for 15 min at room temperature. In this step the positively charged BSA is linked to the negatively charged gold particles by van der Waals forces and, therefore, retaining biological activity, especially not influencing the interaction with the cell receptor. The stability of the BSA-gold complexes was tested by incubation of the BSA-gold solution with 10% NaCl in a 1:1 ratio. A red colour indicates stable BSA-gold complexes, in contrast, colour change from red to blue indicates unstable complexes. Following centrifugation of the BSA-gold solution (15 min at 20.000 rpm and 4°C), the red pellet was collected and used for pre-incubation of HUVEC.

Co-incubation of HUVEC with BSA-gold particles

To pre-load HUVEC lysosomes, HUVEC were fed with BSA-gold particles 18 h prior to infection. HUVEC cultivated in transwell inserts were incubated with 75 µl of the BSA-gold solution per well under standard conditions. On the following day cell layers were washed once with basal medium and infected with streptococci as described in section 3.7.2.

3.7.4 Blocking of the M protein on streptococci

In order to analyse the involvement of the M1 protein of *S. pyogenes* in invasion into HUVEC, GAS A527 cultures were adjusted to 10% transmission as described for the standard infection model (see 3.7.2). Diluted streptococcal suspensions were then pre-treated with increasing concentrations (0 µg/ml, 10 µg/ml, 25 µg/ml, 50 µg/ml and 75 mg/ml) of a rabbit anti-M1 antibody or a control antibody (75 µg/ml) 1 h prior to infection. Following pre-incubation, HUVEC were infected with pre-treated streptococci according to the standard infection protocol (see 3.7.2). Internalization rates were expressed as % invasion compared to the internalization rates of an untreated control with 100% invasion.

3.7.5 Latex bead internalization assay on HUVEC

To assess the invasion potential of the M1 protein of *S. pyogenes*, latex beads were coated with recombinant M1 protein and GST as negative control (see 3.5.6). HUVEC seeded on coverslips or transwell inserts (see 3.7.1) were co-incubated with $2x10^6$ M1- or GST-coated latex beads 1-5 h for immunofluorescence analysis, 60-120 min for field emission scanning electron microscopy (FESEM) or 12 h for transmission electron microscopy (TEM). Cell layers were washed three times with basal medium and fixed with 1% PFA (immunofluorescence analysis) or EM-fixans (electron microscopy, see Table 31). Internalization rates were assessed by immunofluorescence staining of intra- and extracellular beads (see 3.8.1). Internalization rates were determined by enumerating intracellular beads.

3.7.6 Quantification of intracellular viable bacteria in HUVEC (survival assay)

HUVEC cultivated on transwell inserts (see 3.7.1) were infected with M1 GAS A527 according to the standard infection procedure (see 3.7.2). Infection was performed for an initial period of three hours (t_0). Subsequently infected cell layers were washed three times with EBM-2 to remove unbound bacteria. Afterwards samples were incubated for defined time periods in EBM-2 medium supplemented with 2.5% FCS, 5 µg ml^{-1} penicillin G and 100 µg ml^{-1} gentamycin to kill all remaining extracellular bacteria. After 2 h, 4 h, 6 h and 9 h infected cell layers were washed with EBM-2 at least five times to ensure complete removal of antibiotics. Cells were detached from the transwell membrane with 100 µl 0.025% Trypsin/0.01% EDTA per well for 5 min at 37°C. Detached cells were subsequently permeabilized with 400 µl 1% saponin in PBS for 20 min at 37°C. Finally, cell suspensions were diluted in EBM-2. 25 µl of the corresponding serial dilutions were plated on THY agar plates and incubated at 37°C and 5% CO_2 for up to 48 h. The number of viable intracellular

streptococci was evaluated by counting bacterial colonies and calculating the colony forming units (cfu) per ml.

3.7.7 Measurement of EC barrier function using the CellZscope® automated cell monitoring system

Analysis and monitoring of cell cultures, in particular cell layer formation and polarization, was determined with the CellZscope® automated cell monitoring system by measuring the transendothelial impedance of cells grown on permeable membranes. In addition to the transendothelial resistance (TER), the cell layers electric capacitance (Ccl) was measured which gives information about the properties of a cell layer, e.g. expression of microvilli. Measurement of the transendothelial resistance and the cell layers capacitance provides valuable parameters to assess the current state of a cell layer. Confluent polarized cell layers exhibit high TER values and low capacitance, while permeability correlates with low TER values and high capacitance (NanoAnalytics, 2009).

HUVEC were cultivated on gelatinised transwell membranes with a pore size of 0.4 µm as described above (see 3.7.1). Transwells were then placed in the cavities of the CellZscope® system and incubated at 37℃ and 5% CO_2. Two electrodes on either side of the transwell membrane and the application of a small voltage allow the measurement of the electric resistance of the cell layer. The TER and the Ccl was measured automatically every hour over a period of several days. The resulting data was evaluated based on the algorithm of the CellZscope® system and customized Cellzscope® software. After 4-5 days of cultivation HUVEC cell layers exhibited TER values higher than 15 Ω x cm^2 and Ccl values lower than 1 µF/cm^2 indicating that HUVEC cell layers had grown to confluence and were polarized. To assess the influence of streptococcal infection on HUVEC barrier function and integrity, HUVEC cell layers were infected with several M1 GAS strains according to the standard infection protocol (see 3.7.2). Throughout the whole infection period the TER and Ccl were measured and compared to the values of an uninfected control well.

3.7.8 *Ex vivo* infection assay of umbilical cord with *S. pyogenes*

Human umbilical cord was obtained post-delivery from the Hospital Celler Strasse in Braunschweig. The vein (thrombus free) endothelium was infected with $1x10^8$ M1 *S. pyogenes* A527 suspended in EGM-2 medium for 4 ½ h at 37°C and 5% CO_2. Afterwards samples were washed three times with PBS followed by fixation with EM-fixans (see Table 31). Following fixation, several pieces of the vein were processed and analysed by FESEM (see 3.8.2.1). To exclude any effects due to physical damage during the infection process, samples were collected from an area distant from the injection point.

3.8 Microscopic techniques

3.8.1 Fluorescence microscopy

Immunofluorescence staining and immunofluorescence microscopy is a standard technique to visualize target proteins on the cell surface or to localize specific structures within cells or subcellular compartments. This method uses antibodies labelled with specific fluorochromes that specifically, either directly or indirectly, bind to a target antigen. Using light with a specific wavelength the fluorochrome of the sample is excited and emits light with a longer wave length which is detected in the fluorescent microscope (Campbell *et al.*, 2003). Samples were stained as described below and were examined using a Zeiss Axiophot with an attached Zeiss AxioCam HRc digital camera and Zeiss Axiovision software 4.8 or a Zeiss Axio Imager A2 with a Zeiss Axio Cam MRm camera and ZEN 2011 software. Contrast and brightness of images were adjusted using Adobe Photoshop CS3 Extended (Version 10.0).

3.8.1.1 Double-immunofluorescence staining

Irrespective of the different staining set ups described below, fixed samples were washed three times with PBS and first blocked with PBS containing 10% FCS for 30 min at room temperature to prevent unspecific binding of the antibodies. Afterwards streptococci and specific cellular structures were stained according to the protocols described below. For detailed information regarding the antibodies and dilutions used, refer to Table 5 and Table 6. In between each staining step samples were washed three times with PBS. All incubation steps were performed at room temperature in a wet chamber. After the last washing step stained transwell membranes were cut out of the transwell insert and mounted on glass cover slides using ProLong® Gold antifade reagent containing DAPI. Samples were sealed with clear nail polish and stored at 4°C in the dark until fluorescence microscopic analysis.

3.8.1.2 Staining of intra-/extracellular streptococci, lactococci or protein-coated latex beads

First extracellular streptococci were stained with a rabbit polyclonal antibody recognizing *S. pyogenes* (anti-GAS) (Molinari *et al.*, 1997) for 45 min followed by 30 min incubation with an anti-rabbit ALEXA Fluor® 488 coupled secondary antibody. To visualize intracellular streptococci cells were permeabilized with 0.1% Triton-X-100 for 5 min. Following permeabilization, streptococci were again labelled with the anti-GAS primary antibody (see above) and subsequently stained with a secondary anti-rabbit ALEXA Fluor® 568 labelled secondary antibody for 30 min. According to their respective label intracellular bacteria appear red and extracellular streptococci green to yellow.

Intra- and extracellular lactococci were stained according to the protocol described for streptococci except that a rabbit-anti-*L. lactis* antibody was used as primary antibody.

Staining of intra- and extracellular protein-coated latex beads was performed according to the protocol described above for streptococci except that a rabbit anti-M1 or rabbit-anti-GST primary antibody was used.

Following immunofluorescence staining, internalization rates of bacteria or coated latex beads were determined by enumerating intracellular bacteria or latex beads. A minimum of 100 cells was analysed and internalization rates were expressed as intracellular bacteria/beads per 10 cells or % invasion.

3.8.1.3 Staining of streptococci and the actin cytoskeleton

To visualize streptococci as well as cellular components like the actin cytoskeleton, cells were washed three times with PBS and then directly permeabilized with 0.1% Triton-X-100 for 5 min. Following permeabilization, streptococci were labelled with a rabbit anti-GAS antibody (45 min) and subsequently stained with a goat-anti-rabbit ALEXA Fluor® 568 or alternatively A488 coupled secondary antibody for 30 min. Finally, the actin cytoskeleton was stained by incubation with either phalloidin ALEXA Fluor® 488 or phalloidin ALEXA Fluor® 568 for 30 min.

3.8.1.4 Staining of streptococci and late endosomal/lysosomal compartments

In order to analyse co-localization of streptococci with the Lamp-1 positive late endosomal/lysosomal compartment, cells were directly permeabilized with 0.1% Triton-X-100 (5 min), washed with PBS and streptococci stained with a rabbit anti-GAS antibody (45 min) and a species specific ALEXA Fluor® 568 coupled secondary antibody (30 min). The late

endosomal/lysosomal compartment was labelled with a mouse anti-human Lamp-1 (CD107a) primary antibody (1 h) and subsequently stained with a goat-anti-mouse ALEXA Fluor® A488 secondary antibody (30 min).

Following immunofluorescence staining, streptococci residing within the Lamp-1 positive compartment were enumerated and related to the total number of intracellular streptococci.

3.8.1.5 Staining of the Arp2/3 complex

Following permeabilization with 0.1% Triton-X-100 for 5 min, the Arp2/3 complex was labelled with a mouse-anti-Arp2/3 (p16 #323H3) antibody for 1 h followed by incubation with a goat-anti-mouse ALEXA Fluor® 488 coupled secondary antibody (30 min).

3.8.1.6 Staining of streptococci and the β_1-integrin subunit

For visualisation of the β_1-integrin subunit, unpermeabilized cells were incubated with an anti-β_1-integrin antibody (5 µg per well) for 1 h followed by a goat-anti-mouse ALEXA Fluor® 488 coupled secondary antibody (30 min). Subsequently streptococci were labelled with a rabbit anti-GAS antibody (45 min) and a goat-anti-rabbit ALEXA Fluor® 568 coupled secondary antibody (30 min).

3.8.1.7 Bacterial viability staining

Viability testing of intracellular streptococci was performed using the LIVE/DEAD® Baclight™ Bacterial Viability Kit according to the manufacturer's protocol.

3.8.2 Electron microscopy (EM)

3.8.2.1 Field emission scanning electron microscopy (FESEM)

In addition to immunofluorescence analysis, the interaction of M1 *S. pyogenes* as well as M1-coated latex beads with HUVEC or HPMEC was analysed by FESEM. Infected cell layers were washed with EBM-2 or TE-buffer and fixed with EM-fixans for at least 30 min at 4℃. Samples were then washed twice with TE-buffer and dehydrated in a grade series of ethanol (10%, 30%, 50%, 70%, 90%). Each step was performed for 10 min on ice. Samples were incubated twice in 100% ethanol for 15 min at room temperature. Following dehydration, samples underwent critical point drying with liquid CO_2. Finally, samples were sputter coated with a thin gold-palladium film or alternatively with carbon for visualization of

intracellular gold particles. Processed samples were then examined in a field emission scanning electron microscope Zeiss DSM 982 Gemini with an acceleration voltage of 5 kV or a field emission scanning electron microscope Merlin, Zeiss. Sample analysis was carried out by Apl. Prof. Dr. M. Rohde (Department of Medical Microbiology, HZI Braunschweig). Brightness and contrast were adjusted with Adobe Photoshop CS3 Extended (Version 10.0).

3.8.2.2 Transmission electron microscopy (TEM)

Following fixation of infected HUVEC cell layers, transwell membranes were washed twice with 0.1 M cacodylate buffer. Transwell membranes were cut out of the transwell insert and again washed several times with 0.1 M cacodylate buffer. Membranes were again fixed and simultaneously contrasted with 1% aqueous osmium tetroxide for 1 h at room temperature. Afterwards samples were washed with 0.1 M cacodylate buffer and dehydrated in a grade series of ethanol (10%, 30%, 50%, 70%, 90%) with 30 min on ice for each step. Following incubation with 100% ethanol for 30 min at room temperature, samples were embedded in Spurr resin (Spurr, 1969) and polymerized at 70°C for 16 h. After polymerization ultra-thin section of infected cell layers were cut with a diamond knife. Sections were collected onto butvar-coated Cu-grids, contrasted with 4% uranyl-acetate (UAc) for 3 min at room temperature and lead-citrate for 15 sec at room temperature. Following a final washing step with H_2O, sections were air dried and examined with a TEM EM 910. Images were recorded digitally with a Slow-Scan CCD-Camera (ProScan, 1024 x 1024) with ITEM-Software (Olympus Soft Imaging Solutions). Samples analysis was carried out by Apl. Prof. Dr. M. Rohde (Department of Medical Microbiology, HZI Braunschweig). Contrast and brightness of images were adjusted with Adobe Photoshop CS3 Extended (Version 10.0).

In order to stain cellular membranes, samples were subjected to ferrocyanide osmium fixation with thiocarbocyanide (TCH) on the day of infection, immediately after fixation with 0.1 M cacodylate buffer + 5% paraformaldehyde + 2% glutaraldehyde. All solutions were prepared fresh on the day of use. Following fixation, samples were washed twice with 0.1 m cacodylate buffer and then incubated with 1.5% potassiumferrocyanide in 1% aqueous osmium tetroxide for 30 min at room temperature. Afterwards the cell layer was treated with 1% aqueous thiocarbocyanide for 5 min at room temperature followed by another incubation with 1.5% potassiumferrocyanide in 1% aqueous osmium tetroxide for 5 min at room temperature. Finally, samples were washed with 0.1 M cacodylade buffer, dehydrated and processed as described above.

Table 31: Solutions and buffers used for electron microscopy

Fixans for EM analysis	
Glutaraldehyde (GA)	2% (w/v)
Paraformaldehyde (PFA)	5% (w/v)
HEPES buffer	0.1 M

HEPES buffer	
HEPES	23.83 g
H_2O	ad 1 l
Adjust pH 7.4 with NaOH	

Cacodylate buffer	
Cacodylate	100 mM
Sucrose	90 mM
$MgCl_2$	10 mM
$CaCl_2$	10 mM

3.9 Statistical analysis

Data was analysed using Microsoft Office Excel 2010 software. Each assay was repeated at least three times on different days. A minimum of 100 cells was analysed per assay. Statistical comparison was performed using the Student's paired t-test. Results represent mean values ± SD of one representative experiment, unless otherwise stated. p values of 0.05 or less were considered significant.

4. Results

4.1 Analysis of the invasion potential of different serotype M1 S. pyogenes strains

4.1.1 Establishment of an *in vitro* transwell infection model to study streptococcal invasion

Since a direct interaction of the most invasive serotype M1 GAS with an endothelial cell layer (EC) has not been studied before, the invasion potential of M1 GAS was tested by infection of primary human endothelial cells of the umbilical cord (HUVEC). Infection studies were first performed according to a standard infection protocol, in which HUVEC were cultivated on glass coverslips, since previous work within the Department demonstrated successful invasion of serotype M3 GAS into endothelial cells using this infection system (Nerlich *et al.*, 2009, Amelung *et al.*, 2011). Surprisingly, in subsequent immunofluorescence microscopic analysis all clinical M1 isolates appeared non-invasive (data not shown). Thus, in order to characterise the interaction of M1 GAS with EC in more detail, a new *in vitro* transwell infection model had to be established and applied. HUVEC were grown on an artificial semi-permeable membrane of a transwell insert, thereby creating an apical and a basolateral chamber representing the blood stream on the apical side and the tissue side on the basolateral side. Since endothelial cells *in vivo* form functional barriers to ensure the physiological properties of tissues, it was speculated that the confluence status of the EC cell layer is also crucial for streptococcal invasion. Therefore, cell layer formation and polarization were determined with the CellZscope® system by continuously measuring the transendothelial resistance (TER) of cells grown on permeable membranes. In addition to the transendothelial impedance, the CellZscope® allows measurement of the electric capacitance (Ccl) of EC cell layers. Measurement of both, the transendothelial resistance and the cell layers capacitance, provides valuable parameters to assess the current state of a cell layer. Confluent polarized cell layers exhibit high TER values and low capacitance while cell layer permeability correlates with low TER values and high capacitance (NanoAnalytics, 2009).

Directly after seeding HUVEC cell layers exhibit low TER values of ~ 8 Ω/cm^2 (Figure 5a, upper panel). On day three of cultivation the TER value continuously rises and reaches values above 22 Ω/cm^2 by day five (Figure 5a, upper panel). In contrast to the transendothelial resistance, the capacitance of HUVEC layers shows high values (14 $\mu F/cm^2$) directly after seeding (Figure 5a, lower panel). As the transendothelial resistance rises, the capacitance continuously decreases to values below 1 $\mu F/cm^2$ at day five of cultivation. In addition to the measurement of the impedance of HUVEC layers, the confluence was also assessed by electron microscopy. As shown in Figure 5b after five days of cultivation HUVEC

have formed a confluent tight cell layer which correlates with high transendothelial resistance.

Taken together, this *in vitro* transwell system allows the cultivation of a confluent polarised HUVEC cell layer which was subsequently used to analyse the invasion potential of M1 GAS into HUVEC in further detail.

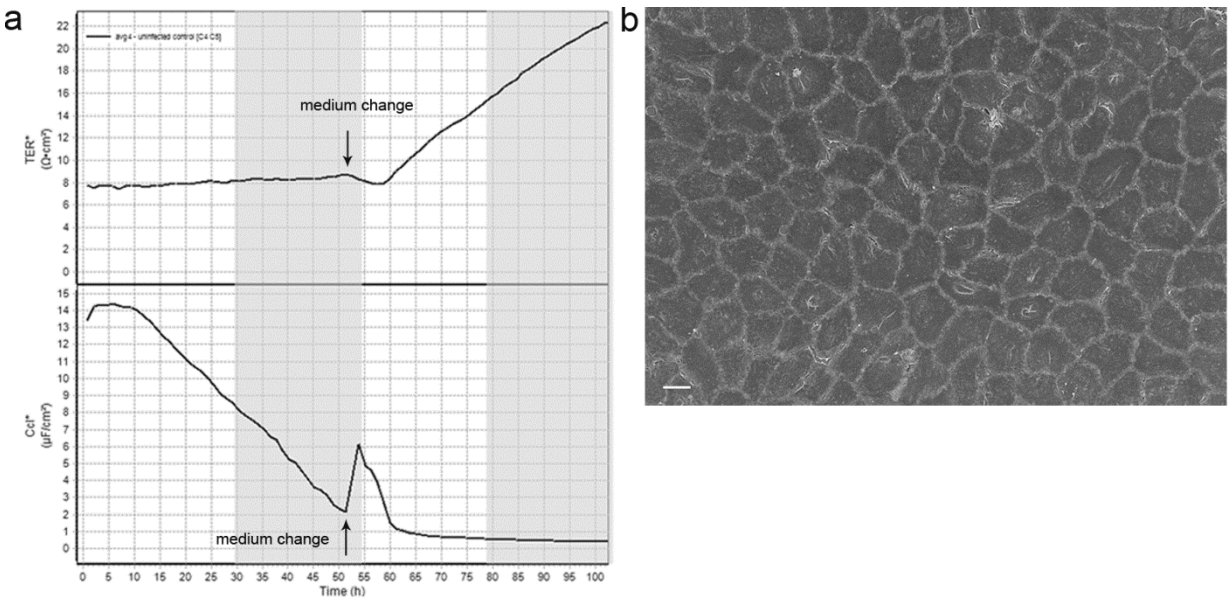

Figure 5: HUVEC cultivated on transwell inserts form confluent polarised cell layers

HUVEC were cultivated on artificial semi-permeable transwell membranes at 37℃ and 5% CO_2 over a period of 5 days.
a. The transendothelial electric resistance TER (upper panel) and capacitance Ccl (lower panel) of HUVEC layers were continuously measured in 60 min intervals using the CellZscope® system. The diagram shows mean values of two independent wells of uninfected HUVEC during the course of cultivation. After 52 h of cultivation the cell culture medium was replaced (arrow medium change).
b. Electron microscopic analysis (FESEM) of the cell layer after 5 days of cultivation confirms the formation of a tight confluent HUVEC cell layer. Bar represents 20 µm.

4.1.2 Different serotype M1 GAS clinical isolates invade EC

Using this transwell system the invasion potential of different clinical isolates of serotype M1 GAS on HUVEC was assessed. Confluent HUVEC cell layers cultivated on transwell inserts were infected with four different M1 GAS isolates (A527, A302, A270 and A271) from patients with invasive diseases. After immunofluorescence staining of intra- (red) and extracellular (green-yellow) bacteria, the number of intracellular streptococci was assessed. Immunofluorescence images of infected HUVEC cell layers show that all M1 GAS isolates tested are able to efficiently invade into EC and intracellular streptococci are localized within the perinuclear region of the cell (Figure 6a-d). Quantification of invasion show that three of

the strains tested exhibit similar invasion rates with more than 100 intracellular bacteria per 10 cells 4 h post infection (Figure 6e). Only strain A271 shows lower infection rates. As all M1 GAS strains display comparable invasion potentials, the following experiments were performed with strain A527 only.

Taken together, these results demonstrate the invasiveness of M1 GAS on EC. Furthermore, a polarized endothelial cell layer proofed to be essential for M1 GAS invasion, since infection assays on glass coverslips using the standard protocol were not successful. Thus, the transwell infection model represents a suitable system to study the invasion mechanisms of M1 GAS in further detail.

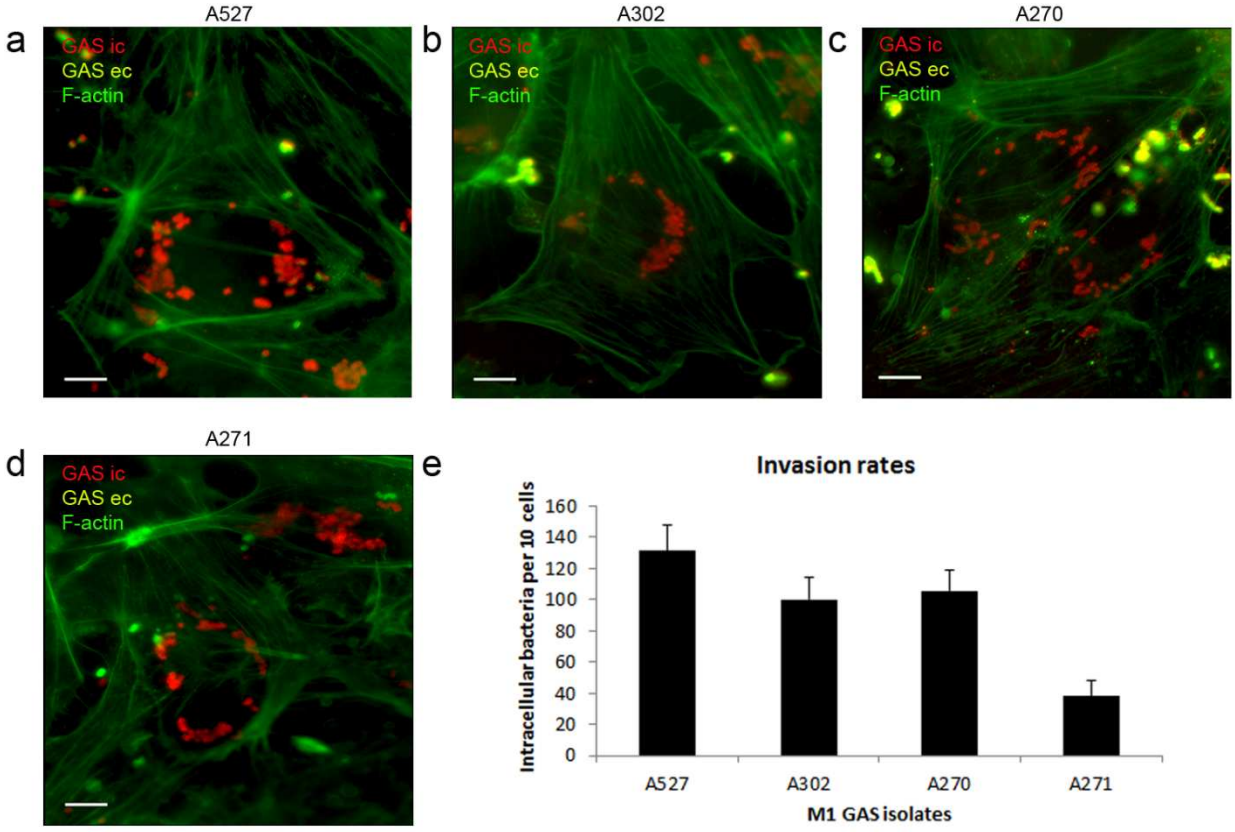

Figure 6: Different clinical isolates of serotype M1 GAS invade confluent HUVEC layers

a-d. Analysis of the invasion potential of M1 GAS clinical isolates on HUVEC layers by immunofluorescence. Confluent HUVEC layers were infected with four clinical isolates of serotype M1 GAS A527 (a), A302 (b), A270 (c) and A271 (d). Following infection, intracellular streptococci are stained in red and extracellular bacteria are visualised in green-yellow. The actin cytoskeleton is depicted in green. Bars represent 5 µm (a-d).
e. Quantification of the invasion potential of M1 GAS strains A527, A302, A270 and A271 on HUVEC 4 h post infection. The graph represents mean values ± SD from one out of three independent experiments.

4.2 Characterization of the invasion mechanism

It has already been shown that several *S. pyogenes* strains efficiently adhere to and invade into different cell types including epithelial and endothelial cells, a process which ensures streptococcal survival and protection from the host cells immune response (LaPenta *et al.*, 1994, Greco *et al.*, 1995, Molinari *et al.*, 1997, Jadoun *et al.*, 1998, Rohde *et al.*, 2003, Nerlich *et al.*, 2009). Depending on the invasin expressed on the surface of GAS, distinct invasion mechanisms are triggered. Serotype M3 GAS, expressing the fibronectin binding protein FbaB, induces the formation of membrane protrusions which engulf the bacteria and mediate a zipper-like uptake into EC (Nerlich *et al.*, 2009, Amelung *et al.*, 2011). Similarly, M1 GAS mediates a zipper-like uptake into epithelial cells (Dombek *et al.*, 1999). In contrast, SfbI-expressing *S. pyogenes* strains trigger the aggregation of caveolae and streptococcal uptake via large membrane invaginations (Molinari *et al.*, 2000, Rohde *et al.*, 2003).

4.2.1 M1 *S. pyogenes* triggers the formation of membrane protrusion and zipper-like uptake into EC

After establishing an *in vitro* infection system, the invasion mechanism and especially the mode of internalization of serotype M1 GAS into HUVEC were assessed in further detail. Therefore, HUVEC were infected with M1 GAS strain A527 and samples were analysed by FESEM.

Following adherence to the apical side of the host cell (Figure 7a), M1 GAS induces actin cytoskeletal rearrangements and the formation of membrane protrusions (Figure 7b). These tightly engulf the streptococcal chain (Figure 7c) until bacteria are completely surrounded by the host cell membrane and internalized into the cell (Figure 7d). Notably, invasion was apparent predominantly at the interfaces between cells in the monolayer and not at the very centre of the cells (data not shown).

These results demonstrate a zipper-like uptake of M1 GAS into endothelial cells which visually parallels the FbaB-mediated uptake of serotype M3 GAS into EC (Amelung *et al.*, 2011). In contrast, this invasion mechanism is morphologically distinct from the caveolae-mediated uptake induced by SfbI-expressing GAS strains (Rohde *et al.*, 2003).

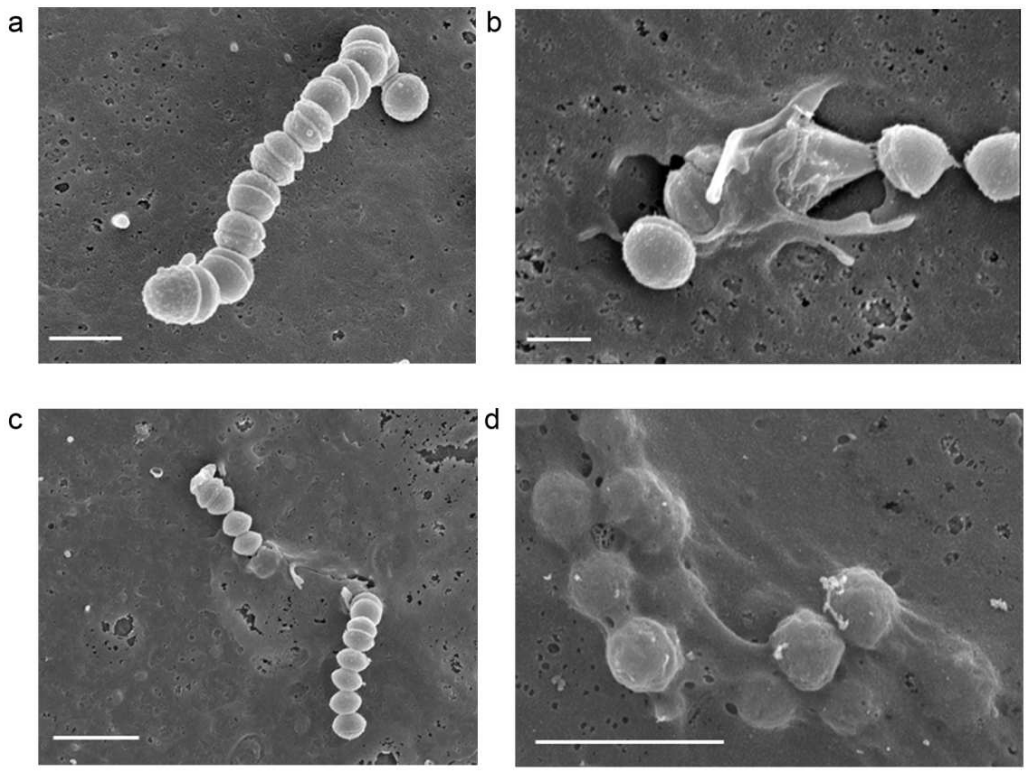

Figure 7: Invasion of M1 GAS into EC is accompanied by the formation of membrane protrusions

Analysis of the invasion mechanism of M1 GAS into EC by field emission scanning electron microscopy. Upon infection of HUVEC, M1 GAS adheres to the host cell surface (a) and induces the formation of membrane protrusions (b, c), which subsequently leads to complete internalization of the streptococcal chain into the host cell (d). Bars represent 1 µm (a), 600 nm (b) and 2 µm (c, d).

4.2.2 M1 GAS entry is characterised by F-actin accumulation and aggregation of the Arp2/3 complex in the vicinity of invading GAS

On the cellular level, the basis for the formation of membrane protrusions are cytoskeletal rearrangements and, in particular, a reorganization of the actin cytoskeleton. The actin related protein complex 2/3 (Arp2/3) has been shown to play a crucial role in actin cytoskeletal remodelling processes. It acts as a nucleation factor that initiates the formation of new actin filaments and, in particular, the assembly of branched actin fibres (Goley *et al.*, 2006, Campellone *et al.*, 2010). Since electron microscopic analysis revealed cytoskeletal rearrangements during the invasion of M1 GAS into EC, the role of actin remodelling and the involvement of the Arp2/3 complex in these processes was investigated.

Therefore, confluent HUVEC layers were infected with M1 GAS. Following infection, F-actin and the Arp2/3 complex were labelled and the samples were analysed by immunofluorescence microscopy.

Upon invasion of M1 GAS into HUVEC, an accumulation of F-actin is induced in the vicinity of invading streptococci. Figure 8a shows a streptococcal chain in the process of invasion. F-actin (stained in green) closely accumulates around the initial three cocci of the streptococcal chain (labelled in red). In contrast, no co-localization with F-actin is observed for the remaining cocci, suggesting that only the front part of the streptococcal chain is already internalized into the cell and the rest of the chain is still localized outside of the cell. In addition to F-actin accumulation at the port of entry, the Arp2/3 complex aggregates around invading bacteria whereas it is statistically distributed within neighbouring cells or within parts of the cell where no bacterial invasion occurs (Figure 8b).

Taken together, upon infection M1 GAS induces actin polymerization at the port of entry, a process which seems to be mediated by Arp2/3 actin filament branching. These cellular processes are the basis for cytoskeletal rearrangements, the formation of membrane protrusion and subsequent internalization of streptococci into the host cell as previously seen by scanning electron microscopy (Figure 7).

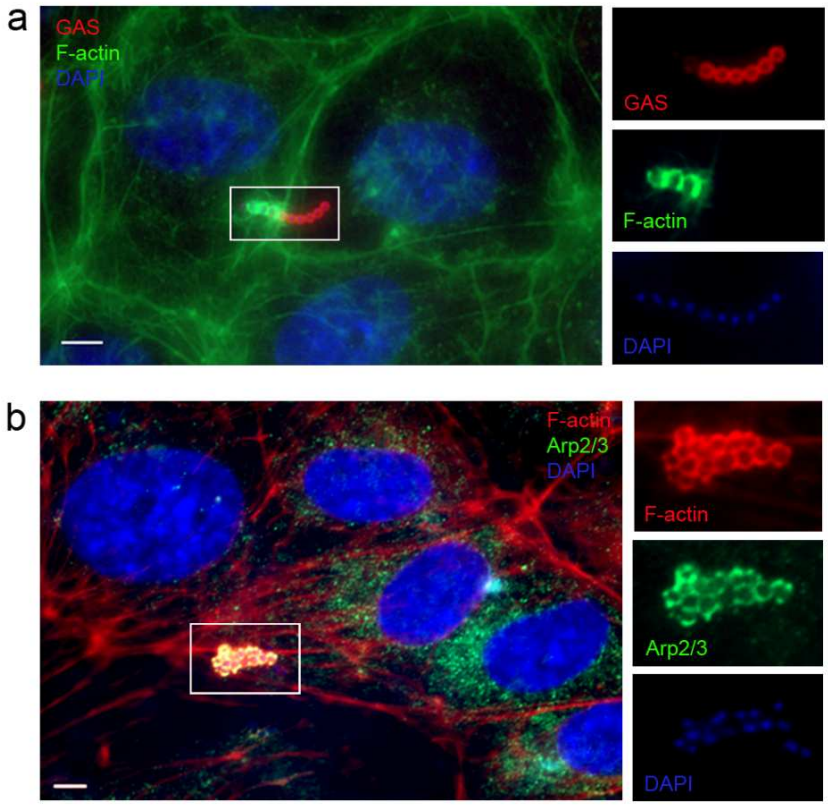

Figure 8: Upon invasion M1 GAS triggers the accumulation of F-actin and the aggregation of the Arp2/3 complex at the port of entry

HUVEC were infected with M1 GAS strain A527 for 60 min. Following infection, samples were stained for immunofluorescence microscopy. M1 GAS (red) invasion into HUVEC induces F-actin accumulation (green) at the site of entry (a). In addition, the Arp2/3 (green) complex aggregates around invading streptococci (blue) (b). Inserts show enlarged sections of split channels of the indicated area in the merged image. Bars represent 5 µm (a,b).

4.3. M1 GAS mediates phagocytic-like uptake processes into HUVEC

Invasion into host cells represents one successful mechanism of *S. pyogenes* to evade host immune defences and to ensure streptococcal survival. It is already known that depending on the mode of internalization *S. pyogenes* strains take distinct intracellular trafficking routes. Strains that trigger invasion by cytoskeletal rearrangements, for example serotype M3 GAS, are localized within phagosomes which traffic along the classical endocytic route and fuse with lysosomes (Amelung *et al.*, 2011) (Talay, unpublished data). In contrast, SfbI-expressing *S. pyogenes* strains showing caveolae-mediated invasion reside within caveosomes and prevent fusion with lysosomes thereby bypassing the endocytic machinery (Rohde *et al.*, 2003).

Thus, the intracellular trafficking route of M1 GAS within EC was analysed in further detail.

4.3.1 M1 GAS mediates co-localization with the late endosomal/lysosomal compartment

A characteristic of the classical endocytic machinery is fusion of phagosomes containing foreign material, e.g. bacteria, with late endosomal and lysosomal compartments. A marker for late endosomal and lysosomal compartments is the lysosomal associated membrane protein 1 (Lamp-1). To analyse the intracellular trafficking route of M1 GAS within endothelial cells, HUVEC were infected with M1 GAS for different time periods ranging from 1 h to overnight infection. Following fixation, the late endosomal lysosomal compartment as well as streptococci were stained differentially and analysed by immunofluorescence microscopy.

Immunofluorescence analysis of infected HUVEC cell layers reveals co-localization of intracellular streptocooci (red) with the Lamp-1 positive late endosomal/lysosomal compartments (green) of the cell (Figure 9a). 1 h until 5 h post infection the majority of the intracellular streptococci is localized within Lamp-1 positive compartments (Figure 9b). In contrast, after overnight infection the number of streptococci co-localizing with Lamp-1 declines to approximately 50% (Figure 9b).

These data suggest that following internalization M1 GAS travels along the endocytic route and acquires late endosomal and lysosomal markers. However, since the number of streptococci residing within these compartments is declining over time, it can be speculated that this is a transient time dependent step in the intracellular trafficking process. This question was addressed in subsequent experiments (refer to chapter 4.4.2).

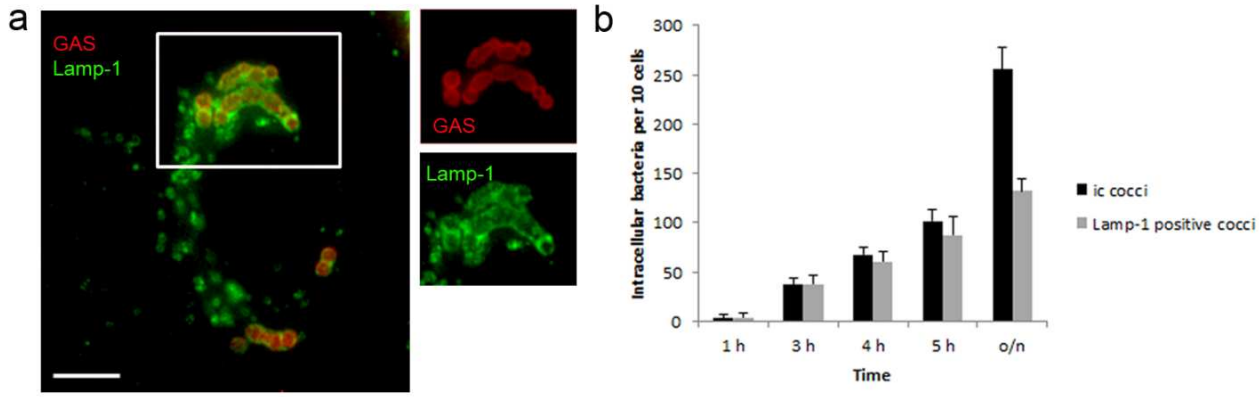

Figure 9: Co-localization of M1 GAS with late endosomal/lysosomal compartments

a. M1 GAS strain A527 (red) co-localizes with Lamp-1 (green), a marker for late endosomal/lysosomal compartments. The inserts show split channels for GAS (red) and Lamp-1 (green) of the indicated area in the merged image. Bar represents 5 µm.
b. Quantification of Lamp-1 association. The graph shows mean values ± SD of one out of three independent experiments. ic cocci: intracellular streptococci.

4.3.2 M1 GAS phagosomes fuse with terminal lysosomes

The results shown above indicate trafficking of M1 GAS along the endocytic route. However, due to the limitation of the Lamp-1 stain, one cannot distinguish between late endosomes and terminal lysosomes. This raised the question if this process eventually ends in fusion of phagosomes with terminal lysosomes. Therefore, HUVEC were pre-incubated with BSA-gold particles 18 h prior to infection. These are internalized into the cell by receptor-mediated endocytosis and, after trafficking along the endocytic route, are delivered into terminal lysosomes. After infection of HUVEC with M1 GAS, the samples were processed for FESEM. Gold-loaded lysosomes are detectable as white material localized within the perinuclear region of HUVEC (Figure 10a, left image white arrow heads; right image shows specific detection of nano gold particles with the EsB-detector due to higher material contrast of nano gold particles). At early infection points, gold-loaded lysosomes are clearly separated from invading streptococci (Figure 10a, white arrow heads indicate gold particles, white arrows indicate invading streptococci) whereas at later time points invading streptococci co-localize with gold-particles (Figure 10b, c left images). Furthermore, electron microscopic images reveal that invading streptococci move from the border of the cell towards the gold-loaded lysosomes which are still surrounding the nucleus of HUVEC (Figure 10b).

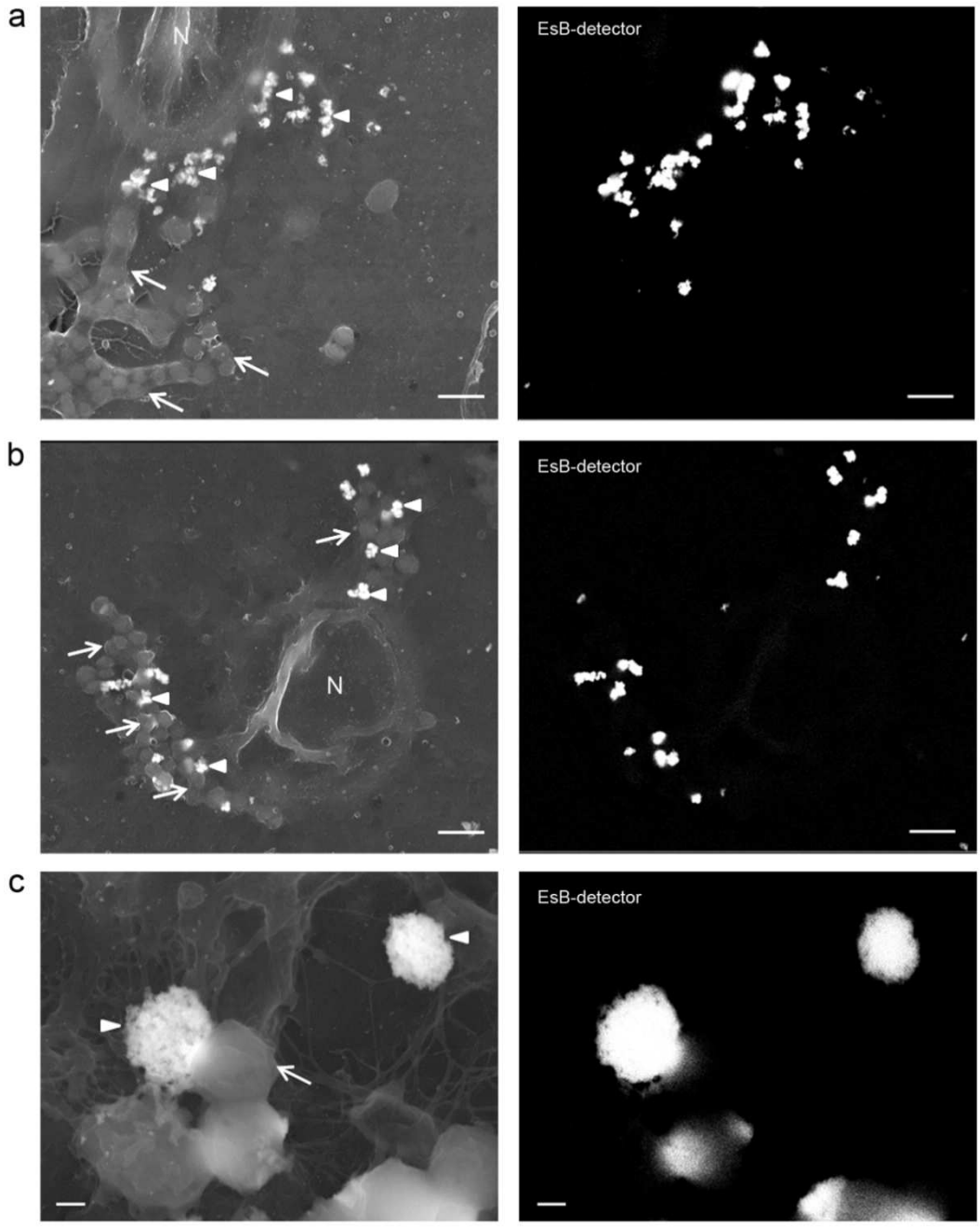

Figure 10: Co-localization of M1 GAS with gold particles indicates phagolysosomal fusion

Analysis of phagolysosomal fusion by FESEM. Prior to infection with M1 GAS, HUVEC lysosomes were pre-loaded with gold particles. Following infection, samples were analysed by FESEM. Right images show corresponding images of the EsB-detector channel used for specific detection of intracellular gold particles.
a. At early time points after infection intracellular streptococci (white arrows) are separated from gold particles (white arrow heads) which accumulate around the cell nucleus (N). Bars represent 2 µm.
b. At later time points invading M1 GAS (white arrows) co-localize with gold particles (white arrow heads). N: HUVEC nucleus. Bars represent 2 µm.
c. Co-localization of M1 GAS (white arrow) with gold particles (white arrow head) at higher magnification. Bars represent 200 nm.

Fusion of streptococci containing phagosomes with terminal lysosomes was further verified by transmission electron microscopy (Figure 11). Again HUVEC lysosomes were pre-loaded with gold particles followed by infection with M1 GAS. Within the cell gold particles are detectable as black and round electron dense material (Figure 11, white arrows). Ultra-thin sections of infected HUVEC layers show fusion events of streptococci with gold particles. At early time points streptococci are still separated from gold-loaded lysosomes (Figure 11, left image). Streptococci then move towards the gold particles (Figure 11, middle image) and at later time points a close co-localization of bacteria with gold particles is detectable (Figure 11, right image, white arrow).

Taken together, the results shown above demonstrate that, after invasion and incorporation into phagosomes, M1 GAS travels along the classical endocytic route and is finally fusing with terminal lysosomes. Thus, this process shows parallels to FbaB-mediated uptake and trafficking of serotype M3 GAS within endothelial cells (Amelung *et al.*, 2011). This is of specific interest since M1 GAS does not harbour the FbaB protein, which is responsible for M3 GAS invasion into HUVEC.

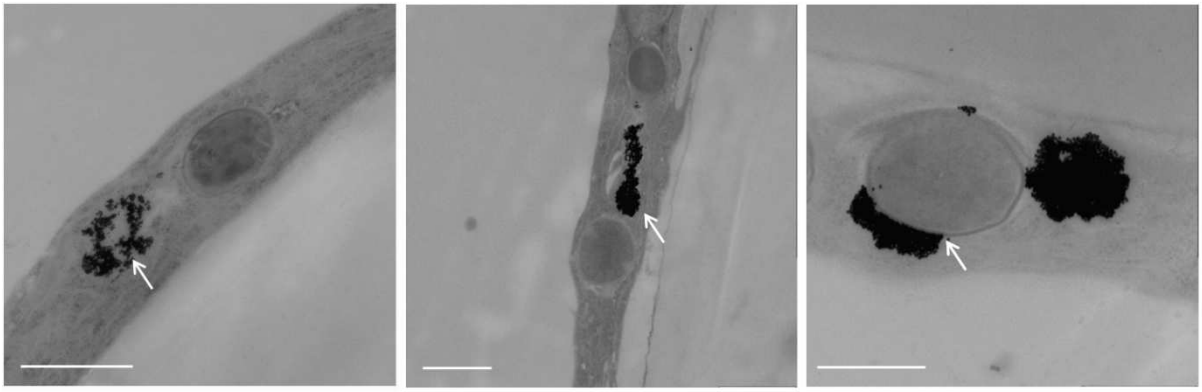

Figure 11: M1 GAS containing phagosomes fuse with terminal lysosomes

HUVEC lysosomes were pre-loaded with BSA-gold particles 18 h prior to infection. Following infection, ultrathin sections of infected HUVEC layers were prepared and analysed by TEM. Electron microscopic images show fusion of the M1 GAS containing phagosome with gold-loaded terminal lysosomes (white arrows). At earlier time points GAS and gold particles are clearly separated (left image). With increasing infection time, GAS and gold particles are found within close proximity (middle image) and finally closely associated and co-localized (right image). Bars represent 1 µm (left and middle image) and 500 nm (right image).

4.4. Intracellular survival of M1 GAS in HUVEC

Classical endocytic uptake processes lead to the delivery of foreign material into lysosomes followed by subsequent degradation and elimination by hydrolytic enzymes, like lipases and proteases (Flannagan *et al.*, 2012). To evade those host defence mechanisms, *S. pyogenes* developed several strategies to ensure its survival. SfbI-expressing streptococci invade target cells by caveolae aggregation and reside in caveosomes which exhibit no fusion with lysosomes and thereby ensure better streptococcal survival (Rohde *et al.*, 2003). Serotype M3 GAS, in contrast, traffics along the phagolysosomal route but induces its release at the basolateral side of the cell by a lysosomal exocytosis process, thereby escaping from the acidic degrading environment of the lysosomes (Talay, unbublished data). Since serotype M1 GAS is one of the most invasive serotypes causing the majority of severe tissue based diseases, the question of intracellular survival and the possible strategy of survival were investigated in further detail.

4.4.1 Quantification of intracellular survival

Bacterial viability staining of HUVEC layers after infection with M1 GAS indicates streptococcal survival within the cell. Immunofluorescence images of infected cell layers reveal live bacteria 5 h post infection (Figure 12a, left image, live bacteria labelled in green). Also after longer infection periods (10 h) at least 50% of the intracellular bacteria are viable (Figure 12a, right image). To quantify intracellular survival, HUVEC were infected with M1 GAS for an initial period of 3 h followed by killing of extracellular bacteria by the addition of antibiotics. After defined time points infected HUVEC were lysed and intracellular viable bacteria were plated. Quantification of survival rates by plating of HUVEC lysates confirms intracellular survival of M1 GAS within HUVEC (Figure 12b). However, one has to note that the bacterial counts are gradually declining over time, yielding $2x10^4$ cfu/ml 2 h post infection, $1,5x10^4$ cfu/ml 4 h post infection, $1x10^4$ cfu/ml 6 h post infection and $5x10^3$ cfu/ml after 9 h of infection (Figure 12b).

Taken together, both, viability staining and plating of HUVEC lysates, indicate that M1 GAS has evolved a strategy to ensure bacterial survival despite the innate defence mechanisms within the host cell.

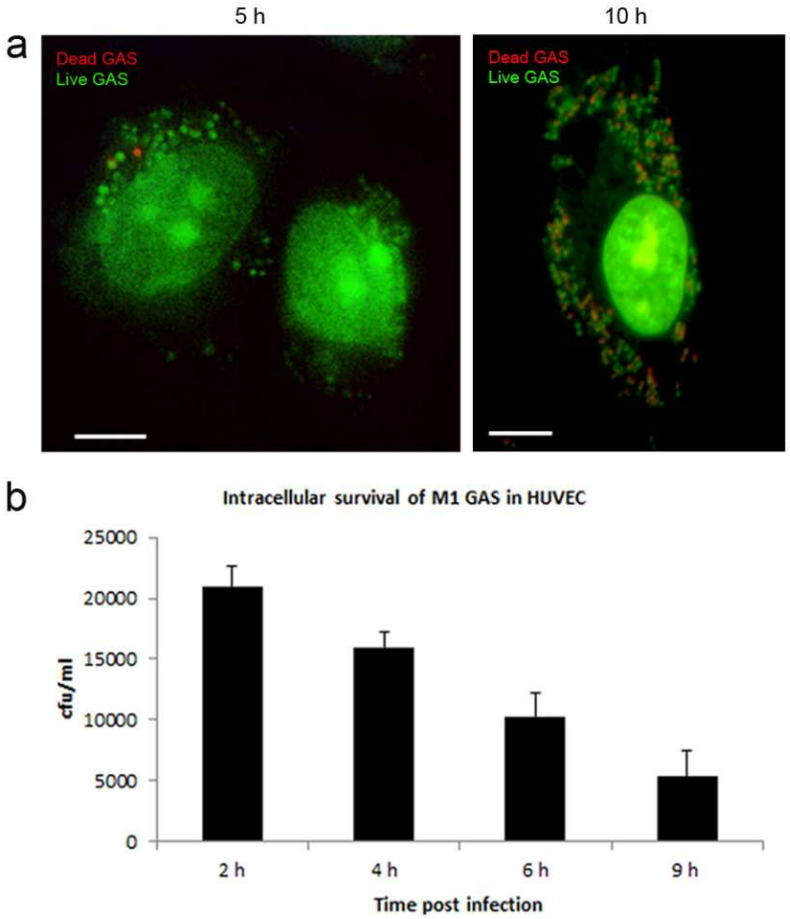

Figure 12: Intracellular survival of M1 GAS within HUVEC

a. Immunofluorescence analysis of the viability of M1 GAS following infection of HUVEC at varying time points. Viable bacteria are stained in green and dead bacteria are labelled in red. HUVEC nuclei also absorb the stain used and, therefore, also appear green. Immunofluorescence images demonstrate viability of intracellular streptococci at 5 h (left image) as well as at 10 h (right image) post infection. Bars represent 5 µm.
b. Quantification of survival rates of M1 GAS. Following infection and killing of extracellular bacteria, HUVEC lysates were plated after defined time points. Survival rates were calculated by enumerating viable bacteria. The graph shows mean values ± SD of triplicates from one representative experiment.

4.4.2 M1 GAS escapes from the phagolysosome into the cytoplasm

The capability of serotype M1 GAS to prevent its degradation within phagolysosomes raised the question how the bacteria mediate this process. To this end HUVEC layers were infected with M1 GAS for different time periods and ultrathin sections of infected HUVEC layers were analysed by transmission electron microscopy. Microscopic images reveal that M1 GAS escapes from the phagolysosomal compartments (Figure 13a, white arrow; Figure 13b) and resides free within the cytoplasm of the host cell (Figure 13a, c). This observation corroborates the findings of the Lamp-1 fluorescent staining which shows that only 50% of the intracellular streptococci co-localize with Lamp-1 after prolonged infection periods, also suggesting escape from phagolysosomal compartments (Figure 9b). In order to verify the cytoplasmic localization of M1 GAS, a staining technique was applied which specifically

visualises cellular membranes. The combined ferrocyanide and osmium tetroxide staining confirms the absence of any cellular membranes surrounding intracellular M1 GAS, giving further evidence of its cytoplasmic localization e.g. in direct proximity to the endoplasmic reticulum (Figure 13c). The electron microscopic images further support viability of intracellular GAS since streptococci seem morphologically intact and bacterial replication is evident.

These results demonstrate that M1 GAS ensures its survival by escaping from the acidic environment of the phagolysosomal compartment into the cytoplasm of the cell, thereby being protected from host cell defence processes.

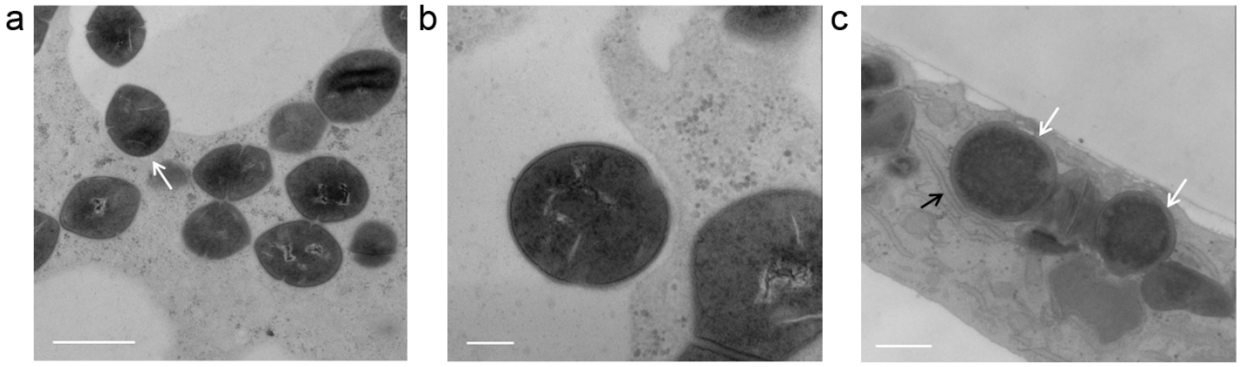

Figure 13: M1 GAS escapes from the phagolysosomal compartment

After infection of HUVEC cell layers with M1 GAS, ultrathin sections were prepared for TEM analysis.
a, b. TEM images of infected HUCEC cell layers show that streptococci escape from the membrane bound compartment of the phagolysosome (a, white arrow). Bars represent 1 µm (a) and 200 nm (b).
c. Free M1 GAS are localized within the cytoplasm (white arrows) of HUVEC in close proximity to the endoplasmic reticulum (black arrow). Bar represents 500 nm.

4.4.3 M1 GAS overcomes the endothelial cell barrier

The data shown above indicate successful survival of M1 GAS within endothelial cells. Since serotype M1 GAS is the leading cause of invasive diseases, the fate of intracellular streptococci had to be addressed next. The development of an invasive disease implies that, at some point, the pathogen is able to overcome endothelial cellular barriers. On this account it was speculated that M1 GAS transmigrates within HUVEC and emerges from the cell at the basolateral side ensuring its spread into deeper tissue layers. Thus, bacteria should be found within the lower compartment of the transwell insert. To test this hypothesis, confluent HUVEC layers were infected with M1 GAS. At defined time points after infection the medium of the lower well was plated and the colony forming units were calculated. Against the expectations plating experiments reveal that no streptococci are present in the lower well

even after 72 h of infection (Figure 14a). Electron microscopic analysis of HUVEC layers confirms the presence of intracellular streptococci (Figure 14b, white arrows). In order to further test the hypothesis of M1 GAS transmigration, infected HUVEC layers were removed from the transwell membrane and the bottom of the cell layer as well as the surface of the transwell membrane itself were analysed for the presence of streptococci. As shown in Figure 14c M1 GAS are present directly attached to the transwell membrane entangled within a mesh of gelatine and extracellular matrix components (Figure 14c, white arrows indicating M1 GAS, white arrow heads label the pores of the transwell membrane). In addition, it became apparent that, as infection progresses, increasing numbers of dead HUVEC are detectable within the intact HUVEC layer (Figure 14d). This observation gives reason for speculation that M1 GAS escape is accompanied with cell lysis. However, since these are preliminary observations the exact mechanism of escape has to be addressed in further detail in subsequent studies.

Taken together, survival of M1 GAS within endothelial cells can be demonstrated. Furthermore, the results indicate that M1 GAS possesses the potential to transmigrate over the endothelial cell barrier via the basolateral side of the HUVEC cells.

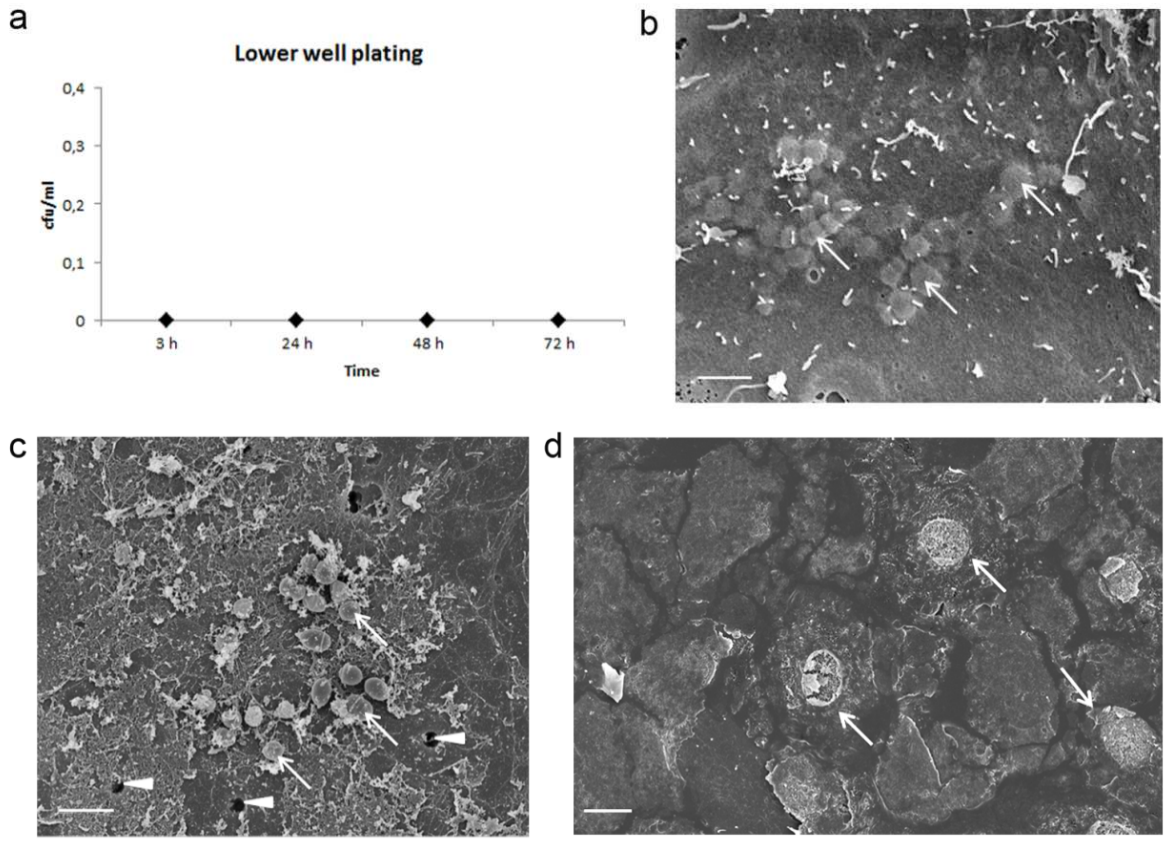

Figure 14: M1 GAS transmigrate through the endothelial cell barrier

a. Plating of streptococci within the lower compartment of the transwell at different time points after infection.
b. Following infection, the presence of intracellular streptococci (white arrows) is confirmed by FESEM demonstrating successful invasion of M1 GAS into HUVEC. Bar represents 2 µm.

c. After removal of the HUVEC layer, M1 GAS (white arrows) are found directly bound to the transwell membrane indicating escape from the cell at the basolateral side. White arrow heads indicate the pores of the transwell membrane. Bar represents 2 µm.
d. FESEM image reveals the presence of dead HUVEC within the cell layer suggesting that M1 GAS escape is accompanied by cell lysis. Bar represents 10 µm.

4.5 Identification of the bacterial factor that determines EC interaction

The data described in the previous chapters show that serotype M1 GAS has evolved strategies to ensure its survival within endothelial cells. Although traditionally viewed as an extracellular pathogen, it successfully invades into endothelial cells, prevents its degradation by hydrolytic enzymes within lysosomes and transmigrates through the endothelial cell barrier to reach deeper tissue layers. However, the bacterial factor or factors that mediate this invasion process remained unidentified. Unlike serotype M3 GAS, in which the fibronectin-binding protein FbaB was identified as the EC invasin (Amelung *et al.*, 2011), serotype M1 GAS lacks this specific protein on its cell surface. Therefore, a series of pre-existing knock-out mutants (GAS 90-226 Δ*emm1*; KTL3 *grab* ko; KTL3 *prtS*::*spc*; KTL3 *slo*::*spc*; KTL3 pJRS 233-Δ*sagA*) was tested in loss of function assays (data not shown). These assays identified the M1 surface protein as a promising candidate. Its role during invasion into EC was analysed in further detail in the following. Previously, Dombek and colleagues have demonstrated that the M1 knock out mutant is deficient in invasion of epithelial cells (Dombek *et al.*, 1999).

4.5.1 Characterization of the GAS M1 knock out mutant strain

Prior to the functional analysis of the M1 protein as the EC invasin, the existing *S. pyogenes* (90-226 ΔM1) M1 knock out mutant strain (Zimmerlein *et al.*, 2005) was characterised and verified for lack of expression of the M1 protein.

First, the expression of the M1 protein on the surface of the M1 knock out mutant strain (90-226 Δ*emm1*) was analysed in comparison to the corresponding wild type M1 GAS strain (90-226 wt). By immunofluorescence staining with a specific α-M1 primary antibody and a labelled secondary antibody the M1 protein is visualised on the surface of the M1 wt GAS stain (Figure 15a, left images). In contrast, as expected, the M1 knock out mutant fails to express the M1 protein on its surface (Figure 15a, right images).

As it is known that the M1 protein of GAS binds several human plasma components, the expression of the M1 protein can be assessed indirectly by analysis of the binding capabilities of the M1 wild type and the M1 knock out mutant strain in a plasma absorbance assay. Following incubation of both strains with human plasma, bound plasma proteins were

eluted with glycine/HCl and were analysed by SDS-PAGE. Figure 15b shows the coomassie stained SDS-gel. The M1 expressing wild type GAS strain binds human albumin, the heavy chain of IgG, fibrinogen and plasminogen, whereas the M1 knock out mutant fails to bind any of these plasma proteins, indicating lack of the M1 protein on its surface (Figure 15b).

As binding of the M1 wild type strain with the light chain of human IgG is not detectable in the SDS-gel, IgG binding was assessed additionally in a radioactive IgG binding assay. Following incubation of the M1 wild type and the M1 knock out mutant with radioactively labelled human IgG, the potential binding was assessed by measuring the radioactive radiation emitted from the bacterial pellets. As shown in Figure 15c the M1 wild type GAS strain binds 75% of the radioactive labelled IgG. In contrast, binding of human IgG is significantly reduced in the mutant strain lacking the M1 protein on its surface.

The results shown above verify the absence of the M1 protein in the M1 knock out mutant which was then used for functional analysis of the M1 protein as a potential invasin.

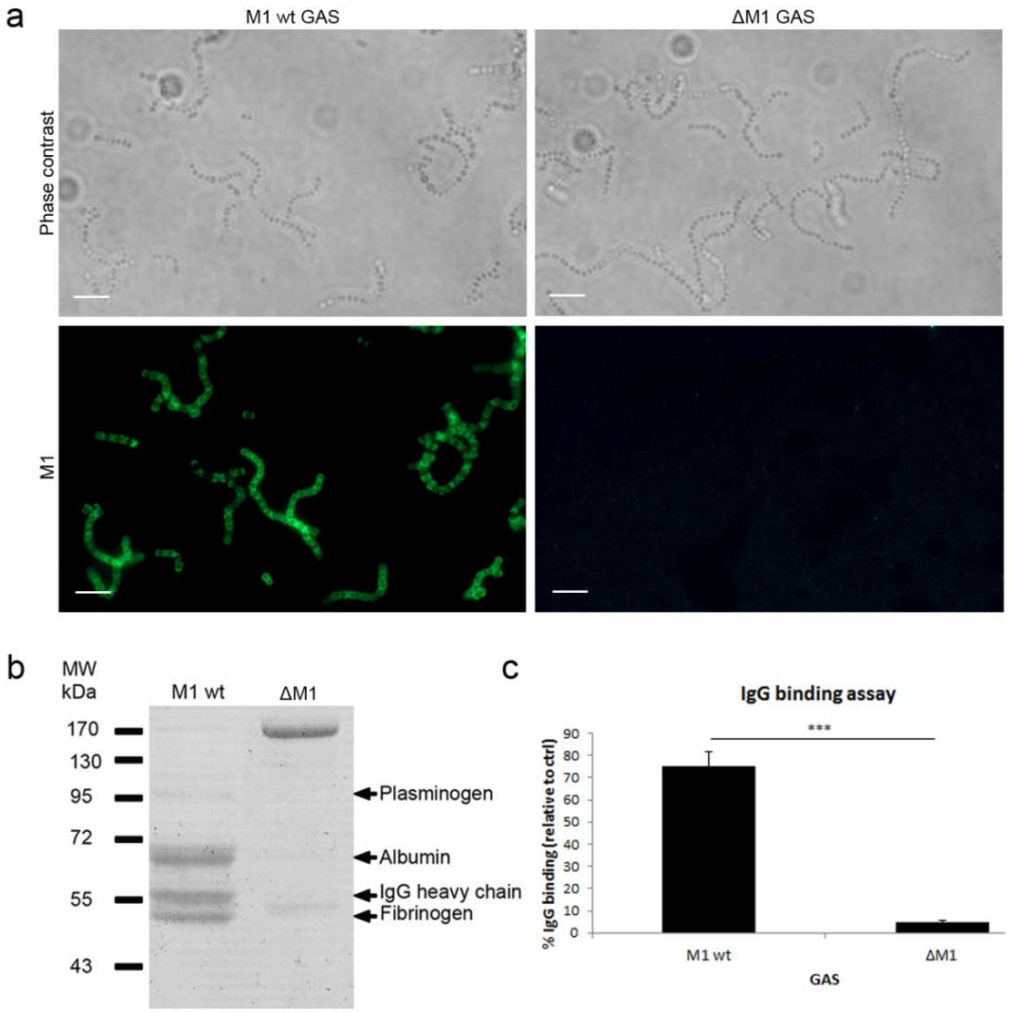

Figure 15: Serotype M1 GAS lacking the M1 surface protein fails to bind human plasma components

a. Analysis of the expression of surface bound M1 on GAS by immunofluorescence staining of the M1 protein. In contrast to the wild type strain (M1 wt GAS, left images), the M1 knock out mutant strain (ΔM1 GAS; right images) shows no expression of the M1 protein (green) on its surface. Bars represent 5 µm.
b. Plasma absorbance assay analysing the binding capacities of GAS strains to human plasma components. The M1 wild type strain (M1 wt) binds plasminogen (faint band with a molecular weight of 95 kDa), albumin, IgG and fibrinogen (arrows). In contrast, the M1 knock out mutant (ΔM1) shows no binding to these plasma proteins. MW: molecular weight
c. Radioactive IgG binding assay. In comparison to the M1 wt strain IgG binding is significantly reduced in the M1 knock out mutant strain. The graph shows mean values ± SD of one experiment done in triplicates.

4.5.2 The M1 protein of *S. pyogenes* is crucial for efficient invasion of GAS into HUVEC

After verification that the M1 knock out mutant could be used to analyse whether the M1 protein represents the invasin of serotype M1 streptococci, loss of function/gain of function infection assays with HUVEC cells were performed. The invasion potential of the M1 protein on EC was analysed by infection of HUVEC with the M1 expressing wild type GAS strain and its isogenic M1 knock out mutant strain. After infection, cell layers were stained differentially for extra- (green-yellow) and intracellular (red) streptococci and samples were assessed by immunofluorescence microscopy.

Figure 16 shows the results of the infection assay on HUVEC. *S. pyogenes*, expressing the M1 protein on its surface, efficiently invades HUVEC with invasion rates of 179 intracellular streptococci per 10 cells 4 h post infection (Figure 16b, M1 wt). In contrast, the invasion of the M1 knock out strain, lacking the M1 protein, is significantly reduced (Figure 16b, ΔM1). By complementation of the deleted *emm1* gene by episomal expression of the M1 protein, the wild type phenotype is restored, yielding internalization rates comparable to that of the wt M1 GAS strain (Figure 16b, compl. ΔM1). Likewise immunofluorescence images of infected HUVEC layers show that the M1 knock out mutant strain is deficient for invasion of HUVEC (Figure 16a, middle image ΔM1 GAS). In comparison both, the M1 wild type GAS strain and the complemented M1 knock out mutant, successfully invade HUVEC (Figure 16a, left and right image respectively).

To further verify the essential role of the M1 protein during the invasion process of GAS into HUVEC, blocking experiments were performed. Prior to infection of HUVEC, streptococci were pre-incubated with increasing concentrations of an α-M1 specific antibody or a control antibody. Following infection, the samples were stained for intra- and extracellular streptococci. In comparison to untreated control bacteria or streptococci treated with a non-M1 specific control IgG, pre-incubation of bacteria with a M1 specific antibody significantly reduces invasion in a concentration dependent manner (Figure 16c).

The data of the infection and blocking assays identified the M1 surface protein of GAS as a crucial factor during the invasion process into endothelial cells. However, it remains to be

clarified if it is the sole factor that mediates streptococcal uptake into EC. In the following its role as a potential invasin on EC was analysed in further detail.

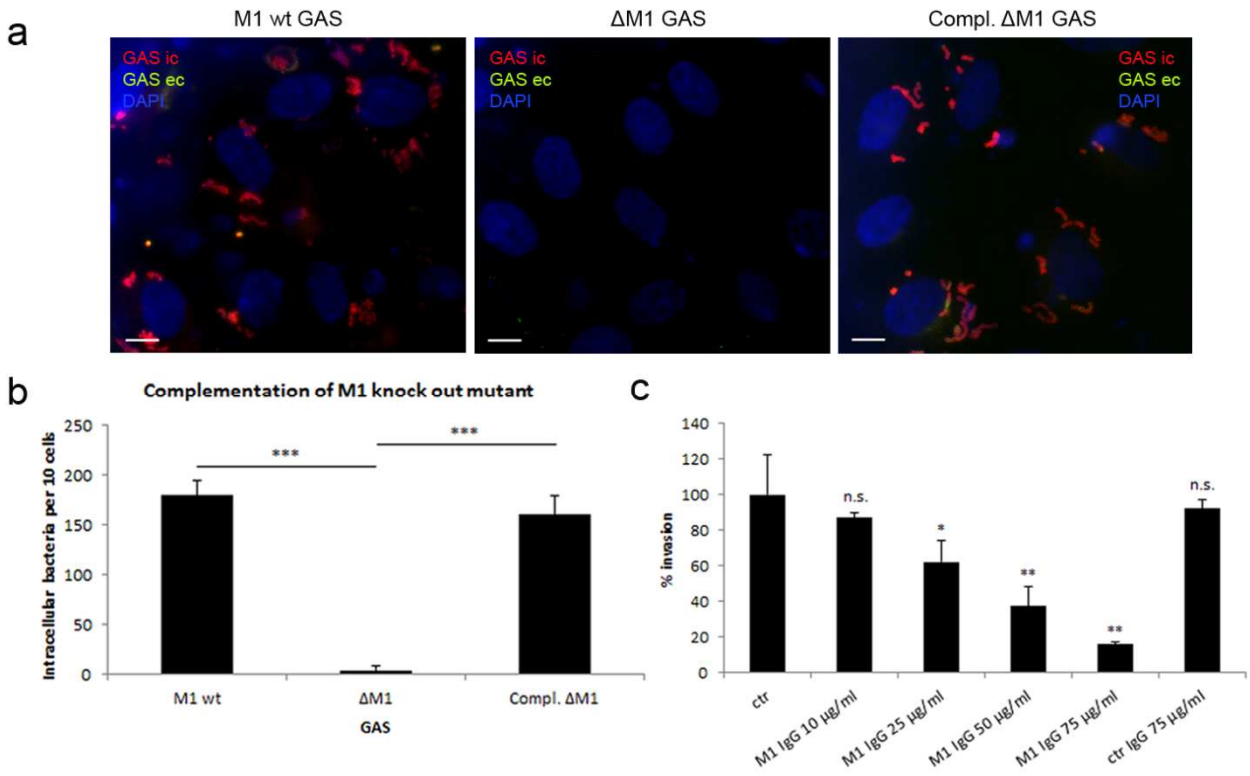

Figure 16: The M1 knock out mutant is deficient for invasion of HUVEC

a. Fluorescence images of HUVEC infected with the M1 wt stain (left image), the ΔM1 knock out mutant (middle image) and the complemented ΔM1 knock out mutant (right image) for 4 h. Intracellular bacteria are depicted in red, extracellular bacteria are shown in green-yellow. HUVEC nuclei are depicted in blue. Bars indicate 20 µm.
b. Internalization rates of the M1 wt GAS strain (strain A766), its isogenic M1 knock out mutant ΔM1 GAS (A767) and the ΔM1 mutant complemented with an *emm1* carrying plasmid (compl. ΔM1 GAS) into HUVEC (4 h post infection). Compared to the M1 wt strain, the ΔM1 knock out mutant is deficient for invasion of HUVEC. After complementation of the ΔM1 GAS strain with *emm1*, bacterial uptake into HUVEC is restored. The graph represents mean values ± SD of one representative out of three independent experiments.
c. Pre-incubation of HUVEC with a polyclonal α-M1 specific antibody significantly reduces invasion of M1 GAS into HUVEC in a concentration dependent manner. Untreated HUVEC and HUVEC treated with a non-M1 control antibody (ctr IgG) served as negative controls. The graph shows mean values ± SD of one out of three independent experiments.

4.5.3 The M1 protein mediates internalization of latex beads into HUVEC

To exclude the involvement of any endogenous streptococcal factors in the invasion process, the invasive properties of the M1 protein were further characterised by latex bead internalization assays. Latex beads with a size of 3 µm are non-invasive and are naturally not internalized into HUVEC. In the following it should be tested if the presence of purified M1 protein on the surface of latex beads promotes uptake of latex beads into HUVEC.

Therefore, the *emm1* gene, omitting the sequence of the signal peptide and the membrane anchor, was amplified, cloned and transformed into *E. coli*. Following overexpression of M1 in *E. coli*, recombinant M1 protein was purified and coated onto latex beads. Latex beads coated with GST protein served as a negative control. The coating efficiency was verified by FACS analysis to ensure successful coating of latex beads with recombinant M1 and GST protein (data not shown). Coated latex beads were then incubated with HUVEC for varying time periods. Following fixation, intra- and extracellular latex beads were stained and the invasion potential of M1 was assessed by immunofluorescence microscopy.

Microscopic samples show that M1-coated latex beads are internalized into HUVEC in a time dependent manner (Figure 17a) and are detectable within the cell surrounding the nucleus (Figure 17b, white arrows). In contrast, GST-coated latex beads are not internalized (Figure 17a). As seen for the M1 wt GAS strain, M1-coated latex beads induce the formation of membrane protrusions which enclose the latex beads (Figure 17c, white arrow heads) until they are completely engulfed by the host cell membrane and internalized into the host cell (Figure 17d). Internalized M1-coated latex beads, like the M1 wt GAS strain, follow the endocytic pathway. M1-coated latex beads induce the accumulation of the late endosomal/lysosomal marker protein Lamp-1 (Figure 17e). Due to the acidic environment within the phagolysosome, the M1 protein on the surface of latex beads is degraded, thus, intracellular latex beads lose their red immunofluorescence stain and appear green. Finally, phagosomes containing M1-coated latex beads fuse with terminal lysosomes as demonstrated by co-localization with gold particles (Figure 17f).

Taken together, the results of the gain of function experiments demonstrate that the M1 protein is sufficient for effective invasion into HUVEC and, therefore, represents the M1 serotype invasin into endothelial cells.

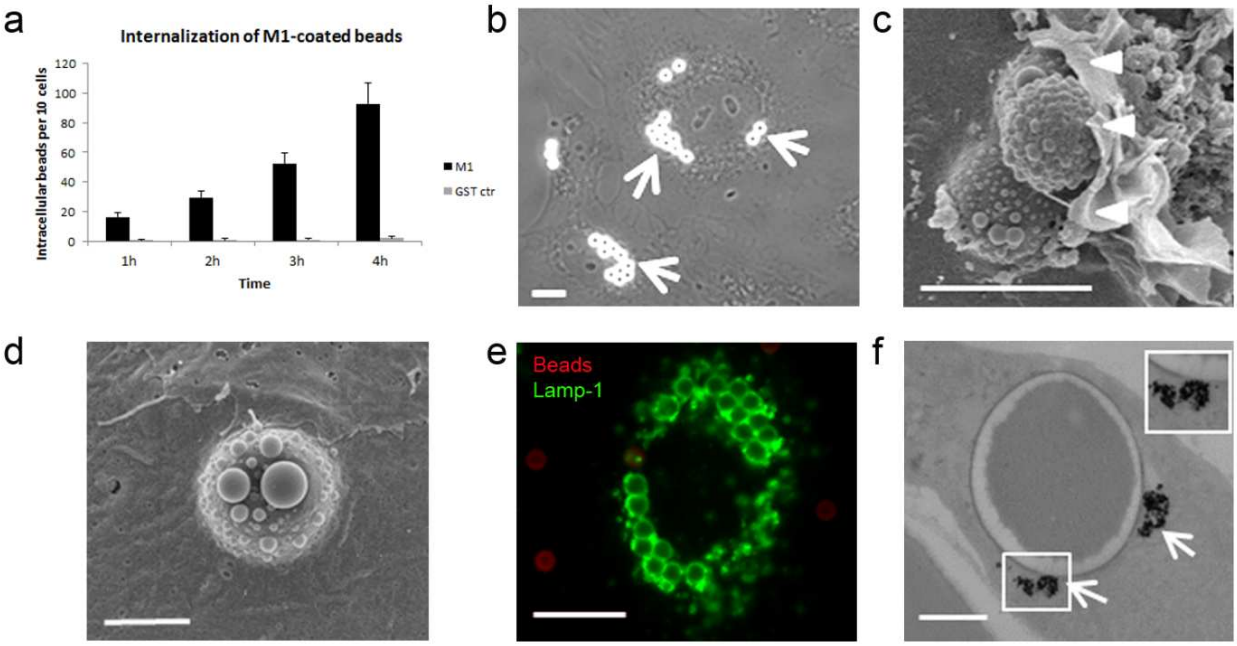

Figure 17: The M1 protein of *S. pyogenes* triggers invasion into HUVEC

Analysis of the invasion potential of M1 by latex bead internalization assays. HUVEC were co-incubated with M1-coated latex beads as well as GST-coated latex beads as negative control. Following infection, the samples were processed for immunofluorescence or electron microscopic analysis.
a. Quantification of internalization of M1- and GST-coated latex beads into HUVEC at varying time points. In contrast to the negative GST-control beads, M1-coated latex beads are internalized into HUVEC in a time dependent manner. The graph shows mean values ± SD of one representative out of three independent experiments.
b. Phase contrast showing HUVEC containing intracellular M1-coated latex beads (white arrows) 60 min post infection. Bar represents 10 µm.
c. FESEM image demonstrating that M1-coated latex beads trigger actin cytoskeletal rearrangements and engulfment of latex beads by host cell membranes 90 min post infection (white arrow heads). Bar represents 5 µm.
d. FESEM of one M1-coated latex bead completely internalized into HUVEC (90 min post infection). Bar represents 2 µm.
e. M1-coated latex beads (red) co-localize with Lamp-1 (green) 4 h post infection. Within the acidic environment of phagolysosome the M1 protein on the surface of latex beads is degraded, thus, intracellular latex beads lose their red immunofluorescence stain and appear green. Bar represents 10 µm.
f. TEM analysis of ultrathin section of HUVEC pre-incubated with BSA-gold particles followed by co-incubation with M1-coated latex beads. Latex beads closely associate with gold particles (white arrows) 12 h post infection indicating fusion of the phagosome with terminal lysosomes. Bar indicates 1 µm.

4.5.4 The M1 protein mediates invasion of *Lactococcus lactis* into HUVEC

Finally, the invasive properties of the M1 protein were further analysed in a bacterial heterologous expression system. *L. lactis* served as a suitable model organism as it is a gram-positive, non-pathogenic bacterium and naturally does not invade human endothelial cells. In the following it should be tested whether the expression of the M1 protein on the surface can convert *L. lactis* into an invasive strain. Two *L. lactis* strains, one expressing the M1 protein heterologous on its surface and the parental wt strain lacking the M1 protein were

kindly provided by Prof. Dr. P. Cleary, Minneapolis, USA (Cue *et al.*, 2001). 16 s rRNA sequencing confirmed that both strains were indeed *L. lactis* strains (data not shown). Furthermore, immunofluorescence analysis confirmed the expression of the M1 protein in the *L. lactis* strain carrying the *emm1* gene whereas in the parental wt strain no expression of M1 was detectable (data not shown). Following verification, both strains were used in infection assays on HUVEC. Infected HUVEC layers were stained for intracellular lactococci by immunofluorescence.

Immunofluorescence analysis of infected HUVEC cell layers confirms that the parental *L. lactis* strain is non-invasive in HUVEC (Figure 18, right bar labelled -M1). In contrast, expression of the M1 protein significantly increases the invasiveness of *L. lactis*, yielding invasion rates of around 60 bacteria per 10 cells (Figure 18, left bar labelled +M1).

These data, together with the results of the experiments described above, clearly identify the M1 protein as a major streptococcal invasin on endothelial cells. In addition, these results demonstrate that the M1 protein alone is sufficient to mediate efficient uptake into HUVEC.

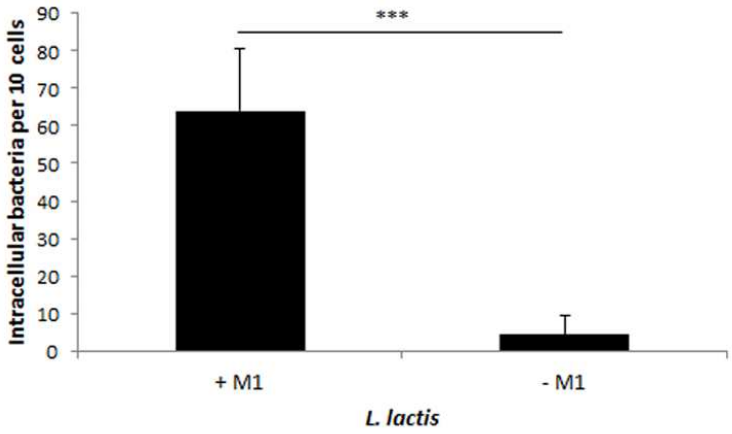

Figure 18: The M1 protein of *S. pyogenes* mediates invasion of lactococci into HUVEC

Quantification of invasion rates of *L. lactis* strains in HUVEC 3 h post infection. Following infection, intra- and extracellular lactococci were stained differentially. *L. lactis* expressing the M1 protein invades into HUVEC. In contrast, the parental wt strain, which lacks the M1 protein on its surface, is non-invasive in HUVEC. The graph shows mean values ± SD of one out of three independent experiments.

4.5.5 Dead M1 GAS are also internalized into HUVEC

In addition to infections with live M1 GAS, infection assays with dead bacteria were also performed. Prior to infection of HUVEC, M1 GAS were heated for 30 min at 95℃ to kill all streptococci. Then HUVEC were infected with heat-killed M1 GAS for varying time periods ranging from 2 h to 5 h. The internalization of M1 GAS into HUVEC was assessed by immunofluorescence microscopy and determination of the number of intracellular bacteria. As depicted in Figure 19, heat-killed M1 GAS are also internalized into HUVEC in a time dependent manner with invasion rates of 180 intracellular streptococci per 10 cells 5 h post infection.

The uptake of dead streptococci indicates that the cellular uptake process of M1 GAS does not require live bacteria or secretion of any effector molecules. In addition, HUVEC, as non-professional phagocytic cells, are able to efficiently internalize M1 GAS depicting the strong potential of M1 as an invasin even in its denatured state.

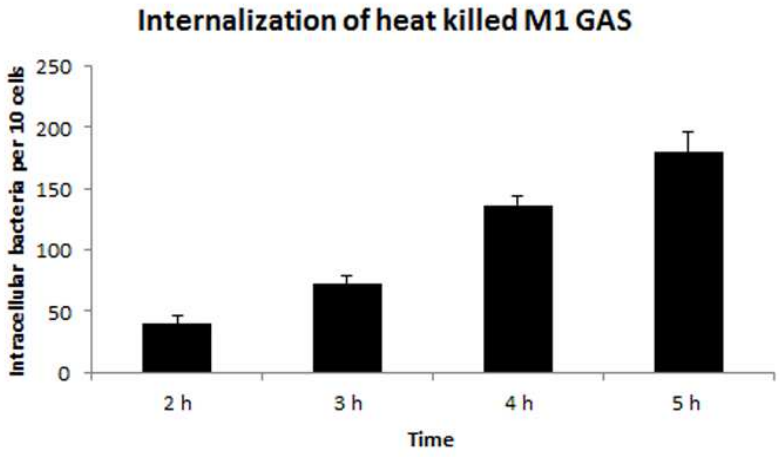

Figure 19: Internalization of heat-killed M1 GAS into HUVEC

HUVEC were infected with heat-killed M1 GAS. Uptake of streptococci into HUVEC was assessed by immunofluorescence staining of intra- and extracellular bacteria. As seen for live bacteria heat-killed M1 GAS strains are also internalized into HUVEC in a time dependent manner. The graph shows mean values ± SD of one representative experiment performed in triplicate.

4.6 Identification of host cell factors that mediate M1 GAS invasion into HUVEC

The basis for actin cytoskeletal rearrangements as triggered by M1 GAS during invasion of HUVEC is the engagement of a cellular receptor and the activation of specific signalling cascades within the host cell which lead to engulfment and internalization of M1 GAS into HUVEC. Next, experiments were performed which aimed to identify cellular factors in particular the cellular receptor and intracellular signalling molecules involved in the invasion process of M1 GAS into HUVEC.

4.6.1 Engagement of beta1-integrins during invasion of M1 GAS into HUVEC

One known host cell receptor involved in invasion of M1 GAS is the family of integrins (Cue *et al.*, 1998). Integrins are heterodimeric glycoprotein receptors consisting of one alpha and one beta subunit. To date, 18 alpha and 8 beta integrin subunits have been identified. Integrins are involved in signal transduction of various cellular processes including organization of the actin cytoskeleton, cell survival, cell proliferation and cell motility (Schwartz *et al.*, 1995, Cary *et al.*, 1999, Hynes, 2002) which makes them an attractive receptor for M1 protein mediated streptococcal uptake.

Next the involvement of integrins in the invasion of M1 GAS into HUVEC was assessed. HUVEC were pre-incubated with monoclonal antibodies against specific alpha and beta integrin subunits. Following pre-incubation, HUVEC were infected with M1 GAS for 2 ½ h and samples were processed for immunofluorescence microscopy. Figure 20a shows the effect of integrin subunit blocking on M1 GAS invasion into HUVEC. Blocking of the α_1- or α_2-integrin subunit has no significant effect on the invasion of M1 GAS into EC. In comparison to the untreated control, invasion rates of more than 90% are observed in these samples. Blocking of the β_1-integrin subunit, however, significantly reduces streptococcal invasion to 56% (Figure 20a). Immunofluorescence images show that β_1-integrins are evenly distributed across the surface of HUVEC (Figure 20b, β_1-integrin labelled in green). In contrast, upon streptococcal invasion, clustering of the β_1-integrins is detectable in the close vicinity of invading streptococci, giving evidence for an outside-inside signalling event (Figure 20b, white box).

The results of the integrin blocking experiments, together with the observation of β_1-integrin subunit clustering around invading streptococci, indicate that M1 GAS induces the activation of host cell integrins. However, further experiments need to be done to clarify which integrin heterodimer is engaged during this process.

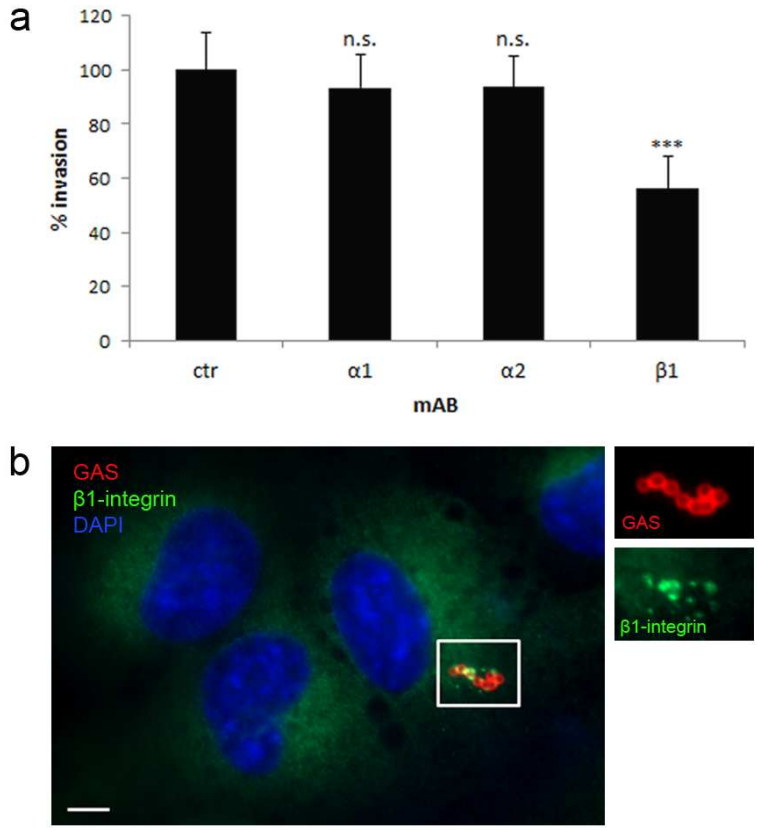

Figure 20: Beta1-integrins are involved in the invasion of M1 GAS into HUVEC

Analysis of the involvement of specific integrin subunits in the invasion of M1 GAS into EC.
a. Quantification of M1 GAS invasion following blocking of the α_1-, α_2- or β_1-integrin subunits by pre-incubation of HUVEC with specific monoclonal antibodies. Blocking of the β_1 subunits significantly reduces streptococcal invasion to 50%. In contrast, neither the α_1 nor α_2 subunit seem to be engaged during M1 GAS invasion as blocking either of those has no effect on invasion rates. n.s.: non-significant
b. Immunofluorescence staining of β_1-integrins on the surface of HUVEC. M1 GAS (red) induces the accumulation of the β_1-integrin subunit (green) around invading streptococci. Inserts show enlarged sections of split channels (GAS in red and β_1-integrin in green) of the indicated area in the merged image. EC nuclei are depicted in blue. Bar represents 5 µm.

4.6.2. Involvement of phospholipase C, protein kinase C and intracellular calcium in the invasion of M1 GAS into HUVEC

The results of the experiments described in the previous chapters highlight that M1 GAS entry into HUVEC comprises features of the classical phagocytic uptake machinery, in particular actin cytoskeletal rearrangements and accumulation of F-actin. During phagocytic uptake of foreign material, receptor engagement leads to the activation of membrane bound phospholipase C which hydrolyses phosphatidylinositol-4,5-bisphosphate ($PI(4,5)P_2$) to diacylglycerol (DAG) and inositol-3,4,5-trisphosphate (IP_3) (Steinberg *et al.*, 2008, Flannagan *et al.*, 2012, Sarantis *et al.*, 2012). IP_3 in turn induces the release of calcium from intracellular stores like the endoplasmic reticulum (Nunes *et al.*, 2010, Sarantis *et al.*, 2012). Intracellular calcium acts as a second messenger and in turn activates protein kinase C and additional

downstream signalling molecules for example small GTPases. These either directly or indirectly induce the re-organization of the actin cytoskeleton and engulfment of foreign material into membrane-bound compartments (Steinberg *et al.*, 2008, Botelho *et al.*, 2011, Flannagan *et al.*, 2012).

Next, it was investigated whether host cell signalling molecules of the phagocytic uptake machinery are also involved in M1 protein mediated streptococcal invasion. Therefore, HUVEC were pre-treated with different chemicals specifically inhibiting single signalling molecules. To specifically impair phospholipase C, HUVEC were pre-incubated with edelfosine. The amount of intracellular calcium within HUVEC was reduced by incubation of HUVEC with the calcium chelating agent BAPTA-AM. A third inhibitor, calphostin C, was used to specifically target protein kinase C. All inhibitors were diluted in DMSO. To exclude any negative effects of the solvent on M1 GAS invasion, HUVEC were also pre-treated with DMSO alone. After pre-treatment HUVEC were infected with M1 GAS for 3 h and afterwards intra- and extracellular streptococci were stained differentially.

Pre-treatment of HUVEC with edelfosine, inhibiting phospholipase C, significantly reduces the invasion of M1 GAS to 16% (Figure 21a). In addition, incubation of HUVEC with the calcium chelator BAPTA-AM completely abolished streptococcal invasion. Inhibition of protein kinase C with calphostin C also significantly reduces the invasion of M1 GAS by 80% (Figure 21a). Immunofluorescence analysis further confirms that, compared to the DMSO treated control (Figure 21b), inhibition of protein kinase C (Figure 21c) and reduction of intracellular calcium (Figure 21d) results in reduced numbers of intracellular streptococci.

The data demonstrate that phospholipase C, intracellular calcium and protein kinase C are involved in the invasion process of M1 GAS into EC since inhibiting either of those significantly reduces or completely abolishes streptococcal internalization. In addition, the results indicate that M1 GAS exploits the phagocytic uptake machinery of EC to ensure internalization into the host cell and protection from the immune system of the host.

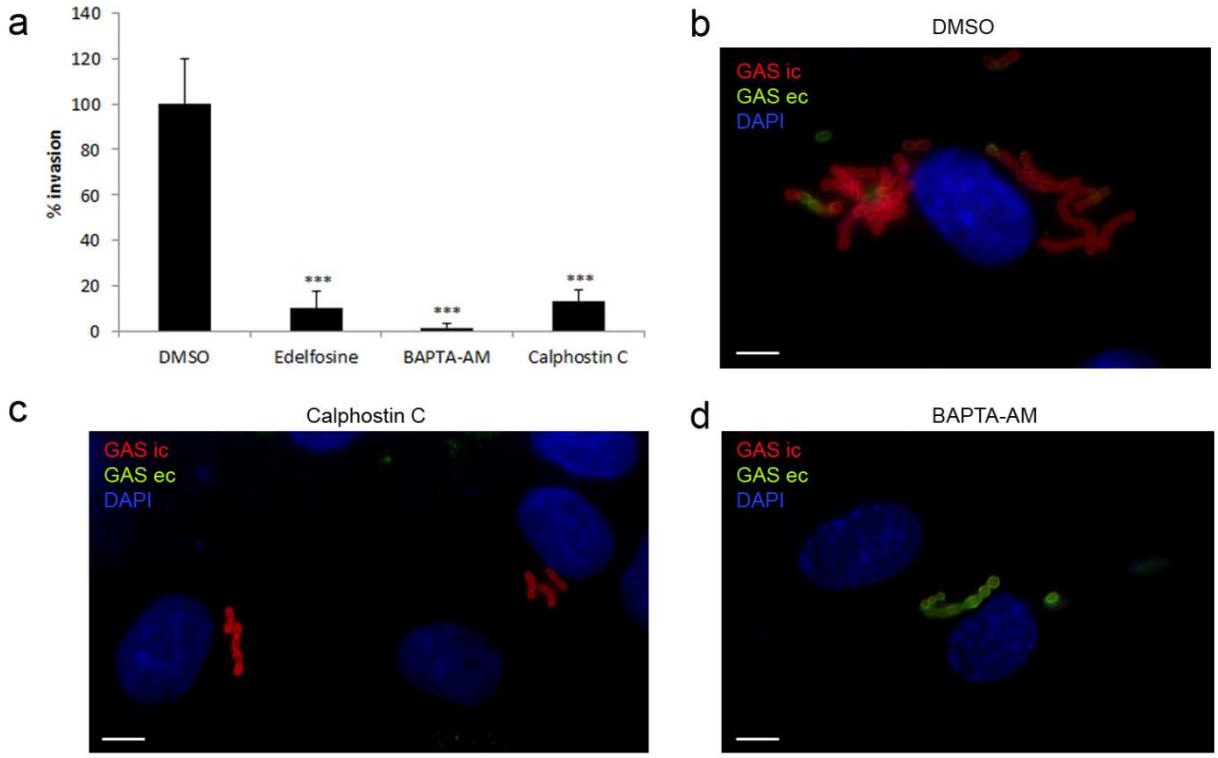

Figure 21: M1 GAS induces phagocytic-like uptake into HUVEC

Specific inhibitors were used to interfere with host cell signalling molecules known to be involved in classical phagocytosis. HUVEC were pre-treated with edelfosine [20 µM], BAPTA-AM [25 µM] and calphostin C [2 µM] for 30 min to inhibit phospholipase C, release of intracellular calcium and protein kinase C respectively. Pre-treated HUVEC were then infected with M1 GAS for 3 h.
a. Quantification of invasion rates. Pre-treatment of HUVEC with edelfosine, BAPTA-AM and calphostin C significantly reduces or completely abolishes M1 GAS mediated uptake into EC. The graph shows mean values ± SD of one representative experiment out of a total of three independent experiments.
b-d. Fluorescence images show less intracellular streptococci in HUVEC when treated with calphostin C (c) and BAPTA-AM (d) when compared to DMSO treated control cells (b). Intracellular bacteria are depicted in red, extracellular bacteria are shown in green-yellow. HUVEC nuclei are depicted in blue. Bars represent 5 µm.

4.7 Infection assays with lung and dermal endothelial cells

4.7.1 Serotype M1 GAS invades into different primary human endothelial cell types

The loss of function/gain of function experiments demonstrate the potential of M1 to act as an invasin on primary endothelial cells. This raised the question whether invasion is restricted to endothelial cells of the human umbilical cord or if invasion into other human endothelial cells might constitute a common mechanism employed by serotype M1 GAS.

Therefore, infection experiments were performed using primary human lung endothelial cells (HPMEC) as well as primary human dermal lymphatic endothelial cells (HDLEC). These cells were infected with M1 GAS as previously described for HUVEC. Afterwards, infected cell layers were processed for immunofluorescence as well as field emission scanning electron microscopy.

The results of the microscopic analysis are depicted in Figure 22. M1 GAS is also able to efficiently invade into human lung endothelial cells (Figure 22a). Similar to invasion into HUVEC, M1 GAS triggers the formation of membrane protrusions tightly engulfing streptococci and subsequent zipper-like uptake into HPMEC (Figure 22a, left FESEM image, white arrow heads indicate membrane ruffles). Immunofluorescence staining of infected cell layers confirms the presence of intracellular streptococci within EC (Figure 22a, right immunofluorescence (IF) image). In addition, also primary human dermal lymphatic endothelial cells represent potential target cells for M1 GAS, as infection assays using these cells also demonstrate invasion of M1 GAS in a time dependent manner (Figure 22b).

In conclusion, the results of the infection experiments described above demonstrate that endothelial cells in general represent target cells for M1 GAS invasion. Thus, invasion into endothelial cells possibly constitutes a common mechanism of M1 GAS to evade the host immune system and reside intracellular.

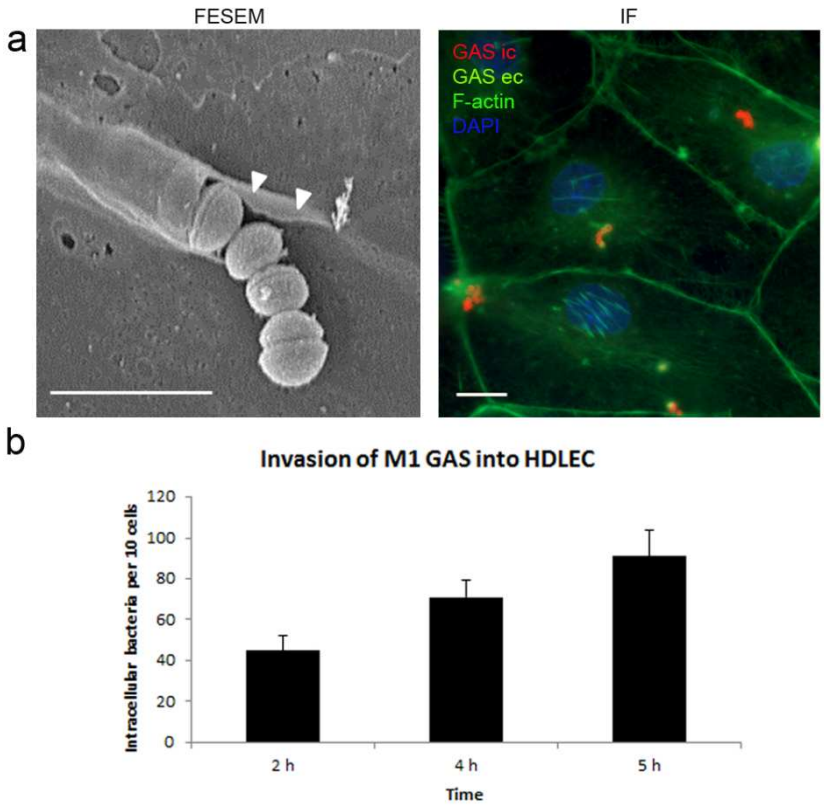

Figure 22: M1 GAS invades into HPMEC as well as HDLEC

Analysis of the invasion potential of M1 GAS on different EC by immunofluorescence microscopy (IF) and FESEM.

a. Upon infection M1 GAS induces rearrangements (left image, white arrow heads) of the actin cytoskeleton and zipper-like uptake into HPMEC. Immunofluorescence staining of intra- (red) and extracellular (green-yellow) streptococci confirms invasion of M1 GAS into HPMEC (right image). The actin cytoskeleton is depicted in green. Bars represent 2 µm (left image) and 10 µm (right image).

b. Quantification of invasion of M1 GAS into primary human dermal endothelial cells (HDLEC) after varying time points. The graph represents mean values ± SD of one representative experiment out of three independent experiments.

4.7.2 *Ex vivo* infection of human endothelium with M1 GAS

In order to verify the invasiveness of M1 GAS on endothelial cells within human tissue, human endothelium was infected with M1 GAS *ex vivo*. Therefore, human umbilical cord was collected directly post-delivery from the Hospital Celler Strasse in Braunschweig and the vein endothelium was infected with M1 GAS. After 4.5 h of infection the samples were washed and processed for electron microscopy.

Figure 23a shows attachment of M1 GAS to the apical side of the endothelium 4.5 h post infection. M1 GAS was found to be closely associated with the endothelial cell lining of the vein within the umbilical cord (Figure 23b). However, analysis of the basal side of the endothelium did not reveal any streptococci. Further experiments are needed in order to demonstrate transmigration of M1 GAS in *ex vivo* derived endothelium.

Taken together, the close association of M1 GAS with the human endothelium in the *ex vivo* experimental set up confirms that human endothelial cells represent potential target cells for M1 GAS invasion.

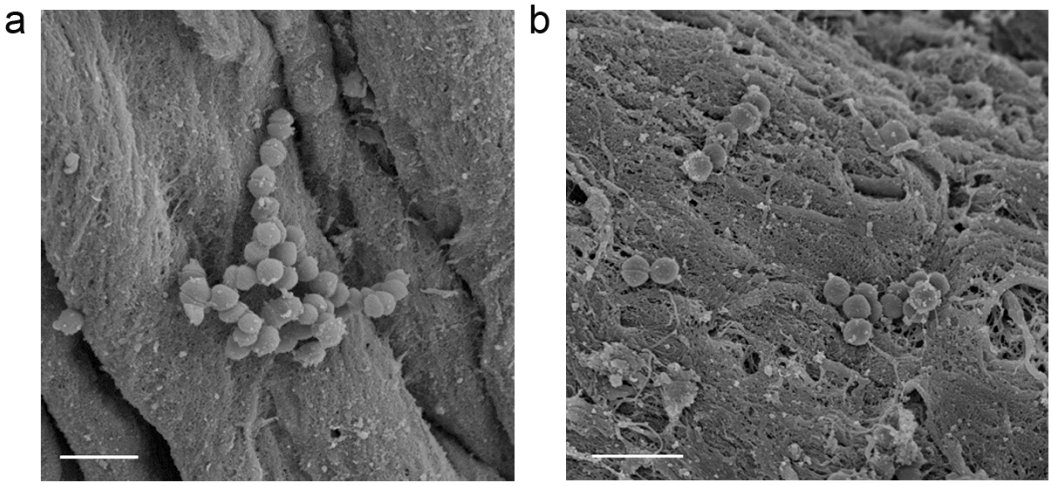

Figure 23: Attachment of M1 GAS to *ex vivo* derived human endothelium

Analysis of the invasion potential of M1 GAS on *ex vivo* derived vein endothelium of human umbilical cord by field emission scanning electron microscopy. Upon infection M1 GAS adheres to (a) and closely associates (b) with the human vein endothelium. Bars represent 2 µm (a, b).

5. Discussion

5.1 Use of an in vitro EC barrier model to study serotype M1 S. pyogenes invasion

S. pyogenes is an extremely versatile organism that causes mild and superficial infections but also severe invasive diseases such as necrotizing fasciitis and streptococcal toxic shock syndrome (Cunningham, 2000). Although antibiotic treatment of streptococcal infections with penicillin is still effective and to date no resistances have occurred, invasive diseases are still the cause for substantial morbidity and mortality worldwide (Kaplan, 1997, Horn *et al.*, 1998, Macris *et al.*, 1998, Carapetis *et al.*, 2005). With over 500.000 deaths per year due to streptococcal infections *S. pyogenes* still represents a major public health problem (Carapetis *et al.*, 2005). Although various serotypes of GAS have been associated with severe invasive infections, serotype M1 and M3 *S. pyogenes* are most frequently isolated from patients with necrotizing fasciitis and STSS (Stevens, 2001, Tart *et al.*, 2007). Invasion into host cells represents one successful mechanism of *S. pyogenes* to circumvent host immune defences and to ensure streptococcal survival. Several studies have already shown that serotype M1 GAS triggers its uptake into various cell types, including epithelial cells and professional phagocytic cells e.g. macrophages and neutrophils and survives and persists intracellular (LaPenta *et al.*, 1994, Medina *et al.*, 2003, Staali *et al.*, 2003, Staali *et al.*, 2006, Hertzen *et al.*, 2010). The ability of *S. pyogenes* to cause invasive diseases, however, implies the ability of GAS to reach the naturally sterile environment of deeper tissue layers, thus, being able to overwind tissue barriers. The observation that in a majority of the patients with invasive diseases no obvious port of entry is detectable led to the hypothesis that streptococcal spread into deeper tissue is associated with a transient bacteraemia originating from the oropharynx (Johansson *et al.*, 2010). This suggests that blood endothelial cells lining the blood vessels might represent potential target cells for pathogenic streptococci and that internalization of *S. pyogenes* into cells of the vascular system might represent a first crucial step during the dissemination into deep tissue. A deeper understanding of the invasion mechanisms itself, as well as the host and bacterial factors involved, might aid in the development of new therapeutic strategies to combat streptococcal infections. The present study, thus, focusses on the invasive potential of one of the most common serotypes, serotype M1 *S. pyogenes,* on EC and, in particular, the mechanisms underlying the interaction of M1 GAS with the endothelial cells of the vascular system.

Studies have already identified a role of invasion of EC in the pathogenesis of serotype M3 GAS which triggers efficient and rapid internalization into EC (Nerlich *et al.*, 2009, Amelung *et al.*, 2011). Preliminary experiments of M1 GAS on EC using a standard infection assay, in which EC are grown and infected on glass coverslips, however suggested fundamental differences between M1 and M3 GAS. Unlike M3 GAS, all M1 clinical GAS isolates were

non-invasive in this standard infection assay (data not shown). These results seem contradictory to the general observation that M1 GAS represents one of the most invasive serotypes, suggesting that the standard infection model is not suitable to study the invasive potential of M1 GAS on EC. Therefore, an additional more complex *in vitro* transwell infection model was employed. In contrast to the standard infection assay, EC are grown on an artificial semi-permeable basement membrane of a transwell insert which allows the establishment of an artificial barrier representing the blood stream on the apical side and the tissue side on the basolateral side. Using this cultivation system allowed the formation of a confluent polarized endothelial cell layer, close to *in vivo* conditions, to study M1 GAS invasion (Figure 5b). Layer formation and polarization was determined by continuous measurement of the transendothelial resistance (TER) and the capacitance providing valuable parameters to assess the current state of the EC layer. Confluent polarized EC layers exhibit high TER values and low capacitance and were then used for infection assays with M1 GAS (Figure 5a). Following infection of confluent polarized EC layers, immunofluorescence analysis demonstrated the invasiveness of M1 GAS on EC. Upon infection, M1 GAS efficiently invade into EC and are localized within the perinuclear region of the cell (Figure 6). The confluence and polarity of the EC layer proofed to be absolutely essential for M1 GAS internalization and correlates with the invasion rates of M1 GAS. Thus, this artificial barrier model represents a suitable system to study the invasion process of M1 GAS into EC in further detail.

5.2 Serotype M1 GAS mediates zipper-like uptake into EC

Invasion into non-phagocytic cells has been shown to represent a common mechanism of various bacterial pathogens to circumvent the host immune system (Alonso *et al.*, 2004). In the case of classical intracellular pathogens two uptake mechanisms have been described and are depicted in Figure 24 (Finlay *et al.*, 1997). *Listeria* and *Yersinia* species for example induce uptake by the zipper invasion mechanism. This is characterized by the initiation of intracellular signalling cascades which are normally involved in host cell processes like cell adhesion and cell migration. The initiation of these signalling cascades induces a rearrangement of the actin cytoskeleton as well as membrane reorganization, resulting in successive engulfment and subsequent internalization of bacteria by the host cell membrane (Alonso *et al.*, 2004, Rottner *et al.*, 2005). The second mechanism, the trigger invasion mechanism, on the other hand is characterized by drastic morphological alterations of the host cell cytoskeleton and membrane ruffling. Uptake by the trigger invasion mechanism has been described for *Salmonella* and *Shigella* species and is induced by the injection of bacterial effector proteins into the cytoplasm of the host cell which then directly target

regulatory host cell factors involved in actin polymerization and actin remodelling processes (Finlay *et al.*, 1997, Alonso *et al.*, 2004, Rottner *et al.*, 2005).

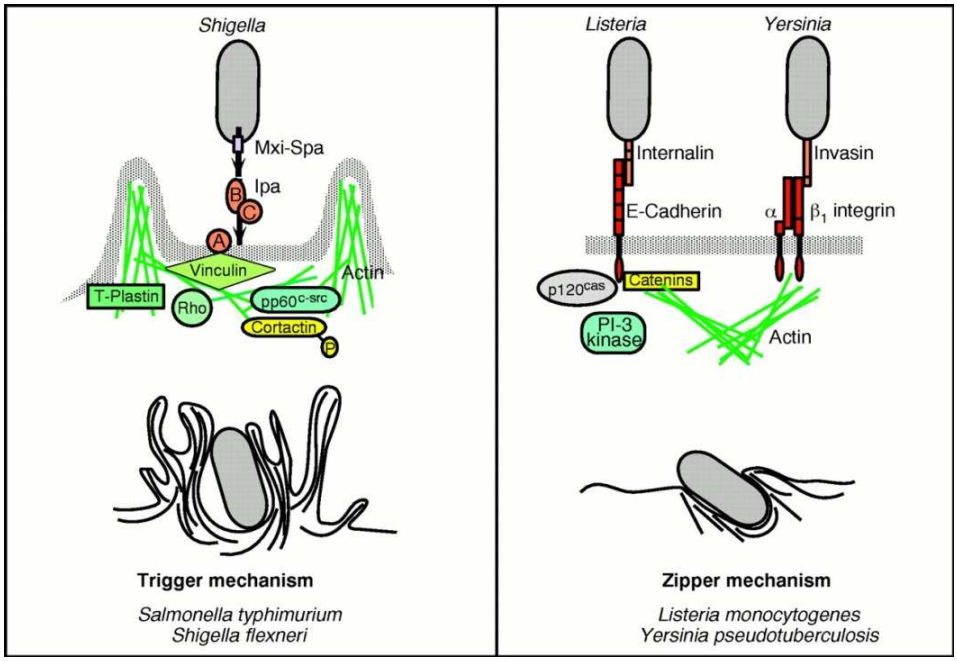

Figure 24: Mechanisms of bacterial invasion

Taken from (Finlay *et al.*, 1997)

Also in the case of streptococci strain dependent morphological differences in the invasion process have been observed (Molinari *et al.*, 2000). Some strains, such as M1-expressing strains and SfbI-negative strains, invade epithelial cells via a zipper-like mechanism, while other strains invade via membrane ruffling similar to the trigger mechanism of classical intracellular pathogens (Dombek *et al.*, 1999, Molinari *et al.*, 2000, Nitsche-Schmitz *et al.*, 2007). In addition, Rohde and colleagues have identified a third invasion mechanism employed by SfbI-expressing streptococci, namely caveolae-mediated endocytosis. This uptake mechanism is completely independent of cytoskeletal rearrangements. Instead, it comprises the accumulation of caveolae at the entry port and subsequent invasion of streptococci into the host cell by the formation of large membrane invaginations (Rohde *et al.*, 2003).

Although the internalization of serotype M1 GAS into epithelial cells is well established, nothing is known about the interaction of M1 GAS with endothelial cells. The results of this study clearly demonstrate that also blood endothelial cells represent target cells for M1 GAS invasion. Immunofluorescence analysis and subsequent quantification of internalization rates

show that M1 GAS efficiently triggers its own uptake into EC (Figure 6). A closer look on the internalization process itself reveals that M1 GAS triggers the formation of membrane protrusions that tightly attach to and engulf invading bacteria resulting in successive zipper-like uptake of M1 GAS into EC (Figure 7). On the cellular level the formation of membrane protrusions is ascribed to a reorganization of the actin cytoskeleton. A key feature in all cytoskeletal remodelling processes is the *de novo* nucleation of actin filaments or site-directed branching and elongation of existing actin fibres (Stradal *et al.*, 2006). These processes are catalysed by the heptameric protein complex Arp2/3 which, by acting as a nucleation factor, promotes the formation and assembly of branched actin filaments. Arp2/3-mediated actin polymerization is induced by the activation of signalling cascades involving small GTPases such as Rac and Cdc42. These act as molecular switches to relate signals to the Arp2/3 complex via the association of nucleation promoting factors, including members of the Wiskott-Aldrich Syndrome proteins (WASP) and WASP family verprolin-homologous (WAVE) proteins (Stradal *et al.*, 2004, Vartiainen *et al.*, 2004, Stradal *et al.*, 2006). The Arp2/3 complex is not only a key component of all cellular processes involving actin dynamics, moreover, several bacterial pathogens e.g. *Shilgella*, *Listeria* and *Rickettsia* exploit the cellular actin cytoskeletal machinery for their own purposes. By specifically targeting the Arp2/3 complex these pathogens induce actin polymerization and actin tail formation, allowing rapid movement within the host cell and spread to adjacent cells (Goldberg, 2001, Gruenheid *et al.*, 2003, Gouin *et al.*, 2004, Alonso *et al.*, 2004). Given the essential function of actin polymerization in the reorganization of the cytoskeleton, it is not surprising that uptake of serotype M1 GAS into EC also involves accumulation of F-actin at the entry port (Figure 8a). Moreover, immunofluorescence analysis of infected EC layers shows that actin accumulation is accompanied with an aggregation and recruitment of the Arp2/3 complex in the vicinity of invading streptococci (Figure 8b). Thus, serotype M1 GAS subverts cellular actin cytoskeletal dynamics possibly by inducing Arp2/3 dependent actin filament branching to trigger its uptake into EC.

5.3 The M1 protein of GAS triggers internalization into EC via the engagement of β_1-integrins on the endothelial cell surface

Internalization of bacterial pathogens by the zipper invasion mechanism is initiated by binding of bacterial ligands to a host cell surface receptor which than triggers intracellular signalling cascades leading to cytoskeletal rearrangements and engulfment of bacteria (Alonso *et al.*, 2004). Previously, the fibronectin binding protein FbaB of serotype M3 GAS was identified as an invasin for endothelial cells driving rapid zipper-like uptake of serotype M3 GAS into EC (Amelung *et al.*, 2011). However, since M1 GAS lacks FbaB on its cell surface, the bacterial factor driving M1 GAS internalization into EC remained so far unknown.

This study clearly identifies the M1 surface protein of serotype M1 GAS as the invasin driving M1 GAS internalization into EC. Using an isogenic M1 knock out mutant, which is deficient in invasion of EC, demonstrates that the M1 protein is absolutely essential for internalization. Complementation of the M1 knock out mutant by episomal expression of M1 restores the wild type phenotype (Figure 16a, b). Gain of function experiments using M1-coated latex beads as well as heterologous expression of M1 in naturally non-invasive *L. lactis* proof that the M1 protein is the sole factor which triggers the internalization process into EC (Figure 17, Figure 18). These findings add yet another role to this multifunctional protein which has already been identified as a major virulence factor of GAS, responsible for subverting various host immune responses thereby ensuring streptococcal survival (reviewed in (Oehmcke *et al.*, 2010) and (Smeesters *et al.*, 2010)). In addition to its well established role as an adhesin/invasin for epithelial cells and its antiphagocytic properties in non-immune human blood, the M1 protein has been described as a crucial factor mediating survival of *S. pyogenes* within neutrophils and macrophages (Bisno, 1979, Dombek *et al.*, 1999, Staali *et al.*, 2003, Staali *et al.*, 2006, Hertzen *et al.*, 2010). Given its antiphagocytic properties, it is quite remarkable that GAS uses the same factor to specifically initiate internalization into non-phagocytic cells. This adds to the extreme versatility of *S. pyogenes*, on the one hand preventing its internalization by professional phagocytes, while on the other hand specifically inducing its entry into non-phagocytic cells including epithelial and endothelial cells.

S. pyogenes has evolved multiple pathways to efficiently invade host cells (Cue *et al.*, 1998, Molinari *et al.*, 2000, Rohde *et al.*, 2003). Invasion into human lung epithelial cells for example involves binding of the M1 protein to components of the extracellular matrix such as fibronectin or laminin (Cue *et al.*, 1998). Fibronectin bound to the M1 protein subsequently interacts with the major fibronectin binding receptor $\alpha_5\beta_1$-integrins on the surface of lung epithelial cells and thereby triggers streptococcal uptake via cytoskeletal rearrangements (Cue *et al.*, 1998, Dombek *et al.*, 1999). The results of the present study clearly demonstrate that, similar to M1 GAS invasion into epithelial cells, efficient invasion into endothelial cells requires the engagement of subsets of the β_1-integrin family on the host cell surface (Figure 20). However, although in both cases binding of β_1-integrins is required, efficient invasion into endothelial cells is highly dependent on a confluent cell layer. Blocking of the β_1-integrin subunit on endothelial cells significantly reduces streptococcal invasion to 56%, proofing that β_1-integrins are required for efficient internalization of serotype M1 GAS into EC (Figure 20a). Moreover, upon invasion an aggregation of β_1-integrins in the vicinity of invading streptococci is detectable (Figure 20b). It is well known that integrin clustering is a prerequisite for triggering an outside to inside signal. Therefore, it is conceivable that, as in the case of invasion into epithelial cells, engagement of $\alpha_5\beta_1$-integrin heterodimers is required for efficient M1-mediated invasion into endothelial cells. Further studies need to be performed to

address whether $\alpha_5\beta_1$-integrins are indeed cell surface receptors for M1-mediated invasion into EC. Moreover, since pre-treatment of EC with an anti-β_1-integrin antibody does not completely abolish M1 GAS invasion into EC, it is likely that the M1 protein targets an additional host cell surface receptor or receptors to ensure efficient entry. Indeed, membrane cofactor protein CD46 has been identified as a receptor for M protein (Okada *et al.*, 1995). Later Rezcallah and colleagues demonstrated that, in addition to $\alpha_5\beta_1$-integrins, CD46 is required for efficient M1-mediated internalization of GAS into epithelial cells and that invasion is dependent on the presence of serum or fibronectin (Rezcallah *et al.*, 2005).

The role of extracellular matrix components (e.g. fibronectin) in the invasion of M1 GAS into EC has also to be clarified in subsequent experiments. SfbI/PrtF1-mediated invasion has been shown to be highly dependent on binding to the host glycoprotein fibronectin (Molinari *et al.*, 1997, Jadoun *et al.*, 1998, Talay *et al.*, 2000). However, little is known about the interaction of the M1 protein with fibronectin. Cue and colleagues suspected that the M1 protein contains two independent binding sites for fibronectin, one present in the A and one in the B domain of the protein, since deletion of either of those significantly inhibited fibronectin binding and subsequent invasion into epithelial cells (Cue *et al.*, 2001). Hence, it would be interesting to study the requirement of M1 protein-fibronectin interactions for efficient invasion into EC. But this question needs to be clarified in subsequent studies.

5.4 M1 GAS exploits the phagocytic uptake machinery to gain access to EC

The molecular basis for membrane remodelling and pseudopod extensions, as seen in M1 GAS invasion into EC, is the initiation of intracellular signalling cascades which activate host cell molecules involved in actin remodelling (Alonso *et al.*, 2004). Thus, it was of interest which signalling molecules are triggered during the internalization of M1 GAS into EC. Function interfering experiments using different chemicals specifically inhibiting single host cell signalling molecules were performed (Figure 21). These experiments identified phospholipase C (PLC), intracellular calcium and protein kinase C (PKC) as key signalling components involved in the uptake of M1 GAS into EC. Pre-treatment of HUVEC with edelfosine, interfering with the activation of phospholipase C, results in a reduction of invasion to 16%. Targeting protein kinase C by calphostin C also significantly reduces M1 GAS invasion by 80%. In addition, intracellular calcium is also absolutely essential for M1 GAS internalization as reducing its release from intracellular stores by the chelator BAPTA-AM completely abolishes M1 GAS invasion into EC (Figure 21).

F-actin accumulation and the formation of membrane protrusions, as seen in M1 GAS invasion, are major characteristics for phagocytic uptake processes. A comparison of the

signalling molecules involved highlights similarities between both processes. Classical receptor-mediated phagocytosis involves multiple ligand receptor interactions resulting in lateral receptor clustering, activation of multiple receptors by phosphorylation and subsequent recruitment of additional adaptor proteins to the activated signalling complex (Flannagan *et al.*, 2012, Sarantis *et al.*, 2012). Lipids, for example phosphatidylinositol-4,5-bisphosphate ($PI(4,5)P_2$), play an important role in signalling events during classical phagocytosis. $PI(4,5)P_2$ is present in the inner leaflet of the cell membrane of resting phagocytes. During phagocytosis its amount first increases within the phagocytic cup but then abruptly decreases (Steinberg *et al.*, 2008, Flannagan *et al.*, 2012). The decrease in the concentration of $PI(4,5)P_2$ is absolutely essential for efficient internalization of foreign particles, most likely by allowing actin disassembly. Phospholipase C γ, which is activated during phagocytosis, binds to $PI(4,5)P_2$ and subsequently hydrolyzes it to yield diacylglycerol (DAG) and inositol-3,4,5-trisphosphate (IP_3) (Steinberg *et al.*, 2008, Flannagan *et al.*, 2012, Sarantis *et al.*, 2012). IP_3 triggers the release of calcium from intracellular stores such as the endoplasmic reticulum (Nunes *et al.*, 2010, Sarantis *et al.*, 2012). Together with DAG, calcium promotes the recruitment of protein kinase C (PKC) (Steinberg *et al.*, 2008). PKC is also a key component enhancing phagocytosis by activating downstream signalling events including the activation of small GTPases (e.g. Rac1 and Cdc42) which relate signals to the Arp2/3 complex promoting cytoskeletal rearrangements during phagocytosis (Botelho *et al.*, 2011, Flannagan *et al.*, 2012).

Taken together, the results of the present study demonstrate that internalization of M1 GAS into EC shows features of classical phagocytic uptake processes in particular ligand receptor binding, activation of calcium dependent intracellular signalling cascades including PLC and PKC, membrane remodelling and engulfment of streptococci. Thus, serotype M1 GAS exploits the phagocytic uptake machinery of the host cell to gain access to non-phagocytic cells, thereby facilitating protection from the immune system. In contrast to the findings of the present study, Purushothaman and colleagues have shown that protein kinase C is not required for M1 GAS invasion into epithelial cells since the inhibitor calphostin C fails to inhibit M1 GAS invasion in this study (Purushothaman *et al.*, 2003). This demonstrates that, although M1 GAS apparently triggers similar internalization processes into both epithelial and endothelial cells, distinct signalling cascades are driving these processes. Hence, further experiments need to be performed to fully understand the signalling cascades generated during M1 GAS uptake into EC. Class I phosphatidylinositol-3-kinases (PI3K) might constitute yet other possible signalling components involved during M1 GAS invasion into EC as they are also known to hydrolyse $PI(4,5)P_2$ into IP_3 (Steinberg *et al.*, 2008, Flannagan *et al.*, 2012). Indeed, Wang and colleagues have previously shown an involvement of PI3K in the internalization of M1 GAS into epithelial cells. Upon association with integrins, M1 GAS

initiate the recruitment and phosphinositide 3-kinase (PI3K) dependent activation of the integrin linked kinase (ILK) and subsequent phosphorylation and assembly of paxillin and the focal adhesion kinase (FAK) at the port of entry (Purushothaman *et al.*, 2003, Wang *et al.*, 2006, Wang *et al.*, 2007). In contrast, Nerlich and colleagues could show that entry of serotype M3 GAS into EC is independent of PI3K (Nerlich *et al.*, 2009).

The small GTPases Rac1 and Cdc42 play also an essential role in processes involving cytoskeletal rearrangements. Both act as molecular switches that relate signals from the cellular receptor to effector proteins. Rac1 induces the formation of lamellipodia and Cdc42 has been shown to mediate the formation of filopodia (Flannagan *et al.*, 2012). Nerlich and colleagues have previously shown that Rac1 is essential to mediate internalization of serotype M3 GAS into EC (Nerlich *et al.*, 2009). Therefore, it will be interesting to analyse the role of Rac1 and Cdc42 in M1 GAS invasion in future experiments.

5.5 Serotype M1 GAS survival within EC is associated with phagolysosomal escape

Following phagocytosis, intracellular bacteria are incorporated into membrane-bound vacuoles called phagosomes (Sarantis *et al.*, 2012). The composition of the newly formed phagosome resembles in its composition the plasma membrane from which it is derived. However, membrane scission is followed by a series of biochemical modifications altering the composition of the phagosome and turning it into a highly microbicidal degradative organelle (Flannagan *et al.*, 2012). These processes involve sequential fusion and fission events of the nascent phagosome with early and late endosomes and finally lysosomes (Sarantis *et al.*, 2012, Flannagan *et al.*, 2012). Early phagosomes acquire the GTPase Rab5 which coordinates early phagosome biogenesis by mediating fusion of the nascent phagosome with early endosomes. Rab5 also recruits other effector proteins such as the early endosomal antigen 1 (EEA1) further facilitating vesical fusion events (Botelho *et al.*, 2011). The transition of the early phagosome into a late phagosome is characterized by the loss of early endosomal markers (e.g. Rab5) but acquisition of other distinct biochemical markers including Rab7 and the lysosome-associated membrane proteins 1 and 2 (Lamp-1 and Lamp-2) (Botelho *et al.*, 2011, Flannagan *et al.*, 2012). Therefore, Rab7 and its effector proteins are essential for phagolysosomal fusion and acidification in the phagosome maturation process. The mature phagolysosome with a pH of 4.5 is rich in degradative enzymes including lysosomal hydrolases, nucleases, lipases, glycosidases, reactive oxygen species and antimicrobial peptides ensuring degradation of foreign material (Botelho *et al.*, 2011, Flannagan *et al.*, 2012). Phagocytosis and subsequent phagosomal maturation, thus, represents one of the first lines of defence against invading pathogens (Flannagan *et al.*, 2012).

Given the importance of phagocytosis in combating infections, it is not surprising that various pathogens, including *S. pyogenes*, have evolved mechanisms to interfere with phagosome maturation and to alter the phagosome for their own benefit avoiding intracellular killing. These mechanisms include (i) the induction of phagosome maturation arrest, (ii) avoidance of fusion of phagosomes with lysosomes, (iii) complete segregation of membrane-bound compartments from the endocytic route and (iiii) escape from the phagosome (Alonso *et al.*, 2004). *Chlamydia*, *Legionella* and *Brucella* for example inhibit endocytic maturation and live within phagosomes segregated from the endocytic route (Meresse *et al.*, 1999, Alonso *et al.*, 2004, Botelho *et al.*, 2011). *Mycobacterium tuberculosis* again mediates an arrest in phagosome maturation by preventing fusion of the phagosome with lysosomes and *Listeria* lyses the phagosomal membrane to escape into the cytoplasm of the host cell (Meresse *et al.*, 1999, Goldberg, 2001, Portnoy *et al.*, 2002, Alonso *et al.*, 2004, Botelho *et al.*, 2011). Also in the case of *S. pyogenes* several evasion mechanisms have been described. Serotype M3 GAS, which triggers invasion by cytoskeletal rearrangements, is localized within phagosomes which traffic along the classical endocytic route and fuse with lysosomes (Amelung *et al.*, 2011). Following transmigration within EC, M3 GAS induces its escape at the basolateral tissue associated membrane via lysosomal exocytosis (Talay, unpublished data). In contrast, SfbI-expressing *S. pyogenes* strains showing caveolae-mediated invasion reside within caveosomes and prevent fusion with lysosomes, thereby bypassing the endocytic machinery (Rohde *et al.*, 2003). In the case of serotype M1 GAS, studies have described that survival within neutrophils and macrophages is mediated by an inhibition of fusion of phagosomes with azurophilic granules and late endosomal/lysosomal compartments (Staali *et al.*, 2006, Hertzen *et al.*, 2010). In contrast to these observations, the results of the present study give evidence that within EC M1 GAS containing phagosomes do travel along the classical endocytic route and fuse with terminal lysosomes (Figure 9, Figure 10, Figure 11). M1 GAS containing phagosomes acquire late endosomal lysosomal markers like Lamp-1. 1 h up to 5 h post infection the majority of intracellular streptococci is localized within Lamp-1 positive compartments (Figure 9). Co-localization of intracellular streptococci with gold loaded-lysosomes by electron microscopy demonstrates that phagosomes in the end fuse with terminal lysosomes, thus, further confirming endosomal/lysosomal intracellular trafficking of M1 GAS within EC (Figure 10, Figure 11). This intracellular pathway of M1 GAS shows parallels to M3 GAS trafficking in EC (Amelung *et al.*, 2011). However, although in both cases fusion events of phagosomes with lysosomes are detectable, differences can be observed. In contrast to M3 GAS which induces movement of gold-loaded lysosomes towards intracellular residing streptococci and the formation of large apertures in the host cells (Talay, unpublished data), the present study shows that serotype M1 GAS moves from the periphery of the cell towards lysosomes which are still localized in

the perinuclear region of the host cell (Figure 10). Furthermore, no formation of apertures is detectable. Most likely this difference between M1 serotype and M3 serotype can be attributed to the nature of subsequent trafficking steps which differ in both strains. Serotype M3 GAS is released at the basolateral side of the host cell by lysosomal exocytosis, a process which is characterized by fusion of the phagolysosomal membrane with the host cell membrane (Talay, unpublished data). Movement of lysosomes towards intracellular residing M3 GAS, thus, strongly supports the observation of streptococcal escape by lysosomal exocytosis. In contrast, the results of this study demonstrate that following fusion with lysosomes M1 GAS escapes from the phagolysosomal compartment into the cytoplasm of the host cell (Figure 13a, b). Visualization of cellular membranes by ferrocyanide-thiocarbocyanide-osmium tetroxide staining confirmed the absence of any cellular membrane surrounding intracellular M1 GAS, further verifying its cytoplasmic localization (Figure 13c). Streptococcal escape from the phagolysosomes also correlates with the observation that after overnight infection the number of M1 GAS co-localized with the Lamp-1 positive late endosomal/lysosomal compartment declines to approximately 50% (Figure 9b). Escape from the phagosome has already been shown for *Listeria*, *Shigella* and *Rickettsia*. These pathogens secrete specific enzymes, e.g. the pore-forming toxin listeriolysine-O of *Listeria*, which lyses the phagosomal membrane releasing the bacteria into the host cytoplasm (Meresse *et al.*, 1999, Alonso *et al.*, 2004). Recruitment of actin to one pole facilitates movement within the host cell and spread to neighbouring cells (Goldberg, 2001). One can speculate that the streptococcal exotoxins streptolysin O and/or streptolysin S are responsible for M1 GAS phagolysosomal escape. Both belong to the group of pore-forming toxins and have been shown to exert cytolytic effects on various cell types and subcellular organelles (Nizet, 2002, Bisno *et al.*, 2003). Experiments within the department are on the way to address this question.

5.6 Survival of serotype M1 GAS within endothelial cells and its ability to overcome the endothelial cell barrier

As described in the previous chapter, M1 GAS mediates its escape from the phagolysosomal compartment, thus, ensuring streptococcal survival within the nutrient-rich host cytoplasm. Bacterial viability staining and plating of intracellular streptococci confirm successful survival of intracellular streptococci up to 10 h post infection (Figure 12). Analysis of ultra-thin sections of infected EC layers also show that intracellular M1 GAS appears morphologically intact. In addition, signs of ongoing bacterial replication are visible, thus, giving further evidence for streptococcal viability (Figure 13). Although quantification of intracellular bacteria by plating of EC lysates also confirms streptococcal survival, bacterial counts are gradually declining over time (Figure 12b) which seems contradictory to the observations made by electron and

immunofluorescence microscopy (Figure 12a, Figure 13). Possible explanations for this discrepancy will be discussed below.

The development of an invasive disease implies that, at some point, the pathogen is able to overcome cellular barriers e.g. the endothelial cell lining. As M1 GAS accounts for the majority of invasive infections, it was hypothesised that following phagolysosomal escape M1 GAS transmigrates within EC and at some point emerges from the host cell at the basolateral side facilitating spread into deeper tissue. Plating of the medium within the lower transwell compartment underneath the EC layer reveals no streptococci even after longer infection times (up to 72 h post infection, Figure 14a). However, after removal of the infected EC layer and examination of the surface of the transwell membrane, M1 GAS was found to be attached to the transwell membrane itself, entangled within a mesh of extracellular matrix and gelatine (Figure 14c). The results of this experiment provide evidence that M1 GAS is indeed able to overcome the endothelial cell lining, a mechanism which potentially favours dissemination into deeper tissue. Due to the tight attachment of streptococci to the gelatine, which was used for coating of transwell membranes, it is not surprising that streptococci are unable to pass through the pores of the transwell membrane and this, therefore, explains the absence of streptococci within the lower transwell compartment (Figure 14a). Moreover, the escape from the host cell might account for the declining numbers of intracellular bacteria after plating of EC lysates (Figure 12b). Presumably, permeabilization and subsequent trypsination of infected EC are not sufficient to detach streptococci from the transwell membrane and, thus, these are not included in the bacterial counts obtained after plating of EC lysates.

With progressive infection time increasing numbers of dead cells are detectable within the EC layer (Figure 14d). This gives reason for speculation that M1 GAS escape is accompanied by host cell lysis. In line with this observation is the study of Hertzén and colleagues also demonstrating morphological changes and cell lysis of macrophages infected with serotype M1 GAS (Hertzen *et al.*, 2010). Whether EC lysis is due to the increasing amount of intracellular streptococci after prolonged infection times or caused by production of streptolysin O and/or streptolysin S remains to be addressed. The morphological changes of the EC layer as described above were only detected by electron microscopy, but not by examination of infected cell layers by immunofluorescence microscopy. This discrepancy highlights the limitations of immunofluorescence microscopy itself. In order to stain intracellular streptococci, all cells are treated with Triton-X-100, thus, all cells are permeabilized. Therefore, during immunofluorescence microscopic analysis, it is impossible to distinguish cells lysed as a consequence of streptococcal infection from those lysed due to Triton-X-100 treatment. Moreover, lysis of host cells implies release of intracellular

streptococci into the surrounding medium. During preparation of EC lysates for quantification of intracellular bacterial survival all extracellular streptococci, including those released during host cell lysis, are killed by the addition of penicillin and gentamycin, thus, impairing the actual viable intracellular bacterial counts. This would also explain the gradual decrease of the intracellular bacteria numbers over time (Figure 12b).

5.7 Summary of the invasion process triggered by serotype M1 GAS

In conclusion, the results of the present study show, for the first time, a direct interaction of M1 GAS, which is one of the most invasive serotypes, with human endothelial cells. Serotype M1 GAS efficiently mediates internalization into polarized EC and, moreover, possesses a strong potential to cross the endothelial cell lining separating the blood stream from the underlying tissue. The M1 surface protein of GAS was identified as a strong invasin which mediates the internalization process into EC. Binding of the M1 protein to β_1-integrin host cell receptors triggers calcium dependent intracellular signalling cascades, involving phospholipase C and protein kinase C, which activate downstream signalling molecules including the Arp2/3 complex. The activation of these effector proteins results in actin recruitment to the port of entry, membrane remodelling and subsequent zipper-like uptake of M1 GAS into endothelial cells. Following internalization, intracellular streptococci, incorporated into phagosomes, traffic along the classical endosomal pathway and finally fuse with terminal lysosomes. With progressive infection time M1 *S. pyogenes* escapes from the phagolysosomal compartment into the cytoplasm of the host cell, subsequently crosses the endothelial cell barrier and is released at the basolateral side of the EC layer.

In summary, the results presented in this study clearly demonstrate new major insights into serotype M1 *S. pyogenes* invasion: i) endothelial cells represent potential target cells for M1 GAS invasion, ii) infection assays show successful invasion of M1 GAS into human umbilical cord, lung as well as human dermal endothelial cells, iii) these results are in favour for and strongly indicate that EC invasion possibly constitutes a general mechanism of M1 GAS to evade innate host immune defences and to reside and persist intracellular before transmigrating into underlying soft tissue, iv) these results give strong evidence about the mechanistic aspects why serotype M1 *S. pyogenes* is very often associated with invasive tissue infections like necrotizing fasciitis.

6. References

Alonso, A. and Garcia-del Portillo, F. (2004). Hijacking of eukaryotic functions by intracellular bacterial pathogens. International microbiology : the official journal of the Spanish Society for Microbiology 7, 181-191.

Amelung, S., Nerlich, A., Rohde, M., Spellerberg, B., Cole, J.N., Nizet, V., et al. (2011). The FbaB-type fibronectin-binding protein of Streptococcus pyogenes promotes specific invasion into endothelial cells. Cellular microbiology 13, 1200-1211.

Aziz, R.K. and Kotb, M. (2008). Rise and persistence of global M1T1 clone of Streptococcus pyogenes. Emerging infectious diseases 14, 1511-1517.

Baorto, D.M., Gao, Z., Malaviya, R., Dustin, M.L., van der Merwe, A., Lublin, D.M. and Abraham, S.N. (1997). Survival of FimH-expressing enterobacteria in macrophages relies on glycolipid traffic. Nature 389, 636-639.

Batzloff, M., Yan, H., Davies, M., Hartas, J. and Good, M. (2004). Preclinical evaluation of a vaccine based on conserved region of M protein that prevents group A streptococcal infection. The Indian journal of medical research 119 Suppl, 104-107.

Batzloff, M.R., Hayman, W.A., Davies, M.R., Zeng, M., Pruksakorn, S., Brandt, E.R. and Good, M.F. (2003). Protection against group A streptococcus by immunization with J8-diphtheria toxoid: contribution of J8- and diphtheria toxoid-specific antibodies to protection. The Journal of infectious diseases 187, 1598-1608.

Bauer, M.J., Georgousakis, M.M., Vu, T., Henningham, A., Hofmann, A., Rettel, M., et al. (2012). Evaluation of novel Streptococcus pyogenes vaccine candidates incorporating multiple conserved sequences from the C-repeat region of the M-protein. Vaccine 30, 2197-2205.

Beachey, E.H. and Ofek, I. (1976). Epithelial cell binding of group A streptococci by lipoteichoic acid on fimbriae denuded of M protein. The Journal of experimental medicine 143, 759-771.

Beall, B., Facklam, R. and Thompson, T. (1996). Sequencing emm-specific PCR products for routine and accurate typing of group A streptococci. Journal of clinical microbiology 34, 953-958.

Bisno, A.L. (1979). Alternate complement pathway activation by group A streptococci: role of M-protein. Infection and immunity 26, 1172-1176.

Bisno, A.L. (2001). Acute pharyngitis. The New England journal of medicine 344, 205-211.

Bisno, A.L., Brito, M.O. and Collins, C.M. (2003). Molecular basis of group A streptococcal virulence. The Lancet infectious diseases 3, 191-200.

Botelho, R.J. and Grinstein, S. (2011). Phagocytosis. Current biology : CB 21, R533-538.

Brakebusch, C. and Fassler, R. (2003). The integrin-actin connection, an eternal love affair. The EMBO journal 22, 2324-2333.

Brook, I. (2010). beta-Lactamase-Producing Bacteria in Upper Respiratory Tract Infections. Current infectious disease reports 12, 110-117.

Brook, I. (2013). Penicillin failure in the treatment of streptococcal pharyngo-tonsillitis. Current infectious disease reports 15, 232-235.

Burns, E.H., Jr., Marciel, A.M. and Musser, J.M. (1996). Activation of a 66-kilodalton human endothelial cell matrix metalloprotease by Streptococcus pyogenes extracellular cysteine protease. Infection and immunity 64, 4744-4750.

Campbell, N.A. and Reece, J.B. (2003) Biologie. 6 edn., Spektrum Akademischer Verlag Heidelberg, pp. 210-231.

Campellone, K.G. and Welch, M.D. (2010). A nucleator arms race: cellular control of actin assembly. Nature reviews. Molecular cell biology 11, 237-251.

Caparon, M.G., Geist, R.T., Perez-Casal, J. and Scott, J.R. (1992). Environmental regulation of virulence in group A streptococci: transcription of the gene encoding M protein is stimulated by carbon dioxide. Journal of bacteriology 174, 5693-5701.

Carapetis, J.R., Steer, A.C., Mulholland, E.K. and Weber, M. (2005). The global burden of group A streptococcal diseases. The Lancet infectious diseases 5, 685-694.

Cary, L.A., Han, D.C. and Guan, J.L. (1999). Integrin-mediated signal transduction pathways. Histology and histopathology 14, 1001-1009.

Courtney, H.S., Simpson, W.A. and Beachey, E.H. (1983). Binding of streptococcal lipoteichoic acid to fatty acid-binding sites on human plasma fibronectin. Journal of bacteriology 153, 763-770.

Courtney, H.S., von Hunolstein, C., Dale, J.B., Bronze, M.S., Beachey, E.H. and Hasty, D.L. (1992). Lipoteichoic acid and M protein: dual adhesins of group A streptococci. Microbial pathogenesis 12, 199-208.

Cue, D., Dombek, P.E., Lam, H. and Cleary, P.P. (1998). Streptococcus pyogenes serotype M1 encodes multiple pathways for entry into human epithelial cells. Infection and immunity 66, 4593-4601.

Cue, D., Lam, H. and Cleary, P.P. (2001). Genetic dissection of the Streptococcus pyogenes M1 protein: regions involved in fibronectin binding and intracellular invasion. Microbial pathogenesis 31, 231-242.

Cue, D., Southern, S.O., Southern, P.J., Prabhakar, J., Lorelli, W., Smallheer, J.M., et al. (2000). A nonpeptide integrin antagonist can inhibit epithelial cell ingestion of Streptococcus pyogenes by blocking formation of integrin alpha 5beta 1-fibronectin-M1 protein complexes. Proceedings of the National Academy of Sciences of the United States of America 97, 2858-2863.

Cue, D.R. and Cleary, P.P. (1997). High-frequency invasion of epithelial cells by Streptococcus pyogenes can be activated by fibrinogen and peptides containing the sequence RGD. Infection and immunity 65, 2759-2764.

Cunningham, M.W. (2000). Pathogenesis of group A streptococcal infections. Clinical microbiology reviews 13, 470-511.

Dale, J.B. and Beachey, E.H. (1985). Multiple, heart-cross-reactive epitopes of streptococcal M proteins. The Journal of experimental medicine 161, 113-122.

Dale, J.B., Fischetti, V.A., Carapetis, J.R., Steer, A.C., Sow, S., Kumar, R., et al. (2013). Group A streptococcal vaccines: paving a path for accelerated development. Vaccine 31 Suppl 2, B216-222.

Dale, J.B., Penfound, T.A., Chiang, E.Y. and Walton, W.J. (2011). New 30-valent M protein-based vaccine evokes cross-opsonic antibodies against non-vaccine serotypes of group A streptococci. Vaccine 29, 8175-8178.

Dinkla, K., Rohde, M., Jansen, W.T., Kaplan, E.L., Chhatwal, G.S. and Talay, S.R. (2003). Rheumatic fever-associated Streptococcus pyogenes isolates aggregate collagen. The Journal of clinical investigation 111, 1905-1912.

Dombek, P.E., Cue, D., Sedgewick, J., Lam, H., Ruschkowski, S., Finlay, B.B. and Cleary, P.P. (1999). High-frequency intracellular invasion of epithelial cells by serotype M1 group A streptococci: M1 protein-mediated invasion and cytoskeletal rearrangements. Molecular microbiology 31, 859-870.

Facklam, R. (2002). What happened to the streptococci: overview of taxonomic and nomenclature changes. Clinical microbiology reviews 15, 613-630.

Ferretti, J.J., McShan, W.M., Ajdic, D., Savic, D.J., Savic, G., Lyon, K., et al. (2001). Complete genome sequence of an M1 strain of Streptococcus pyogenes. Proceedings of the National Academy of Sciences of the United States of America 98, 4658-4663.

Finlay, B.B. and Cossart, P. (1997). Exploitation of mammalian host cell functions by bacterial pathogens. Science 276, 718-725.

Flannagan, R.S., Jaumouille, V. and Grinstein, S. (2012). The cell biology of phagocytosis. Annual review of pathology 7, 61-98.

Gibson, C., Fogg, G., Okada, N., Geist, R.T., Hanski, E. and Caparon, M. (1995). Regulation of host cell recognition in Streptococcus pyogenes. Developments in biological standardization 85, 137-144.

Goldberg, M.B. (2001). Actin-based motility of intracellular microbial pathogens. Microbiology and molecular biology reviews : MMBR 65, 595-626, table of contents.

Goley, E.D. and Welch, M.D. (2006). The ARP2/3 complex: an actin nucleator comes of age. Nature reviews. Molecular cell biology 7, 713-726.

Gouin, E., Egile, C., Dehoux, P., Villiers, V., Adams, J., Gertler, F., et al. (2004). The RickA protein of Rickettsia conorii activates the Arp2/3 complex. Nature 427, 457-461.

Greco, R., De Martino, L., Donnarumma, G., Conte, M.P., Seganti, L. and Valenti, P. (1995). Invasion of cultured human cells by Streptococcus pyogenes. Research in microbiology 146, 551-560.

Gruenheid, S. and Finlay, B.B. (2003). Microbial pathogenesis and cytoskeletal function. Nature 422, 775-781.

Guilherme, L., Dulphy, N., Douay, C., Coelho, V., Cunha-Neto, E., Oshiro, S.E., et al. (2000). Molecular evidence for antigen-driven immune responses in cardiac lesions of rheumatic heart disease patients. International immunology 12, 1063-1074.

Hanski, E. and Caparon, M. (1992). Protein F, a fibronectin-binding protein, is an adhesin of the group A streptococcus Streptococcus pyogenes. Proceedings of the National Academy of Sciences of the United States of America 89, 6172-6176.

Hasty, D.L., Ofek, I., Courtney, H.S. and Doyle, R.J. (1992). Multiple adhesins of streptococci. Infection and immunity 60, 2147-2152.

Hellenthal, W. (2002) Physik für Mediziner und Biologen. 7 edn., Wissenschaftliche Verlagsgesellschaft.

Henningham, A., Chiarot, E., Gillen, C.M., Cole, J.N., Rohde, M., Fulde, M., et al. (2012). Conserved anchorless surface proteins as group A streptococcal vaccine candidates. Journal of molecular medicine 90, 1197-1207.

Hertzen, E., Johansson, L., Wallin, R., Schmidt, H., Kroll, M., Rehn, A.P., et al. (2010). M1 protein-dependent intracellular trafficking promotes persistence and replication of Streptococcus pyogenes in macrophages. Journal of innate immunity 2, 534-545.

Horn, D.L., Zabriskie, J.B., Austrian, R., Cleary, P.P., Ferretti, J.J., Fischetti, V.A., et al. (1998). Why have group A streptococci remained susceptible to penicillin? Report on a symposium. Clinical infectious diseases : an official publication of the Infectious Diseases Society of America 26, 1341-1345.

Horstmann, R.D., Sievertsen, H.J., Knobloch, J. and Fischetti, V.A. (1988). Antiphagocytic activity of streptococcal M protein: selective binding of complement control protein factor H. Proceedings of the National Academy of Sciences of the United States of America 85, 1657-1661.

Hynes, R.O. (2002). Integrins: bidirectional, allosteric signaling machines. Cell 110, 673-687.

Jadoun, J., Ozeri, V., Burstein, E., Skutelsky, E., Hanski, E. and Sela, S. (1998). Protein F1 is required for efficient entry of Streptococcus pyogenes into epithelial cells. The Journal of infectious diseases 178, 147-158.

Jeng, A., Sakota, V., Li, Z., Datta, V., Beall, B. and Nizet, V. (2003). Molecular genetic analysis of a group A Streptococcus operon encoding serum opacity factor and a novel fibronectin-binding protein, SfbX. Journal of bacteriology 185, 1208-1217.

Ji, Y., McLandsborough, L., Kondagunta, A. and Cleary, P.P. (1996). C5a peptidase alters clearance and trafficking of group A streptococci by infected mice. Infection and immunity 64, 503-510.

Ji, Y., Schnitzler, N., DeMaster, E. and Cleary, P. (1998). Impact of M49, Mrp, Enn, and C5a peptidase proteins on colonization of the mouse oral mucosa by Streptococcus pyogenes. Infection and immunity 66, 5399-5405.

Johansson, L., Thulin, P., Low, D.E. and Norrby-Teglund, A. (2010). Getting under the skin: the immunopathogenesis of Streptococcus pyogenes deep tissue infections. Clinical infectious diseases : an official publication of the Infectious Diseases Society of America 51, 58-65.

Kaplan, E.L. (1997). Recent evaluation of antimicrobial resistance in beta-hemolytic streptococci. Clinical infectious diseases : an official publication of the Infectious Diseases Society of America 24 Suppl 1, S89-92.

Kaplan, E.L., Chhatwal, G.S. and Rohde, M. (2006). Reduced ability of penicillin to eradicate ingested group A streptococci from epithelial cells: clinical and pathogenetic implications. Clinical infectious diseases : an official publication of the Infectious Diseases Society of America 43, 1398-1406.

Kaplan, M.H. and Suchy, M.L. (1964). Immunologic Relation of Streptococcal and Tissue Antigens. Ii. Cross-Reaction of Antisera to Mammalian Heart Tissue with a Cell Wall Constituent of Certain Strains of Group a Streptococci. The Journal of experimental medicine 119, 643-650.

Kapur, V., Majesky, M.W., Li, L.L., Black, R.A. and Musser, J.M. (1993). Cleavage of interleukin 1 beta (IL-1 beta) precursor to produce active IL-1 beta by a conserved extracellular cysteine protease from Streptococcus pyogenes. Proceedings of the National Academy of Sciences of the United States of America 90, 7676-7680.

Kawabata, S., Kunitomo, E., Terao, Y., Nakagawa, I., Kikuchi, K., Totsuka, K. and Hamada, S. (2001). Systemic and mucosal immunizations with fibronectin-binding protein FBP54 induce protective immune responses against Streptococcus pyogenes challenge in mice. Infection and immunity 69, 924-930.

Koller, T., Manetti, A.G., Kreikemeyer, B., Lembke, C., Margarit, I., Grandi, G. and Podbielski, A. (2010). Typing of the pilus-protein-encoding FCT region and biofilm formation as novel parameters in epidemiological investigations of Streptococcus pyogenes isolates from various infection sites. Journal of medical microbiology 59, 442-452.

Laemmli, U.K. (1970). Cleavage of structural proteins during the assembly of the head of bacteriophage T4. Nature 227, 680-685.

Lancefield, R.C. (1928). The Antigenic Complex of Streptococcus Haemolyticus : I. Demonstration of a Type-Specific Substance in Extracts of Streptococcus Haemolyticus. The Journal of experimental medicine 47, 91-103.

Lancefield, R.C. (1933). A Serological Differentiation of Human and Other Groups of Hemolytic Streptococci. The Journal of experimental medicine 57, 571-595.

Lancefield, R.C. (1962). Current knowledge of type-specific M antigens of group A streptococci. Journal of immunology 89, 307-313.

LaPenta, D., Rubens, C., Chi, E. and Cleary, P.P. (1994). Group A streptococci efficiently invade human respiratory epithelial cells. Proceedings of the National Academy of Sciences of the United States of America 91, 12115-12119.

Long, S.S., Pickering, L.K. and Prober, C.G. (2012) Principles and Practices of Pediatic Infectious Diseases. 4 edn., Elsevier, pp. 698-707.

Macris, M.H., Hartman, N., Murray, B., Klein, R.F., Roberts, R.B., Kaplan, E.L., et al. (1998). Studies of the continuing susceptibility of group A streptococcal strains to penicillin during eight decades. The Pediatric infectious disease journal 17, 377-381.

Marjomaki, V., Pietiainen, V., Matilainen, H., Upla, P., Ivaska, J., Nissinen, L., et al. (2002). Internalization of echovirus 1 in caveolae. Journal of virology 76, 1856-1865.

McNeil, S.A., Halperin, S.A., Langley, J.M., Smith, B., Warren, A., Sharratt, G.P., et al. (2005). Safety and immunogenicity of 26-valent group a streptococcus vaccine in healthy adult volunteers. Clinical infectious diseases : an official publication of the Infectious Diseases Society of America 41, 1114-1122.

Medina, E., Rohde, M. and Chhatwal, G.S. (2003). Intracellular survival of Streptococcus pyogenes in polymorphonuclear cells results in increased bacterial virulence. Infection and immunity 71, 5376-5380.

Meresse, S., Steele-Mortimer, O., Moreno, E., Desjardins, M., Finlay, B. and Gorvel, J.P. (1999). Controlling the maturation of pathogen-containing vacuoles: a matter of life and death. Nature cell biology 1, E183-188.

Molinari, G., Rohde, M., Guzman, C.A. and Chhatwal, G.S. (2000). Two distinct pathways for the invasion of Streptococcus pyogenes in non-phagocytic cells. Cellular microbiology 2, 145-154.

Molinari, G., Talay, S.R., Valentin-Weigand, P., Rohde, M. and Chhatwal, G.S. (1997). The fibronectin-binding protein of Streptococcus pyogenes, SfbI, is involved in the internalization of group A streptococci by epithelial cells. Infection and immunity 65, 1357-1363.

Moses, A.E., Wessels, M.R., Zalcman, K., Alberti, S., Natanson-Yaron, S., Menes, T. and Hanski, E. (1997). Relative contributions of hyaluronic acid capsule and M protein to virulence in a mucoid strain of the group A Streptococcus. Infection and immunity 65, 64-71.

Mullis, K.B. and Faloona, F.A. (1987). Specific synthesis of DNA in vitro via a polymerase-catalyzed chain reaction. Methods in enzymology 155, 335-350.

NanoAnalytics (2009) CellZscope Operating Manual Version 1.32.

Nerlich, A., Rohde, M., Talay, S.R., Genth, H., Just, I. and Chhatwal, G.S. (2009). Invasion of endothelial cells by tissue-invasive M3 type group A streptococci requires Src kinase and activation of Rac1 by a phosphatidylinositol 3-kinase-independent mechanism. The Journal of biological chemistry 284, 20319-20328.

Nitsche-Schmitz, D.P., Rohde, M. and Chhatwal, G.S. (2007). Invasion mechanisms of Gram-positive pathogenic cocci. Thrombosis and haemostasis 98, 488-496.

Nizet, V. (2002). Streptococcal beta-hemolysins: genetics and role in disease pathogenesis. Trends in microbiology 10, 575-580.

Nizet, V. (2007). Understanding how leading bacterial pathogens subvert innate immunity to reveal novel therapeutic targets. The Journal of allergy and clinical immunology 120, 13-22.

Norkin, L.C., Wolfrom, S.A. and Stuart, E.S. (2001). Association of caveolin with Chlamydia trachomatis inclusions at early and late stages of infection. Experimental cell research 266, 229-238.

Nunes, P. and Demaurex, N. (2010). The role of calcium signaling in phagocytosis. Journal of leukocyte biology 88, 57-68.

Oehmcke, S., Shannon, O., Morgelin, M. and Herwald, H. (2010). Streptococcal M proteins and their role as virulence determinants. Clinica chimica acta; international journal of clinical chemistry 411, 1172-1180.

Okada, N., Liszewski, M.K., Atkinson, J.P. and Caparon, M. (1995). Membrane cofactor protein (CD46) is a keratinocyte receptor for the M protein of the group A streptococcus. Proceedings of the National Academy of Sciences of the United States of America 92, 2489-2493.

Olivier, C. (2000). Rheumatic fever--is it still a problem? The Journal of antimicrobial chemotherapy 45 Suppl, 13-21.

Olsen, R.J. and Musser, J.M. (2010). Molecular pathogenesis of necrotizing fasciitis. Annual review of pathology 5, 1-31.

Olsen, R.J., Shelburne, S.A. and Musser, J.M. (2009). Molecular mechanisms underlying group A streptococcal pathogenesis. Cellular microbiology 11, 1-12.

Osterlund, A., Popa, R., Nikkila, T., Scheynius, A. and Engstrand, L. (1997). Intracellular reservoir of Streptococcus pyogenes in vivo: a possible explanation for recurrent pharyngotonsillitis. The Laryngoscope 107, 640-647.

Ozeri, V., Rosenshine, I., Ben-Ze'Ev, A., Bokoch, G.M., Jou, T.S. and Hanski, E. (2001). De novo formation of focal complex-like structures in host cells by invading Streptococci. Molecular microbiology 41, 561-573.

Ozeri, V., Rosenshine, I., Mosher, D.F., Fassler, R. and Hanski, E. (1998). Roles of integrins and fibronectin in the entry of Streptococcus pyogenes into cells via protein F1. Molecular microbiology 30, 625-637.

Pelkmans, L., Kartenbeck, J. and Helenius, A. (2001). Caveolar endocytosis of simian virus 40 reveals a new two-step vesicular-transport pathway to the ER. Nature cell biology 3, 473-483.

Phillips, G.N., Jr., Flicker, P.F., Cohen, C., Manjula, B.N. and Fischetti, V.A. (1981). Streptococcal M protein: alpha-helical coiled-coil structure and arrangement on the cell surface. Proceedings of the National Academy of Sciences of the United States of America 78, 4689-4693.

Podbielski, A., Schnitzler, N., Beyhs, P. and Boyle, M.D. (1996). M-related protein (Mrp) contributes to group A streptococcal resistance to phagocytosis by human granulocytes. Molecular microbiology 19, 429-441.

Portnoy, D.A., Auerbuch, V. and Glomski, I.J. (2002). The cell biology of Listeria monocytogenes infection: the intersection of bacterial pathogenesis and cell-mediated immunity. The Journal of cell biology 158, 409-414.

Prescott, L.M., Harley, J.P. and Klein, D.A. (2005) Microbiology. 6 edn., McGraw Hill, pp. 503-520.

Pries, A.R. and Kuebler, W.M. (2006). Normal endothelium. Handbook of experimental pharmacology, 1-40.

Purushothaman, S.S., Wang, B. and Cleary, P.P. (2003). M1 protein triggers a phosphoinositide cascade for group A Streptococcus invasion of epithelial cells. Infection and immunity 71, 5823-5830.

Rezcallah, M.S., Hodges, K., Gill, D.B., Atkinson, J.P., Wang, B. and Cleary, P.P. (2005). Engagement of CD46 and alpha5beta1 integrin by group A streptococci is required for efficient invasion of epithelial cells. Cellular microbiology 7, 645-653.

Rohde, M., Muller, E., Chhatwal, G.S. and Talay, S.R. (2003). Host cell caveolae act as an entry-port for group A streptococci. Cellular microbiology 5, 323-342.

Rottner, K., Stradal, T.E. and Wehland, J. (2005). Bacteria-host-cell interactions at the plasma membrane: stories on actin cytoskeleton subversion. Developmental cell 9, 3-17.

Salyers, A.A. and Whitt, D.D. (2002) Bacterial Pathogenesis, A Molecular Approach. 2 edn., ASM Press, pp. 232-246.

Sarantis, H. and Grinstein, S. (2012). Subversion of phagocytosis for pathogen survival. Cell host & microbe 12, 419-431.

Saunders, M. (2009). Transplacental transport of nanomaterials. Wiley interdisciplinary reviews. Nanomedicine and nanobiotechnology 1, 671-684.

Schottmüller, H. (1903) Die Artunterscheidung der für den Menschen pathogenen Streptokokken durch Blutagar, Münch. Med. Wochenschr.

Schrager, H.M., Alberti, S., Cywes, C., Dougherty, G.J. and Wessels, M.R. (1998). Hyaluronic acid capsule modulates M protein-mediated adherence and acts as a ligand for attachment of group A Streptococcus to CD44 on human keratinocytes. The Journal of clinical investigation 101, 1708-1716.

Schwartz, M.A., Schaller, M.D. and Ginsberg, M.H. (1995). Integrins: emerging paradigms of signal transduction. Annual review of cell and developmental biology 11, 549-599.

Schwarz-Linek, U., Hook, M. and Potts, J.R. (2006). Fibronectin-binding proteins of gram-positive cocci. Microbes and infection / Institut Pasteur 8, 2291-2298.

Sela, S. and Barzilai, A. (1999). Why do we fail with penicillin in the treatment of group A streptococcus infections? Annals of medicine 31, 303-307.

Shet, A., Kaplan, E.L., Johnson, D.R. and Cleary, P.P. (2003). Immune response to group A streptococcal C5a peptidase in children: implications for vaccine development. The Journal of infectious diseases 188, 809-817.

Shin, J.S. and Abraham, S.N. (2001a). Caveolae as portals of entry for microbes. Microbes and infection / Institut Pasteur 3, 755-761.

Shin, J.S. and Abraham, S.N. (2001b). Cell biology. Caveolae--not just craters in the cellular landscape. Science 293, 1447-1448.

Shin, J.S. and Abraham, S.N. (2001c). Co-option of endocytic functions of cellular caveolae by pathogens. Immunology 102, 2-7.

Simpson, W.A. and Beachey, E.H. (1983). Adherence of group A streptococci to fibronectin on oral epithelial cells. Infection and immunity 39, 275-279.

Smeesters, P.R., McMillan, D.J. and Sriprakash, K.S. (2010). The streptococcal M protein: a highly versatile molecule. Trends in microbiology 18, 275-282.

Smeets, E.F., von Asmuth, E.J., van der Linden, C.J., Leeuwenberg, J.F. and Buurman, W.A. (1992). A comparison of substrates for human umbilical vein endothelial cell culture. Biotechnic & histochemistry : official publication of the Biological Stain Commission 67, 241-250.

Spurr, A.R. (1969). A low-viscosity epoxy resin embedding medium for electron microscopy. Journal of ultrastructure research 26, 31-43.

Staali, L., Bauer, S., Morgelin, M., Bjorck, L. and Tapper, H. (2006). Streptococcus pyogenes bacteria modulate membrane traffic in human neutrophils and selectively inhibit azurophilic granule fusion with phagosomes. Cellular microbiology 8, 690-703.

Staali, L., Morgelin, M., Bjorck, L. and Tapper, H. (2003). Streptococcus pyogenes expressing M and M-like surface proteins are phagocytosed but survive inside human neutrophils. Cellular microbiology 5, 253-265.

Steinberg, B.E. and Grinstein, S. (2008). Pathogen destruction versus intracellular survival: the role of lipids as phagosomal fate determinants. The Journal of clinical investigation 118, 2002-2011.

Stevens, D.L. (2001). Invasive streptococcal infections. Journal of infection and chemotherapy : official journal of the Japan Society of Chemotherapy 7, 69-80.

Stradal, T.E., Rottner, K., Disanza, A., Confalonieri, S., Innocenti, M. and Scita, G. (2004). Regulation of actin dynamics by WASP and WAVE family proteins. Trends in cell biology 14, 303-311.

Stradal, T.E. and Scita, G. (2006). Protein complexes regulating Arp2/3-mediated actin assembly. Current opinion in cell biology 18, 4-10.

Sumpio, B.E., Riley, J.T. and Dardik, A. (2002). Cells in focus: endothelial cell. The international journal of biochemistry & cell biology 34, 1508-1512.

Talay, S.R. (2005). Gram-positive adhesins. Contributions to microbiology 12, 90-113.

Talay, S.R., Valentin-Weigand, P., Jerlstrom, P.G., Timmis, K.N. and Chhatwal, G.S. (1992). Fibronectin-binding protein of Streptococcus pyogenes: sequence of the binding domain involved in adherence of streptococci to epithelial cells. Infection and immunity 60, 3837-3844.

Talay, S.R., Zock, A., Rohde, M., Molinari, G., Oggioni, M., Pozzi, G., et al. (2000). Co-operative binding of human fibronectin to Sfbl protein triggers streptococcal invasion into respiratory epithelial cells. Cellular microbiology 2, 521-535.

Tart, A.H., Walker, M.J. and Musser, J.M. (2007). New understanding of the group A Streptococcus pathogenesis cycle. Trends in microbiology 15, 318-325.

Valentin-Weigand, P., Talay, S.R., Kaufhold, A., Timmis, K.N. and Chhatwal, G.S. (1994). The fibronectin binding domain of the Sfb protein adhesin of Streptococcus pyogenes occurs in many group A streptococci and does not cross-react with heart myosin. Microbial pathogenesis 17, 111-120.

Vartiainen, M.K. and Machesky, L.M. (2004). The WASP-Arp2/3 pathway: genetic insights. Current opinion in cell biology 16, 174-181.

Wang, B., Li, S., Dedhar, S. and Cleary, P.P. (2007). Paxillin phosphorylation: bifurcation point downstream of integrin-linked kinase (ILK) in streptococcal invasion. Cellular microbiology 9, 1519-1528.

Wang, B., Yurecko, R.S., Dedhar, S. and Cleary, P.P. (2006). Integrin-linked kinase is an essential link between integrins and uptake of bacterial pathogens by epithelial cells. Cellular microbiology 8, 257-266.

Wessels, M.R., Moses, A.E., Goldberg, J.B. and DiCesare, T.J. (1991). Hyaluronic acid capsule is a virulence factor for mucoid group A streptococci. Proceedings of the National Academy of Sciences of the United States of America 88, 8317-8321.

Wexler, D.E., Chenoweth, D.E. and Cleary, P.P. (1985). Mechanism of action of the group A streptococcal C5a inactivator. Proceedings of the National Academy of Sciences of the United States of America 82, 8144-8148.

Yamaguchi, M., Terao, Y. and Kawabata, S. (2012). Pleiotropic virulence factor - Streptococcus pyogenes fibronectin-binding proteins. Cellular microbiology.

Zimmerlein, B., Park, H.S., Li, S., Podbielski, A. and Cleary, P.P. (2005). The M protein is dispensable for maturation of streptococcal cysteine protease SpeB. Infection and immunity 73, 859-864.

Internet sources

http://www.siumed.edu/~dking2/crr/cvguide.htm

Acknowledgment

I would like to take the opportunity to thank all who have contributed to the success of this thesis:

First of all, I would like to thank Prof. Dr. Singh Chhatwal for the opportunity to conduct the laboratory work of this thesis in the Department of Medical Microbiology.

I would like to sincerely thank my supervisors Apl. Prof. Dr. Manfred Rohde and Dr. Susanne Talay for their support, scientific advices and many motivating discussions. Special thanks go to Apl. Prof. Dr. Manfred Rohde for his commitment and great support, especially during the last year of this thesis.

Furthermore, sincere thanks go to PD Dr. Simone Bergmann, my referee and member of the thesis committee, for supporting me during my thesis and for offering many valuable discussions. In addition, I would like to acknowledge Prof. Dr. Michael Steinert who agreed to act as second referee for this thesis.

I also would like to thank Dr. Dagmar Wirth, who accompanied my thesis as a member of my thesis committee, for her support and helpful suggestions.

I am very grateful for funding from the President's Initiative and Networking Fund of the Helmholtz Association of German Research Centers under the contract number VH-GS-202. Moreover, I would like to acknowledge the HZI Graduate School for the opportunity to participate in laboratory as well as scientific courses and international conferences.

In addition, I would like to extend many thanks to Dr. Henk Garritsen (Institute for Transfusion Medicine, Hospital Celler Strasse, Braunschweig) who kindly provided the umbilical cord for *ex vivo* infection assays.

I am very grateful to my colleagues of the whole MMIK and INI group for their help in various aspects of my laboratory work. In particular, I would like to thank our technician Stephanie Peter for many valuable advices and the kind working atmosphere. Special thanks also go to Dr. Oliver Goldmann for experimental advices, for his help with the FACS analysis and for critically reading this thesis. Furthermore, I also thank Dr. Marcus Fulde for his support with the radioactive binding assays.

Moreover, special thanks go to Apl. Prof. Dr. Manfred Rohde and Ina Schleicher for the excellent electron microscopic images and for introducing me into the world of electron microscopy. Many thanks go to Ina Schleicher for sharing her knowledge and for always helping me.

I am especially grateful to my good friends and colleagues Katja Branitzki-Heinemann, Alva Rosendahl and Angela Hitzmann. Thank you for your scientific, but more importantly, your emotional support that helped me get through the difficult times and for the fun we had together. Also, special thanks to my friend Gitta Lipps for her support and for carefully reading this thesis.

Finally, I would like to thank my whole family, especially my parents, for their continous support, love and faith in me.

Most importantly, Aaron, thank you so much for your love, your motivation, your faith in me and your endless patience. Thank you for always being there for me.